Xavier Pennec

Asclepios team, INRIA Sophia-Antipolis – Mediterranée, France

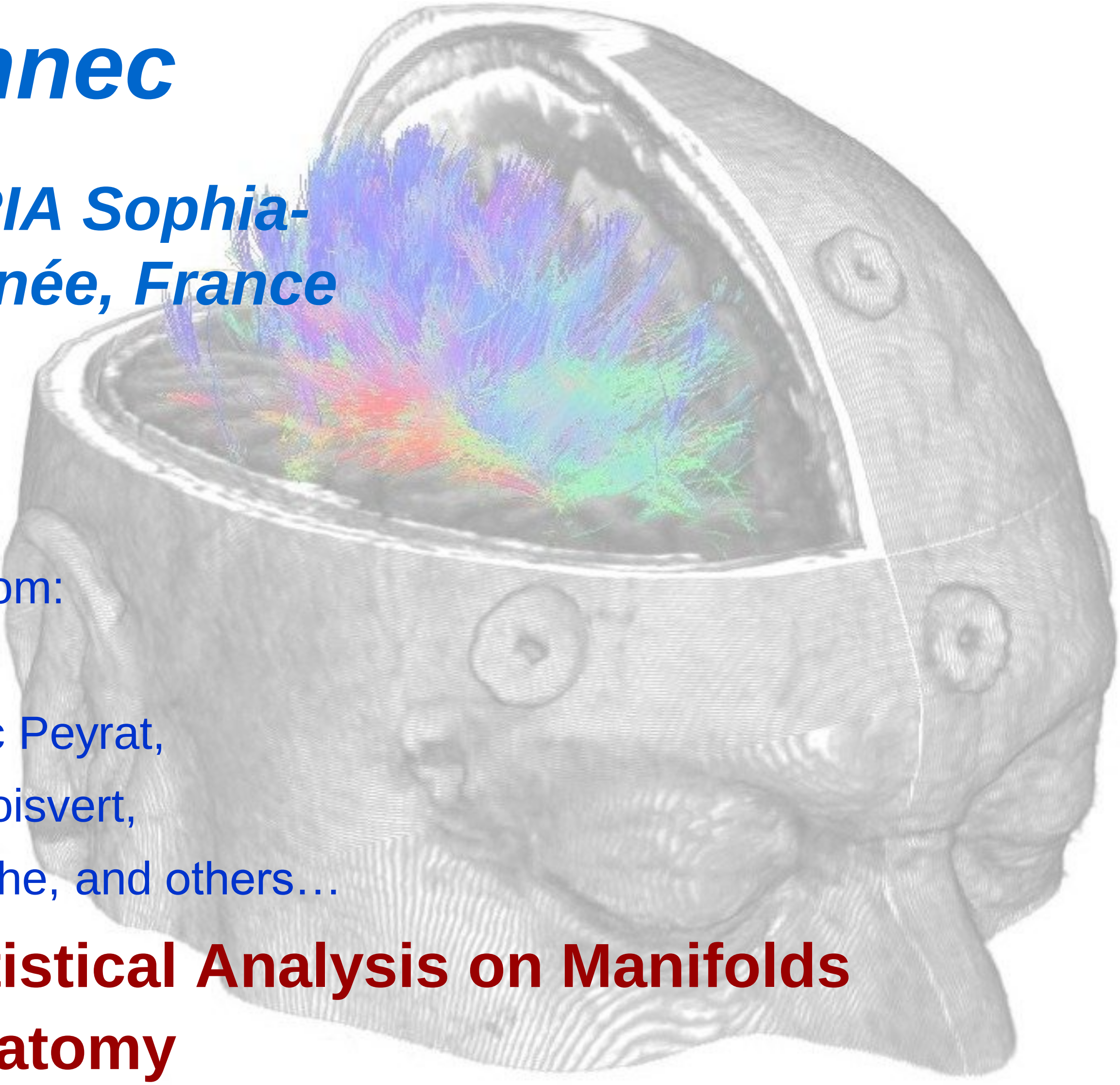

With indebting contributions from:

Pierre Fillard, Vincent Arsigny,

Stanley Durrleman, Jean-Marc Peyrat,

Tom Vercauteren, Jonathan Boisvert,

Thomas Mansi, Nicholas Ayache, and others…

Current issues in Statistical Analysis on Manifolds for Computational Anatomy

Seminaire Brillouin, IRCAM

May 28, 2010

INRIA SOPHIA ANTIPOLIS

Anatomy

Science that studies the structure and the relationship in space of different organs and tissues in living systems [Hachette Dictionary]

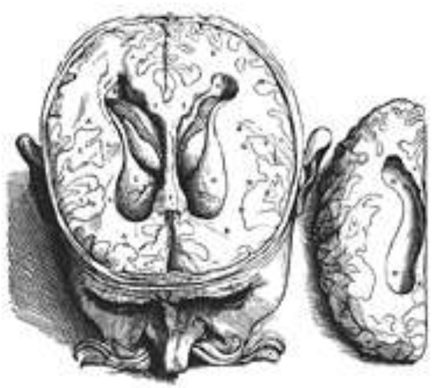

1er cerebral atlas, Vesale, 1543

Paré, 1585

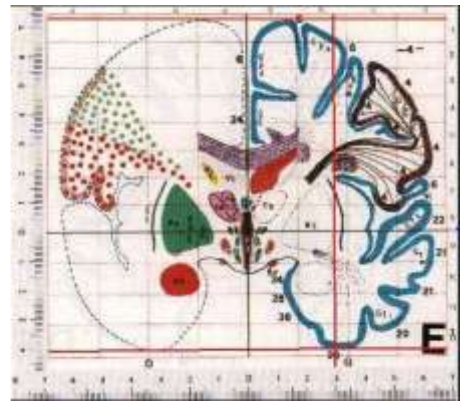

Talairach & Tournoux, 1988

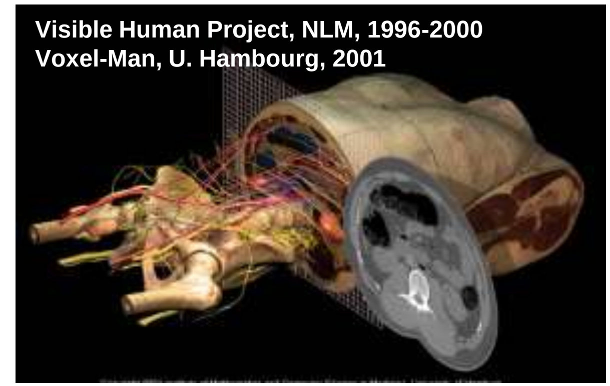

Antiquity
- Animal models
- Philosophical physiology

Renaissance:
- Dissection, surgery
- Descriptive anatomy

17-20e century:
- Anatomo-physiology
- Microscopy, histology

1990-2000:
- Explosion of imaging
- Computer atlases
- Brain decade

Galien (131-201) → **Vésale (1514-1564) Paré (1509-1590)** → **Sylvius (1614-1672) Willis (1621-1675)** → **Gall (1758-1828) : *Phrenology* Talairach (1911-2007)**

Revolution of observation means (1988-2007) :

- From dissection to in-vivo in-situ imaging
- From representative individual to population
- From descriptive atlases to interactive and generative models (simulation)

Modeling and image analysis: a virtuous loop

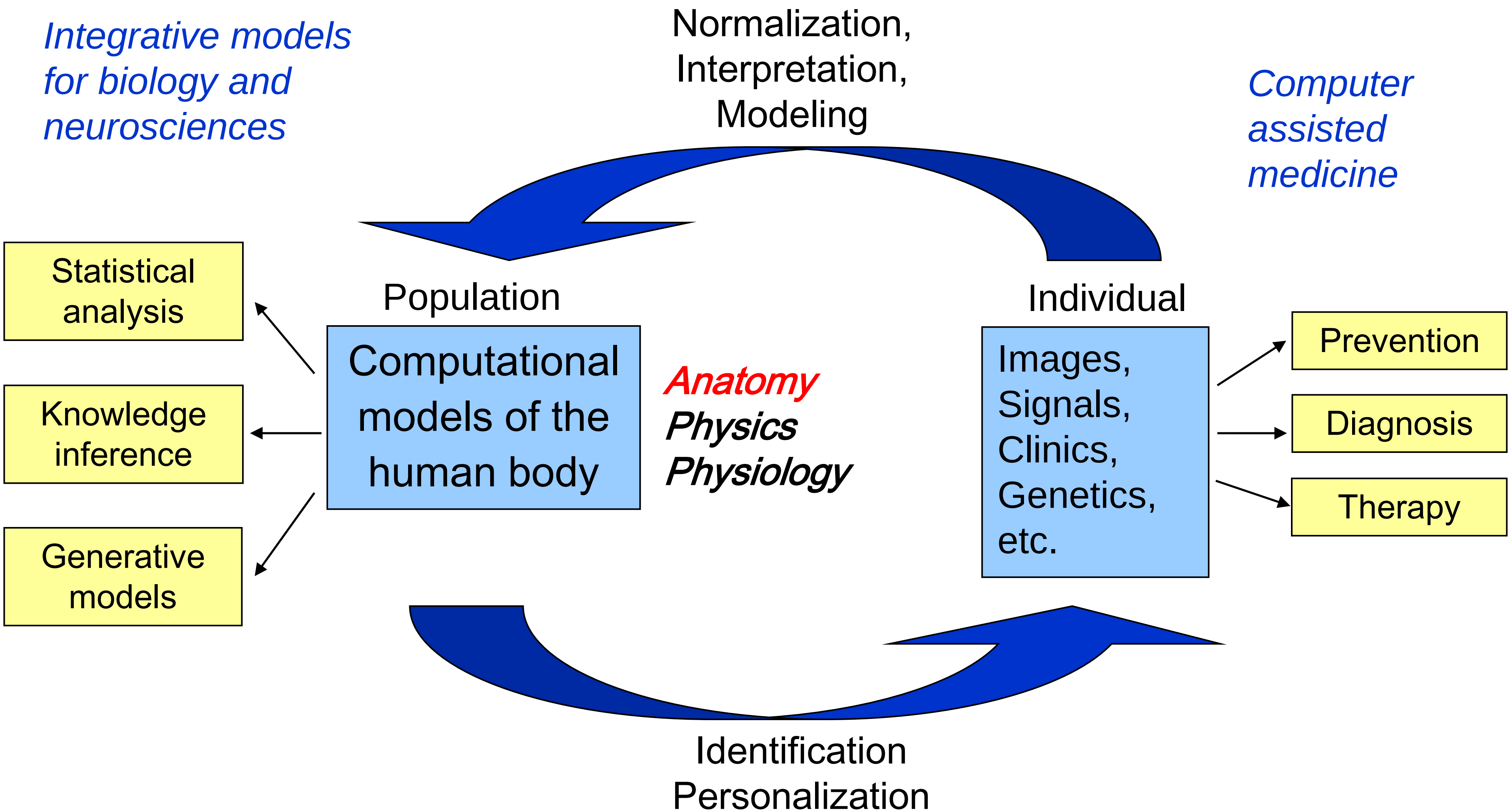

Computational Anatomy


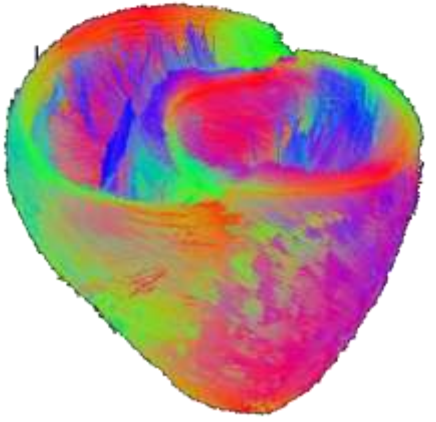
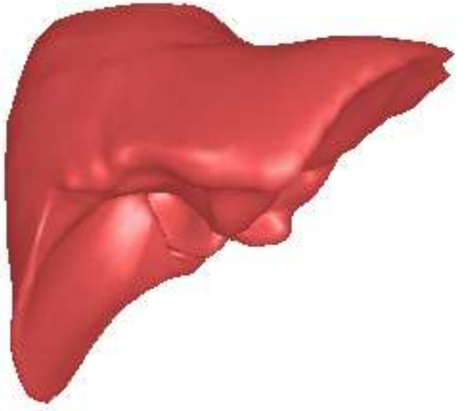


Design Mathematical Methods and Algorithms to Model and Analyze the Anatomy

- Estimate representative organ anatomies across species, populations, diseases, aging, ages…
- Model organ development across time
- Establish normal variability

To understand and to model how life is functioning

- Classify pathologies from structural deviations (**taxonomy**)
- Relate anatomy and **function** at the population level
- Build prior knowledge to **simulate** new anatomies

To detect, understand and correct dysfunctions

- From generic (atlas-based) to **patients-specific models**
- Quantitative and objective measures for **diagnosis**
- Help **therapy** planning (before), control (during) and follow-up (after)

Methods of computational anatomy

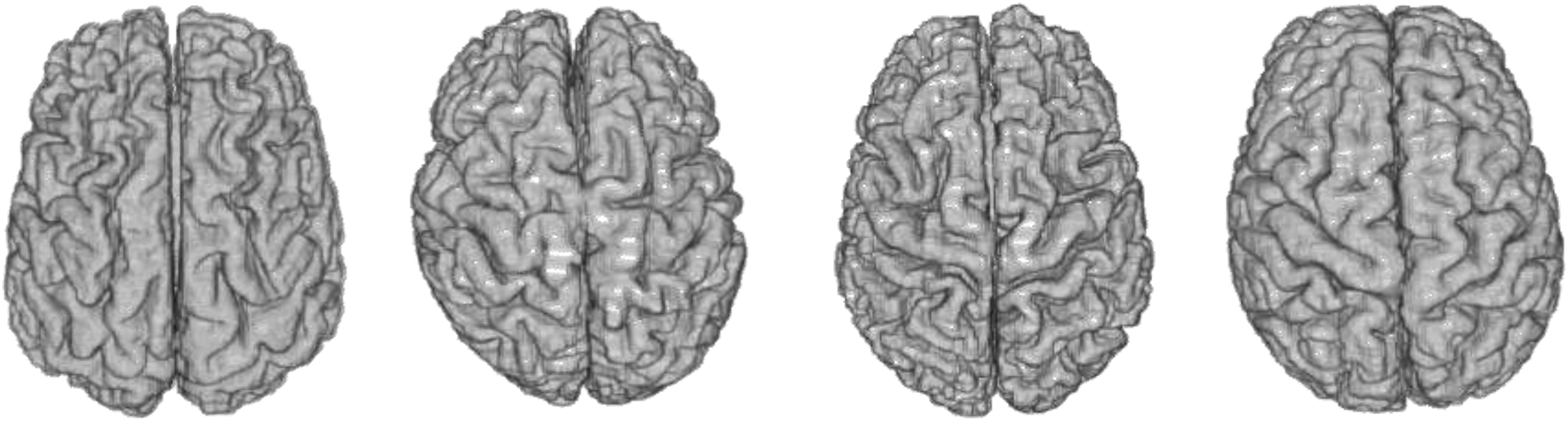

Structural variability of the cortex

Hierarchy of anatomical manifolds (structural models)

- Landmarks [0D]: AC, PC [Talairach et Tournoux, Bookstein], functional landmarks
- Curves [1D]: crest lines, sulcal lines [Mangin, Barillot, Fillard…]
- Surfaces [2D]: cortex, sulcal ribbons [Thompson, Mangin, Miller…],
- Images [3D functions]: VBM, Tensors in Diffusion imaging
- Transformations: rigid, multi-affine, local deformations (TBM), diffeomorphisms [Asburner, Arsigny, Miller, Trouve, Younes…]

Groupwise correspondances in the population

Model observations and its structural variability

→ Statistical computing on Riemannian manifolds

Statistical analyses on manifolds in Medical image analysis

Noisy geometric measures

- Feature extracted from images
  - Lines, oriented points, extremal points (frames)
  - Curves, surfaces
  - Tensors from DTI

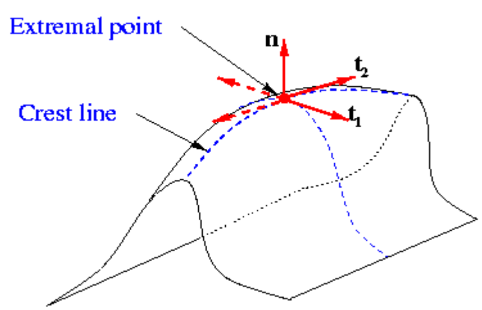

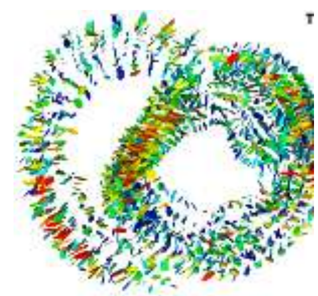

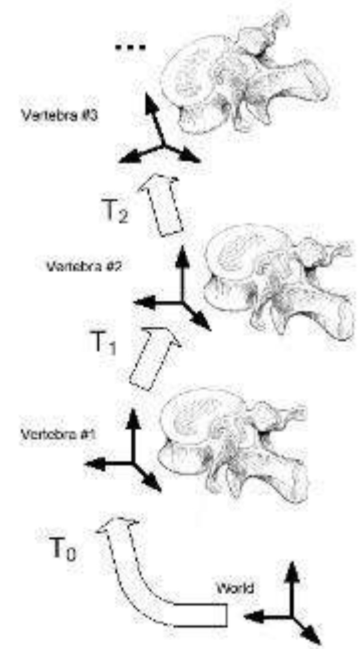

- Transformations in registrations
  - Rigid, Affine, locally affine, families of deformations

Goal:

- Deal with noise consistently on these non-Euclidean manifolds
- A consistent computing framework

Diffusion Tensor Imaging

Covariance of the Brownian motion of water
-> Architecture of axonal fibers

Very noisy data

- Tensor image processing
  - Robust estimation
  - Filtering, regularization
  - Interpolation / extrapolation
- Information extraction (fibers)

Symmetric positive definite matrices

- Convex operations are stable
  - mean, interpolation
- More complex operations are not
  - PDEs, gradient descent…
  - Null and negatives eigenvalues are not physical

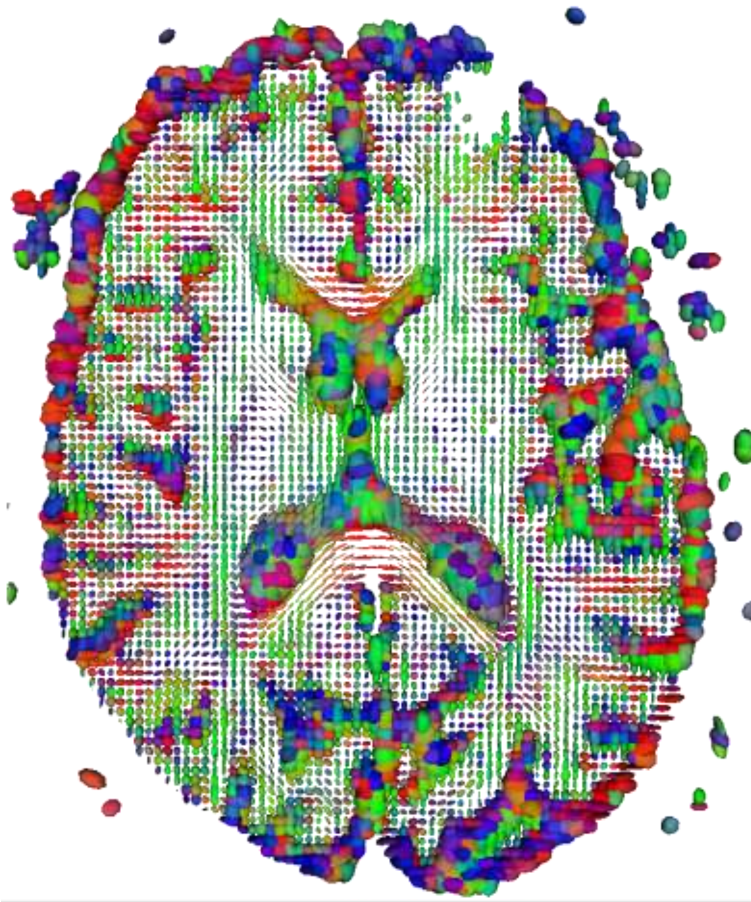

Diffusion Tensor Filed
(slice of a 3D volume)

Intrinsic computing on Manifold-valued images?

Roadmap

Goals and methods of Computational anatomy

Statistical computing on manifolds

A Riemannian framework for tensor computing

Currents: an embedding space for curves and surfaces

Log-Euclidean statistics on image deformations

Conclusion and challenges

Roadmap

Goals and methods of Computational anatomy

Statistical computing on manifolds

- The mathematical framework
  - Riemannian geometry
  - Simple statistics
- Example applications on rigid body transformations

A Riemannian framework for tensor computing

Currents: an embedding space for curves and surfaces

Log-Euclidean statistics on image deformations

Conclusion and challenges

Riemannian geometry is a powerful structure to build consistent statistical computing algorithms

Shape spaces & directional statistics

- [Kendall StatSci 89, Small 96, Dryden & Mardia 98]

Numerical integration, dynamical systems & optimization

- [Helmke & Moore 1994, Hairer et al 2002]
- Matrix Lie groups [Owren BIT 2000, Mahony JGO 2002]
- Optimization on Matrix Manifolds [Absil, Mahony, Sepulchre, 2008]

Information geometry (statistical manifolds)

- [Amari 1990 & 2000, Kass & Vos 1997]
- [Oller Annals Stat. 1995, Battacharya Annals Stat. 2003 & 2005]

Statistics for image analysis

- Rigid body transformations [Pennec PhD96]
- General Riemannian manifolds [Pennec JMIV98, NSIP99, JMIV06]
- PGA for M-Reps [Fletcher IPMI03, TMI04]
- Planar curves [Klassen & Srivastava PAMI 2003]

The geometric framework: Riemannian Manifolds

Riemannian metric :

- Dot product on tangent space
- Speed, length of a curve
- Distance and geodesics
  - Closed form for simple metrics/manifolds
  - Optimization for more complex

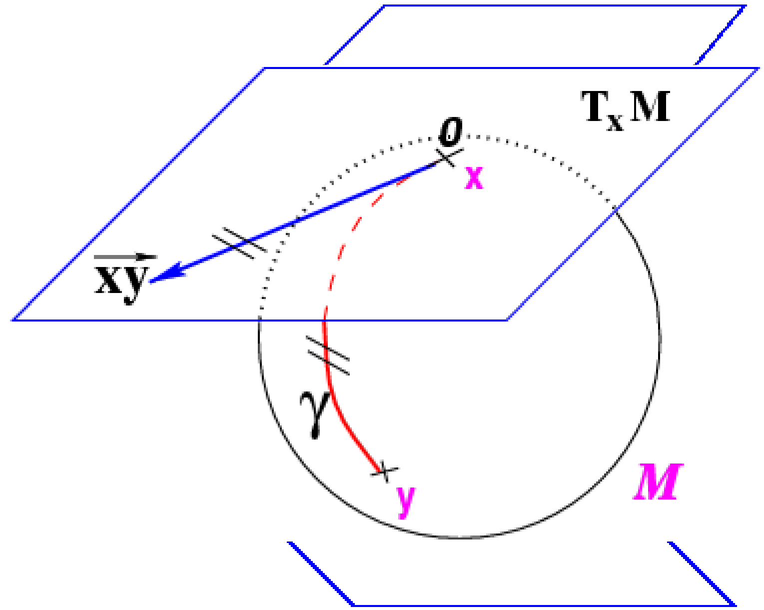

Exponential map (Normal coord. syst.) :

- Geodesic shooting: $Exp_x(v) = \gamma_{(x,v)}(1)$
- Log: find vector to shoot right

Unfolding (Log_x), folding (Exp_x)

- Vector -> Bipoint (no more equivalent class)

Operator	Euclidean space	Riemannian manifold
Subtraction	$\overrightarrow{xy} = y - x$	$\overrightarrow{xy} = Log_x(y)$
Addition	$y = x + \overrightarrow{xy}$	$y = Exp_x(\overrightarrow{xy})$
Distance	$\mathrm{dist}(x, y) = \\|y - x\\|$	$\mathrm{dist}(x, y) = \\|\overrightarrow{xy}\\|_x$
Gradient descent	$x_{t+\varepsilon} = x_t - \varepsilon \nabla C(x_t)$	$x_{t+\varepsilon} = Exp_{x_t}(-\varepsilon \nabla C(x_t))$

Metric choice

Transformations (Lie group):

- Left (or right) invariant $\quad \mathrm{dist}(g,h) = \mathrm{dist}(f \circ g, f \circ h) = \left\| f^{(-1)} \circ g \right\|_{Id}$
- Practical computations $\quad \exp_{\vec{f}}\left(\overrightarrow{\delta f}\right) = f \circ \overrightarrow{\delta f} \qquad \overrightarrow{fg} = f^{(-1)} \circ g$
- *No bi-invariant metric*

Homogeneous manifolds

$$\mathrm{dist}(x,y) = \mathrm{dist}(g * x, g * y)$$

- Choose a metric invariant wrt the isotropy group of an origin o
- Choose one family of transformations f_x such that $f_x(o) = x$
- Practical computations $\quad \exp_x\left(\overrightarrow{\delta x}\right) = f_x * \overrightarrow{\delta x} \qquad \overrightarrow{xy} = f_x^{(-1)} * \vec{y}$

General Riemannian manifolds

- Exp and log through numerical optimization / integration

Example on 3D rotations

Space of rotations SO(3):

- Manifold: $R^t.R=Id$ and $\det(R)=+1$
- Lie group:
  - Composition: $R_1 \text{ o } R_2 = R_1.R_2$
  - Inversion: $R^{(-1)} = R^t$

Tangent space

- At Identity (skew symmetric matrices)
- At any point by left or right translation

Metrics on SO(3)

- Left / right invariant metrics
- Induced by the ambient space: bi-invariance

Group exponential

- One parameter subgroups = bi-invariant Geodesic starting at Id
  - Matrix exponential and Rodrigue's formula
- Geodesic everywhere by left (or right) translation

Roadmap

Goals and methods of Computational anatomy

Statistical computing on manifolds

- The mathematical framework
  - Riemannian geometry
  - Simple statistics
- Example applications on rigid body transformations

A Riemannian framework for tensor computing

Currents: an embedding space for curves and surfaces

Log-Euclidean statistics on image deformations

Conclusion and challenges

Basic probabilities and statistics

Measure: random vector x of pdf $p_{\mathbf{x}}(z)$

Approximation: $\mathbf{x} \sim (\overline{\mathrm{x}}, \mathbf{\Sigma_{xx}})$

- Mean: $\overline{\mathrm{x}} = \mathrm{E}(\,\mathbf{x}\,) = \int z.p_{\mathbf{x}}(z).dz$
- Covariance: $\Sigma_{\mathbf{xx}} = \mathrm{E}\left[(\mathbf{x}-\overline{\mathrm{x}}).(\mathbf{x}-\overline{\mathrm{x}})^{T}\right]$

Propagation:

$$\mathbf{y} = h(\mathbf{x}) \sim \left(h(\overline{\mathrm{x}}),\ \frac{\partial h}{\partial \mathrm{x}}.\mathbf{\Sigma_{xx}}.\frac{\partial h}{\partial \mathrm{x}}^{\mathrm{T}} \right)$$

Noise model: additive, Gaussian...

Principal component analysis

Statistical distance: Mahalanobis and χ^2

Statistical tools on Riemannian manifolds

Metric -> Volume form (measure) $d\mathcal{M}(\mathrm{x})$

Probability density functions $\forall X, P(x \in X) = \int_X p_{\mathbf{x}}(y).d\mathcal{M}(y)$

Expectation of a function ϕ from M into R :

- Definition : $\mathrm{E}\left[\phi(x)\right] = \int_{\mathcal{M}} \phi(y).p_{\mathbf{x}}(y).d\mathcal{M}(y)$

- Variance : $\sigma_{\mathbf{x}}^2(y) = \mathrm{E}\left[\mathrm{dist}(y, \underline{\mathrm{x}})^2\right] = \int_{\mathcal{M}} \mathrm{dist}(y, z)^2.p_{\mathbf{x}}(z).d\mathcal{M}(z)$

- Information (neg. entropy): $\mathrm{I}[\mathbf{x}] = \mathrm{E}\left[\log(p_{\mathbf{x}}(\mathbf{x}))\right]$

Fréchet expectation (1944)

Minimizing the variance

$$\mathrm{E}[\mathbf{x}] = \underset{y \in \mathrm{M}}{\mathrm{argmin}} \left(\mathrm{E}\left[\mathrm{dist}(y, \mathbf{x})^2 \right] \right)$$

- **Existence and uniqueness : Karcher and Kendall**

Characterization as an exponential barycenter (P(C)=0)

$$\mathrm{grad}\left(\sigma_{\mathbf{x}}^2(y)\right) = 0 \quad \Rightarrow \quad \mathrm{E}\left[\overrightarrow{\bar{\mathrm{x}}\mathbf{x}}\right] = \int_{\mathrm{M}} \overrightarrow{\bar{\mathrm{x}}\mathbf{x}}.p_{\mathbf{x}}(z).d\mathrm{M}(z) = 0$$

The case of points: classical expectation $\bar{\mathrm{x}} \in \mathrm{E}[\mathbf{x}] \quad \Rightarrow \quad \mathrm{E}[-\bar{\mathrm{x}} + \mathbf{x}] = 0$

Other central primitives

$$\mathrm{E}^{\alpha}[\mathbf{x}] = \underset{y \in \mathrm{M}}{\mathrm{argmin}} \left(\mathrm{E}\left[\mathrm{dist}(y, \mathbf{x})^{\alpha} \right] \right)^{1/\alpha}$$

[Pennec, JMIV06, RR-5093, NSIP'99]

Other definitions of the mean

Doss [1949] / Herer [1988]: $\mathrm{E}[\mathbf{x}] = \{ y \in M \, / \, \mathrm{dist}(y, \bar{x}) \leq \mathrm{E}[\mathrm{dist}(y, \mathbf{x})] \}$

Convex barycenters (Emery / Arnaudon)

$$\mathrm{E}[\mathbf{x}] = \{ y \in M \, / \, \alpha(y) \leq \mathrm{E}[\alpha(\mathbf{x})] \text{ for } \alpha \text{ convex on the support of } \mathbf{x} \}$$

- Convex functions in compact spaces are constant

Emery 1991:

- if the support of **x** is included in a strongly convex open set:

$$\text{Exponential barycenters} \subset \text{Convex Barycenters}$$

Picard 1994: Connector (->) Connection (->) metric

- Difference between barycenters is O(σ)

Statistical tools: Moments

Frechet / Karcher mean minimize the variance

$$\mathrm{E}[\mathbf{x}] = \underset{y \in \mathcal{M}}{\mathrm{argmin}} \left(\mathrm{E}\left[\mathrm{dist}(y, \mathbf{x})^2 \right] \right) \quad \Rightarrow \quad \mathrm{E}\left[\overrightarrow{\bar{\mathrm{x}}\mathbf{x}} \right] = \int_{\mathcal{M}} \overrightarrow{\bar{\mathrm{x}}\mathbf{x}} . p_{\mathbf{x}}(z).d\mathrm{M}(z) = 0 \quad [P(C) = 0]$$

Gauss-Newton Geodesic marching

$$\bar{\mathrm{x}}_{t+1} = \exp_{\bar{\mathrm{x}}_t}(v) \quad \text{with} \quad v = \mathrm{E}\left[\overrightarrow{\mathrm{y}\mathbf{x}} \right]$$

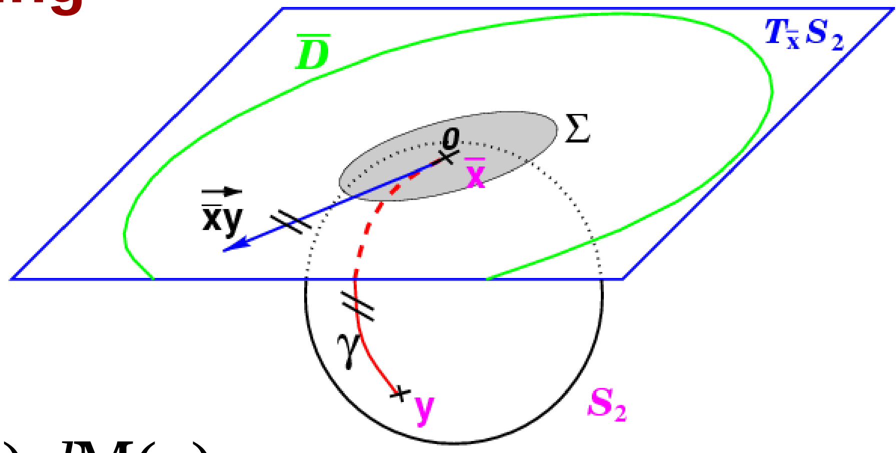

Covariance et higher moments

$$\Sigma_{\mathbf{xx}} = \mathrm{E}\left[\left(\overrightarrow{\bar{\mathrm{x}}\mathbf{x}} \right) \left(\overrightarrow{\bar{\mathrm{x}}\mathbf{x}} \right)^{\mathrm{T}} \right] = \int_{\mathcal{M}} \left(\overrightarrow{\bar{\mathrm{x}}z} \right) \left(\overrightarrow{\bar{\mathrm{x}}z} \right)^{\mathrm{T}} . p_{\mathbf{x}}(z).d\mathrm{M}(z)$$

[Pennec, JMIV06, RR-5093, NSIP’99]

Distributions for parametric tests

Uniform density:

- maximal entropy knowing X $\qquad p_{\mathbf{x}}(z) = \mathrm{Ind}_X(z) / \mathrm{Vol}(X)$

Generalization of the Gaussian density:

- Stochastic heat kernel p(x,y,t) [complex time dependency]
- Wrapped Gaussian [Infinite series difficult to compute]
- Maximal entropy knowing the mean and the covariance

$$N(y) = k.\exp\left(\left(\overrightarrow{\bar{\mathrm{x}}\mathbf{x}} \right)^{\mathrm{T}} .\mathbf{\Gamma}.\left(\overrightarrow{\bar{\mathrm{x}}\mathbf{x}} \right) / 2 \right)$$

$$\mathbf{\Gamma} = \mathbf{\Sigma}^{(-1)} - \tfrac{1}{3}\mathrm{Ric} + O(\sigma) + \varepsilon(\sigma / r)$$

$$k = (2\pi)^{-n/2}.\det(\mathbf{\Sigma})^{-1/2}.\left(1 + O(\sigma^3) + \varepsilon(\sigma / r)\right)$$

Mahalanobis D2 distance / test: $\qquad \mu_{\mathbf{x}}^2(\mathrm{y}) = \overrightarrow{\bar{\mathrm{x}}\mathrm{y}}^t .\Sigma_{\mathbf{xx}}^{(-1)}.\overrightarrow{\bar{\mathrm{x}}\mathrm{y}}$

- Any distribution: $\qquad \mathrm{E}\left[\mu_{\mathbf{x}}^2(\mathbf{x})\right] = n$
- Gaussian: $\qquad \mu_{\mathbf{x}}^2(\mathbf{x}) \propto \chi_n^2 + O(\sigma^3) + \varepsilon(\sigma / r)$

[Pennec, JMIV06, NSIP'99]

Gaussian on the circle

Exponential chart: $x = r\theta \in \left]-\pi.r\,;\pi.r\right[$

Gaussian: truncated standard Gaussian

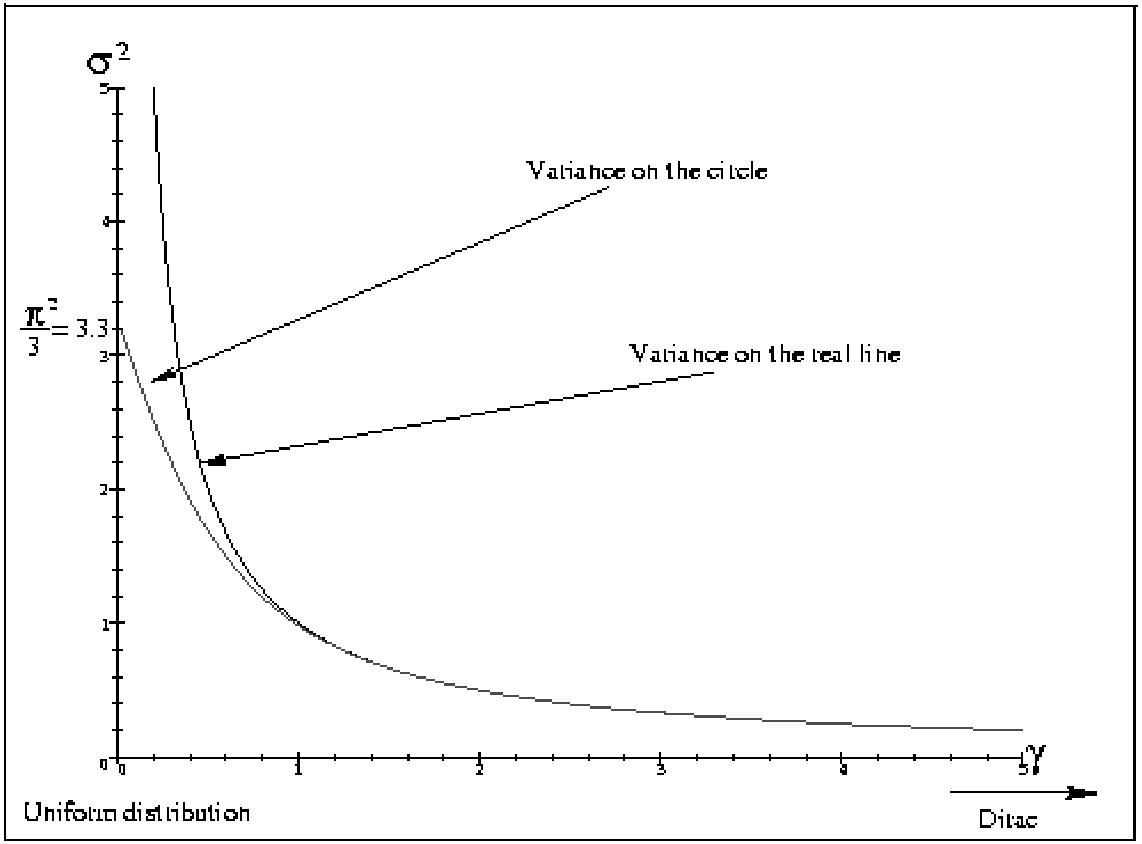

$r \to \infty$: standard Gaussian
(Ricci curvature → 0)

$\gamma \to 0$: uniform pdf with

$$\sigma^2 = (\pi.r)^2 / 3$$

(compact manifolds)

$\gamma \to \infty$: Dirac

PCA vs PGA

PCA

- find the subspace that best explains the variance
- → Maximize the squared distance to the mean
- Generative model: Gaussian

PGA (Fletcher, Joshi, Lu, Pizer, MMBIA 2004)

- find a low dimensional sub-manifold generated by geodesic subspaces that best explain measurements
- → Minimize the squared Riemannian distance from the measurements to that sub-manifold (no closed form)
- Generative model:
  - Implicit uniform distribution within the subspace
  - Gaussian distribution in the vertical space

Different models in curved spaces (no Pythagore thm)

Computing on manifolds: a summary

The Riemannian metric easily gives

- Intrinsic measure and probability density functions
- Expectation of a function from M into R (variance, entropy)

Integral or sum in M: minimize an intrinsic functional

- Fréchet / Karcher mean: minimize the variance
- Filtering, convolution: weighted means
- Gaussian distribution: maximize the conditional entropy

The exponential chart corrects for the curvature at the reference point

- Gradient descent: geodesic walking
- Covariance and higher order moments
- Laplace Beltrami for free

[Pennec, NSIP'99, JMIV 2006, Pennec et al, IJCV 66(1) 2006, Arsigny, PhD 2006]

Roadmap

Goals and methods of Computational anatomy

Statistical computing on manifolds

- The mathematical framework
- Example applications on rigid body transformations

A Riemannian framework for tensor computing

Currents: an embedding space for curves and surfaces

Log-Euclidean statistics on image deformations

Conclusion and challenges

Statistical Analysis of the Scoliotic Spine

[J. Boisvert et al. ISBI'06, AMDO'06 and IEEE TMI 27(4), 2008]

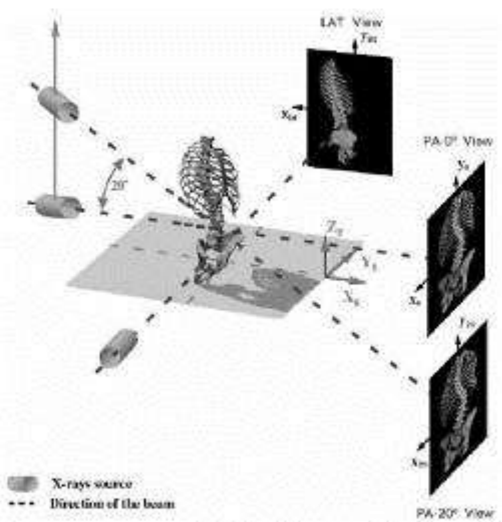

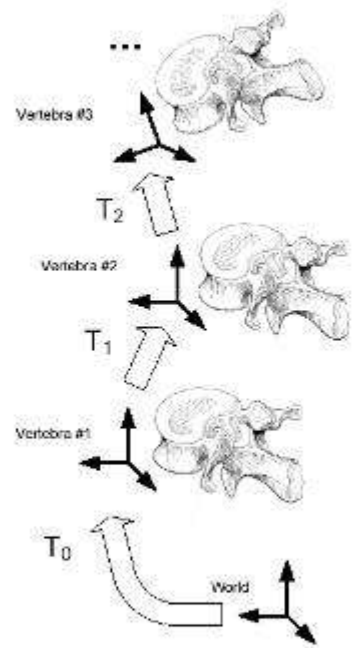

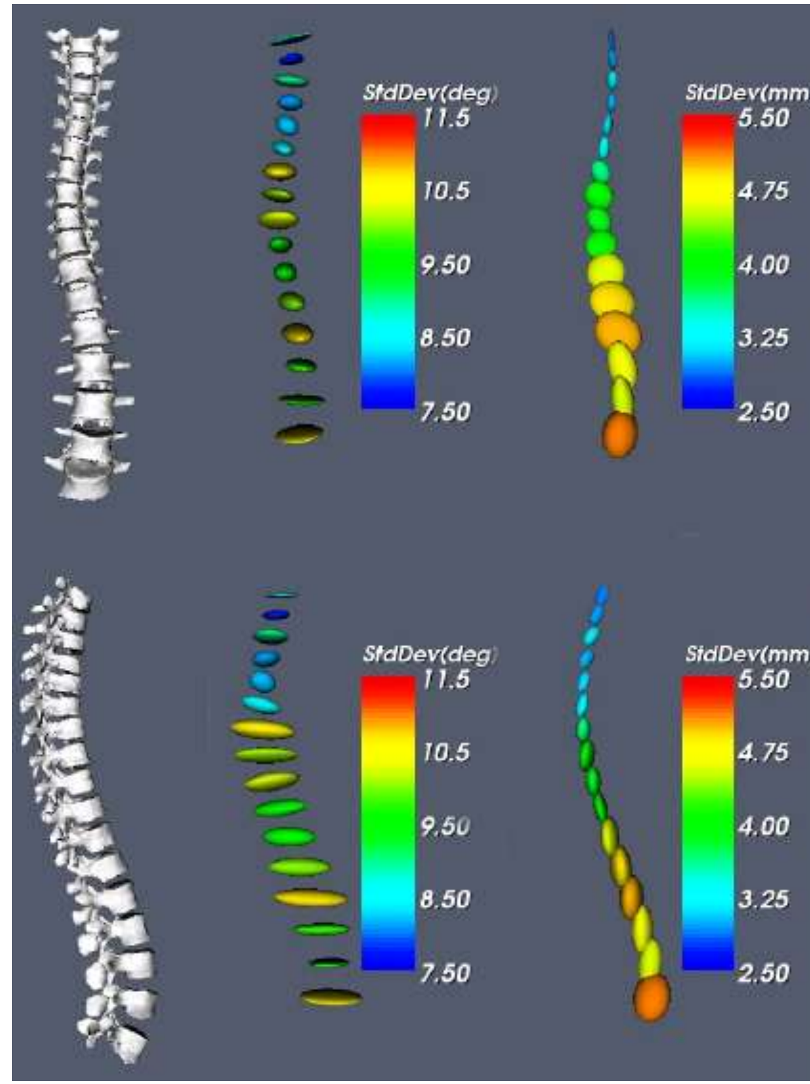

Database

- 307 Scoliotic patients from the Montreal's Sainte-Justine Hospital.
- 3D Geometry from multi-planar X-rays

Mean

- Main translation variability is axial (growth?)
- Main rot. var. around anterior-posterior axis

Statistical Analysis of the Scoliotic Spine

[J. Boisvert et al. ISBI'06, AMDO'06 and IEEE TMI 27(4), 2008]

PCA of the Covariance:
4 first variation modes
have clinical meaning

- Mode 1: King's class I or III
- Mode 2: King's class I, II, III
- Mode 3: King's class IV + V
- Mode 4: King's class V (+II)

Validation of the rigid registration accuracy

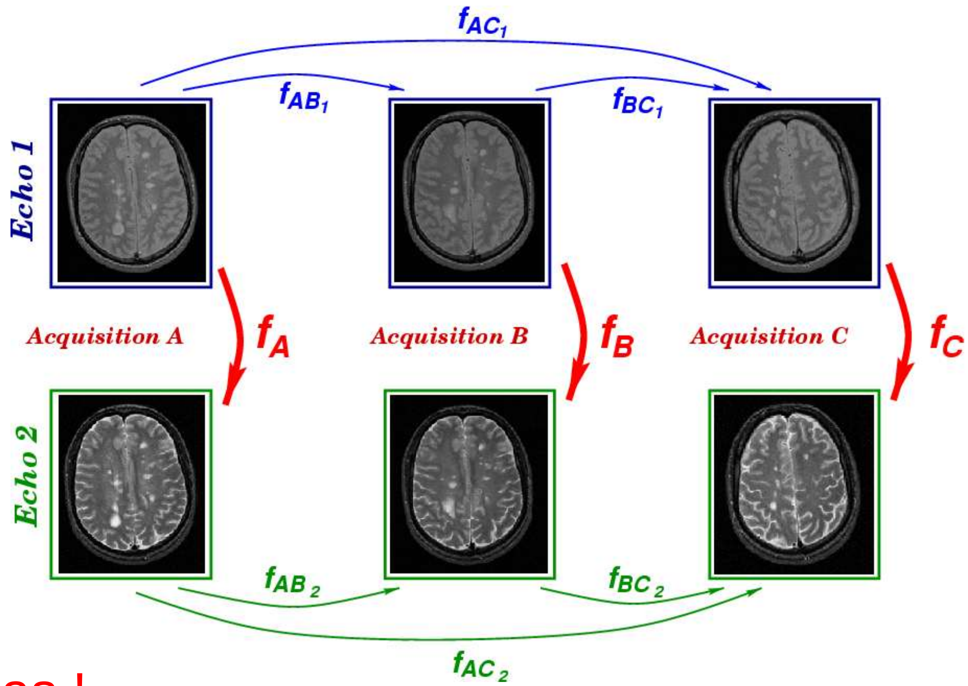

Comparing two transformations and their Covariance matrix :

$$\mu^2(T_1, T_2) \approx \chi_6^2$$

Mean: 6, Var: 12

KS test

Intra-echo: $\mu^2 \approx 6$, KS test OK

Inter-echo: $\mu^2 > 50$, KS test failed, Bias !

Bias estimation: (chemical shift, susceptibility effects)

- $\sigma_{rot} = 0.06 \text{ deg}$ (not significantly different from the identity)
- $\sigma_{trans} = 0.2 \text{ mm}$ (significantly different from the identity)

Inter-echo with bias corrected: $\mu^2 \approx 6$, KS test OK

[X. Pennec et al., Int. J. Comp. Vis. 25(3) 1997, MICCAI 1998]

Validation using Bronze Standard

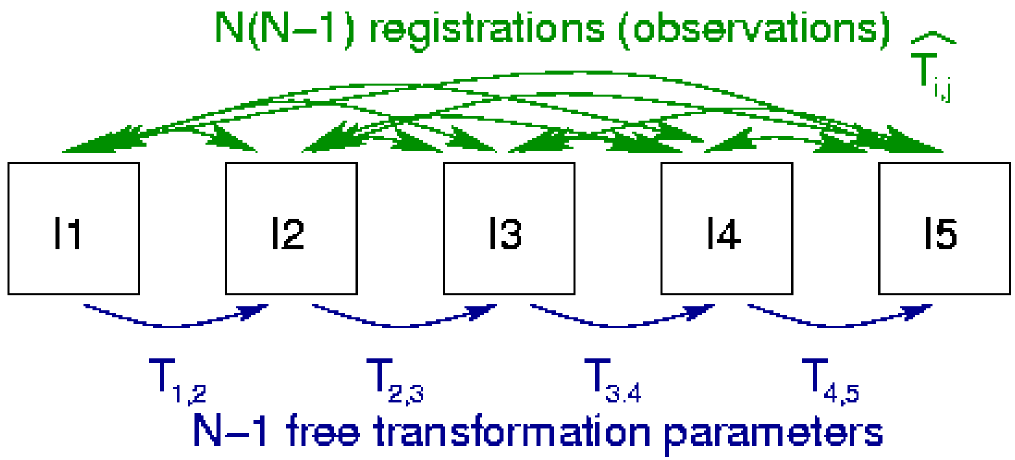

Best explanation of the observations (ML) : $C = \sum_{ij} d^2(T_{ij}, \hat{T}_{ij})$

- LSQ criterion
- Robust Fréchet mean $d^2(T_1, T_2) = \min\left(\mu^2(T_1, T_2), \chi^2\right)$
- Robust initialization and Newton gradient descent

Result $\boxed{T_{i,j}, \sigma_{rot}, \sigma_{trans}}$

[T. Glatard & al, MICCAI 2006, Int. Journal of HPC Apps, 2006]

Derive tests on transformations for accuracy / consistency

Liver puncture guidance using augmented reality

3D (CT) / 2D (Video) registration

- 2D-3D EM-ICP on fiducial markers
- Certified accuracy in real time

Validation

- Bronze standard (no gold-standard)
- Phantom in the operating room (2 mm)
- 10 Patient (passive mode): < 5mm (apnea)

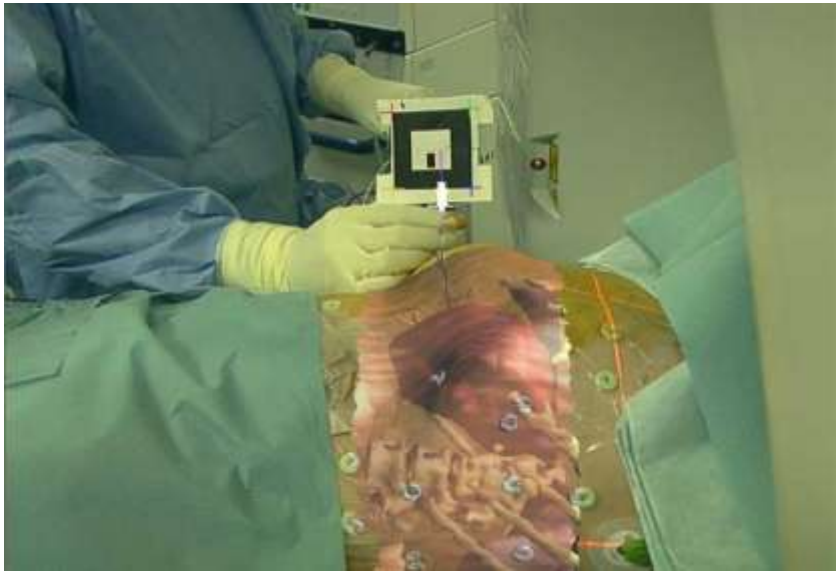

[S. Nicolau, PhD'04 MICCAI05, ECCV04, IS4TM03, Comp. Anim. & Virtual World 2005]

Roadmap

Goals and methods of Computational anatomy

Statistical computing on manifolds

A Riemannian framework for tensor computing

- Tensor image processing
  - Affine-invariant metrics
  - Log-Euclidean and other metrics
- Application
  - Diffusion tensor images (DTI)
  - Morphometry of sulcal lines on the brain

Currents: an embedding space for curves and surfaces

Log-Euclidean statistics on image deformations

Conclusion and challenges

Isotropic/Anisotropic Diffusion

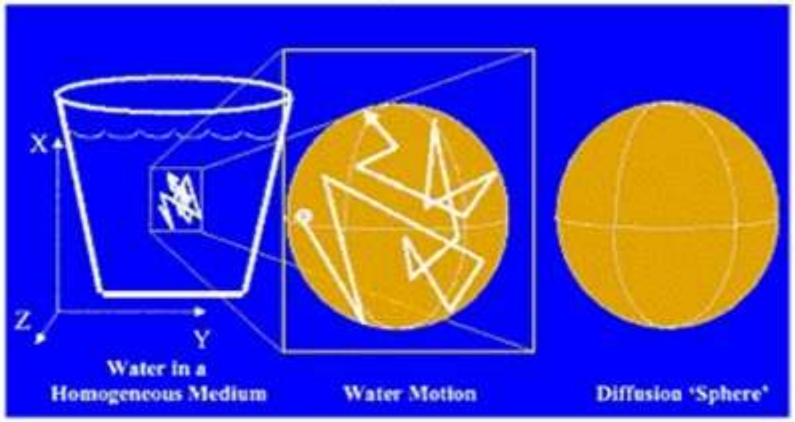

Isotropic diffusion
$(\lambda_1 = \lambda_2 = \lambda_3)$

Anisotropic diffusion
$(\lambda_1 > \lambda_2 > \lambda_3)$

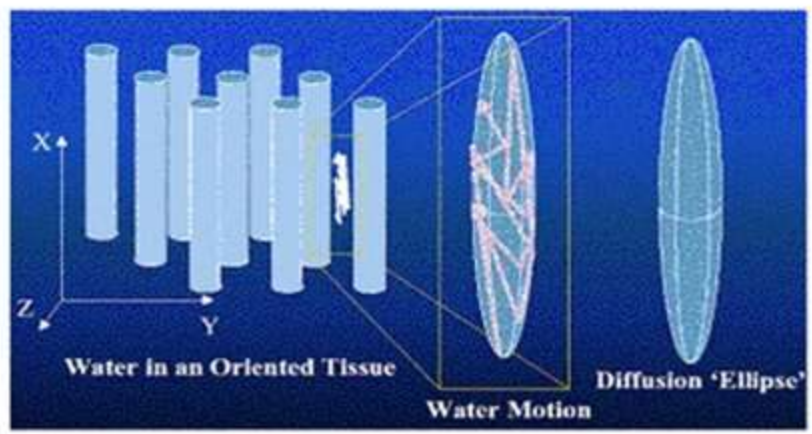

Anatomy of a diffusion MRI

T2 image

+

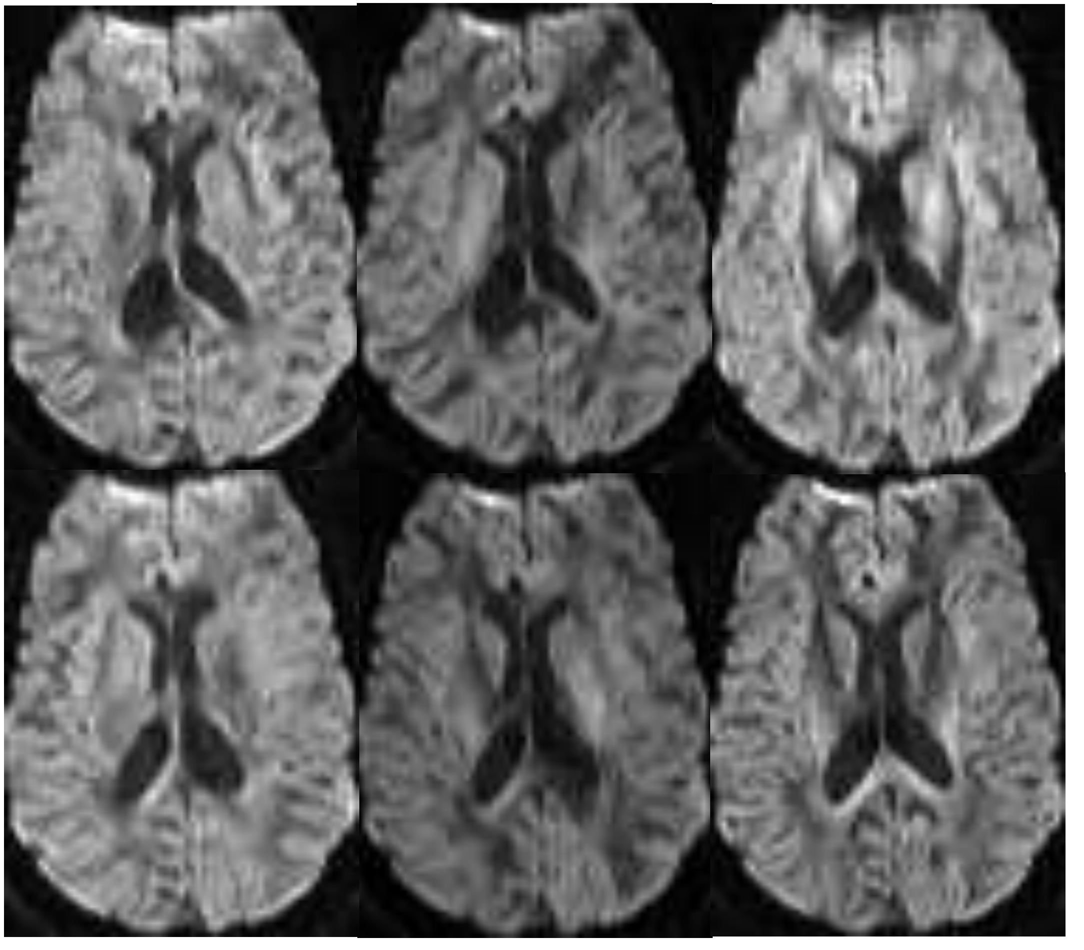

6 diffusion weighted images

Stejskal & Tanner equation

Signal attenuation related to tensor using:

$$S_i = S_0 \exp\left(-b \, \vec{g}_i^T D \, \vec{g}_i\right)$$

- S_i: diffusion weighted images;
- S_0: T2 image;
- g_i: spatial direction of the diffusion gradient;
- b: b-value (related to physical parameters of the acquisition, including field strength and diffusion time);
- D: diffusion tensor;

Reconstruction of the diffusion tensor

- **Tensor : 6 degrees of freedom.**
  - At least 6 images acquired with non collinear gradients.
- **Linearization of the Stejskal & Tanner equation:**

$$log\left(\frac{S_0}{S_i}\right) = b\,\vec{g}_i^T D(x)\,\vec{g}_i$$

- **Least squares estimation:**

$$D(x) = min \sum_{i=1}^{N}\left(\log\left(\frac{S_0}{S_i}\right) - b\,\vec{g}_i^T D(x)\,\vec{g}_i\right)^2$$

- **Other possible methods:**
  - - non-linear equations, m-estimators.

Visualization using ellipsoids

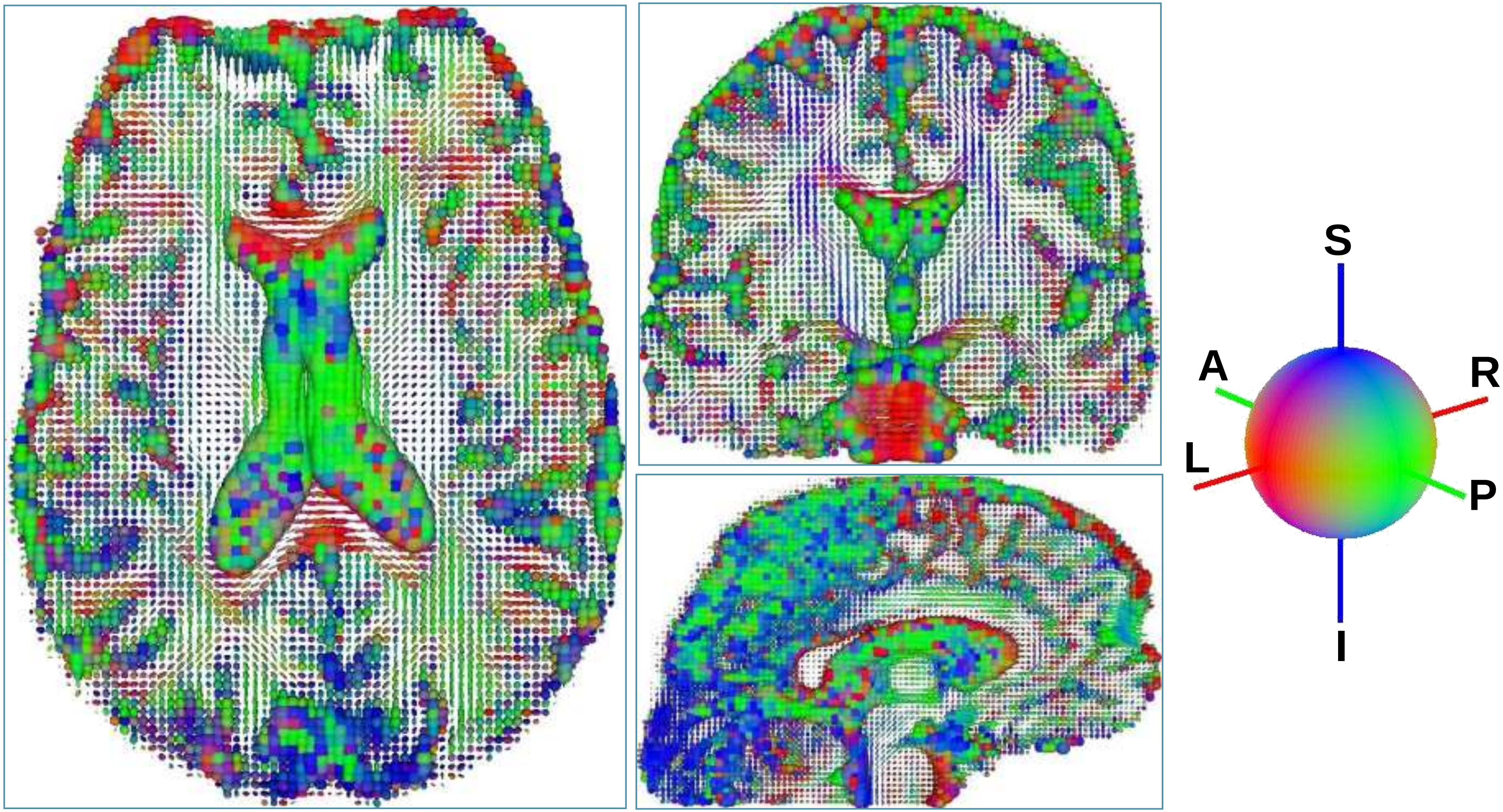

Diffusion Tensor Imaging

Covariance of the Brownian motion of water
-> Architecture of axonal fibers

Very noisy data

- Tensor image processing
  - Robust estimation
  - Filtering, regularization
  - Interpolation / extrapolation
- Information extraction (fibers)

Symmetric positive definite matrices

- Convex operations are stable
  - mean, interpolation
- More complex operations are not
  - PDEs, gradient descent…

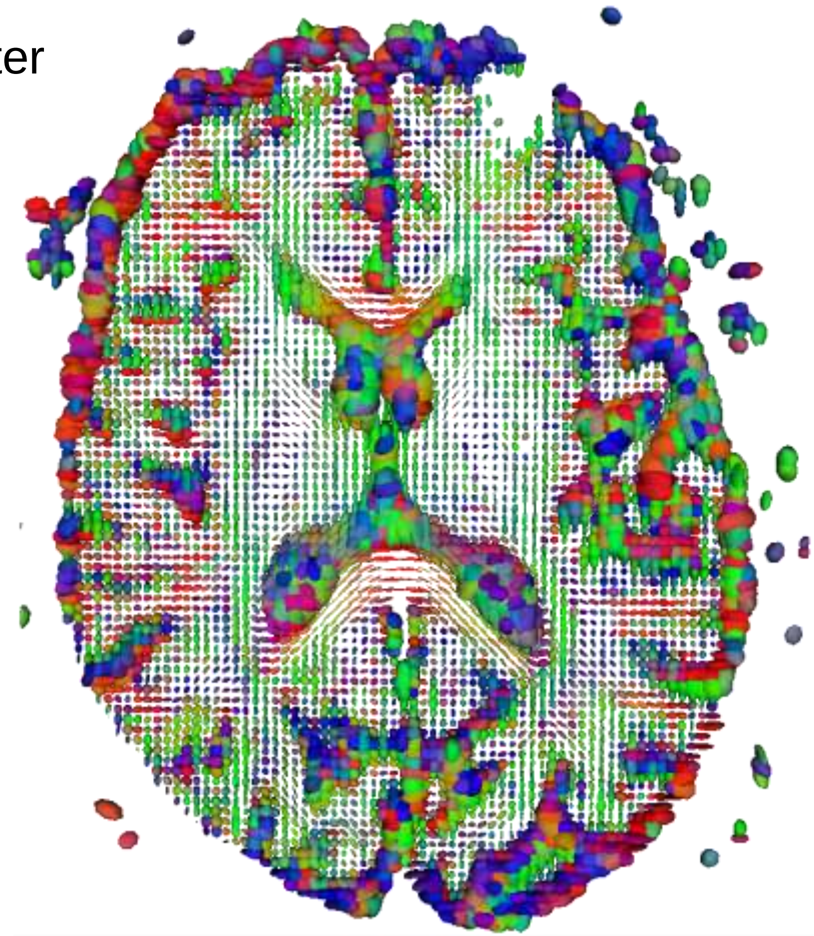

Diffusion Tensor Filed
(slice of a 3D volume)

Intrinsic computing on Manifold-valued images?

Affine Invariant Metrics on Tensors

Action of the Linear Group GL$_n$ $$A * \Sigma = A.\Sigma.A^T$$

Invariant metric $$\langle W_1 \mid W_2 \rangle_\Sigma = \langle A W_1 A^t \mid A W_2 A^t \rangle_{A\Sigma A^t} \overset{def}{=} \langle \Sigma^{-1/2} * W_1, \Sigma^{-1/2} * W_2 \rangle_{Id}$$

- Isotropy group at the identity: Rotations
- All rotationally invariant scalar products:

$$\langle W_1 \mid W_2 \rangle_{Id} \overset{def}{=} \mathrm{Tr}\left(W_1^T W_2\right) + \beta\, \mathrm{Tr}(W_1).\mathrm{Tr}(W_2) \quad (\beta > \text{-}1/\mathrm{n})$$

- Geodesics at Id $\Gamma_{Id,W}(t) = \exp(tW)$
- Exponential map $Exp_\Sigma(\overrightarrow{\Sigma\Psi}) = \Sigma^{1/2} \exp(\Sigma^{-1/2}.\overrightarrow{\Sigma\Psi}.\Sigma^{-1/2})\Sigma^{1/2}$
- Log map $\overrightarrow{\Sigma\Psi} = Log_\Sigma(\Psi) = \Sigma^{1/2} \log(\Sigma^{-1/2}.\Psi.\Sigma^{-1/2})\Sigma^{1/2}$
- Distance $\boxed{dist(\Sigma, \Psi)^2 = \langle \overrightarrow{\Sigma\Psi} \mid \overrightarrow{\Sigma\Psi} \rangle_\Sigma = \left\| \log(\Sigma^{-1/2}.\Psi.\Sigma^{-1/2}) \right\|_{Id}^2}$

[Pennec, Fillard, Ayache, IJCV 66(1), 2006, Lenglet JMIV'06, etc]

Affine Invariant Metrics on Tensors

$$\|W\|_{\Sigma}^{2} = \mathrm{Tr}\left(W.\Sigma^{-1}W\Sigma^{-1}\right) + \beta\,\mathrm{Tr}\left(W\Sigma^{-1}\right)^{2} \quad (\beta > \text{-}1/\mathrm{n})$$

Space of Gaussian distributions (β=0)

- Fisher information metric [Burbea & Rao J. Multivar Anal 12 1982, Skovgaard Scand J. Stat 11 1984, Calvo & Oller Stat & Dec. 9 1991]
- DTI segmentation [Lenglet RR04 & JMIV 25(3) 2006]

DTI processing (β=0)

- [Pennec, Fillard, Ayache, IJCV 66(1), Jan 2006 / INRIA RR-5255, 2004]
- PGA on tensors [Fletcher & Joshi CVMIA04, SigPro 87(2) 2007]

Geometric means (β=0)

- Covariance matrices in computer vision [Forstner TechReport 1999]
- Math. properties [Moakher SIAM J. Matrix Anal App 26(3) 2004]
- Geodesic Anisotropy [Batchelor MRM 53 2005]

Homogeneous Embedding (β=-1/(n+1))

- [Lovric & Min-Oo, J. Multivar Anal 74(1), 2000]

Linear vs. Riemannian Interpolation: walking along geodesics

Interpolation of the coefficients:

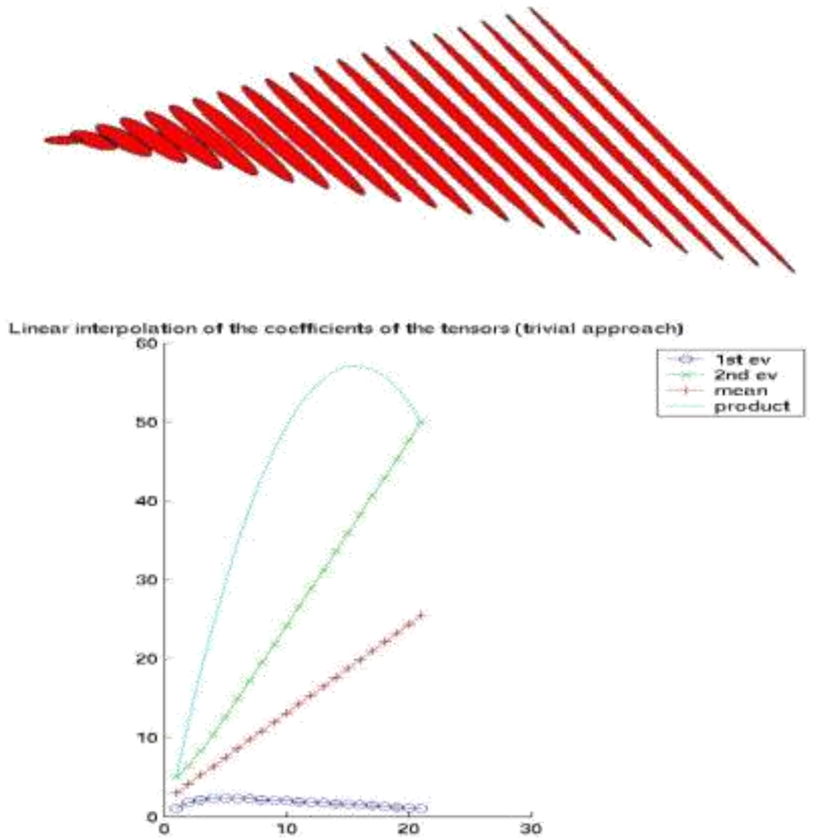

Interpolation along the Riemannian geodesic:

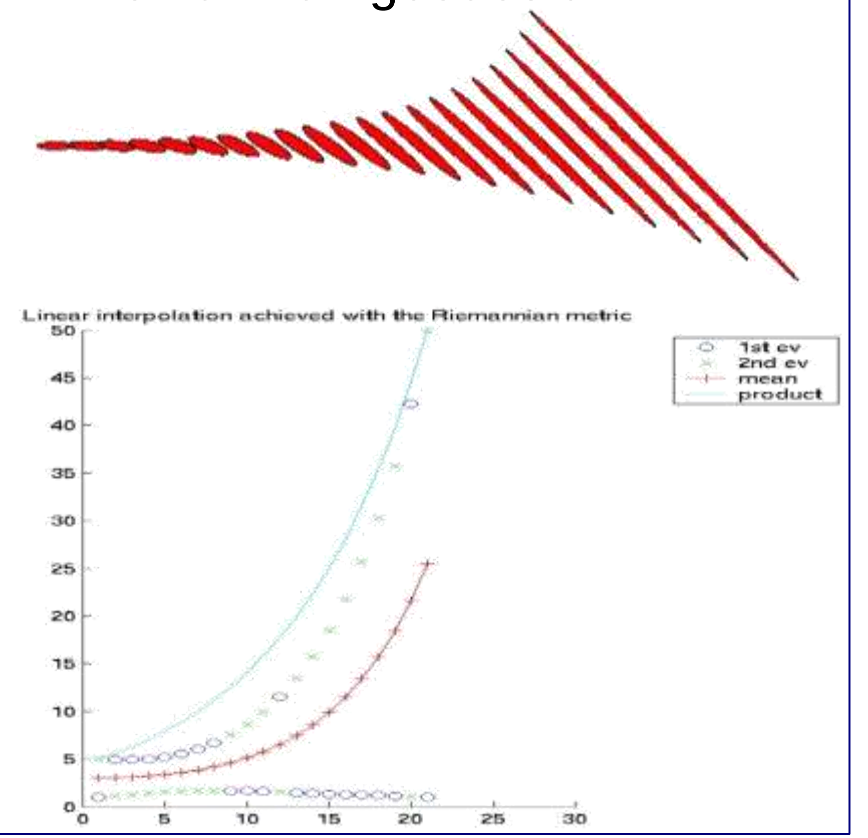

X Pennec,P.Fillard,N.Ayache:Riemannian Tensor Computing, IJCV 66(1), Jan 2006

Tensor interpolation

Geodesic walking in 1D

$$\Sigma(t) = \exp_{\Sigma_1}(t\overrightarrow{\Sigma_1\Sigma_2})$$

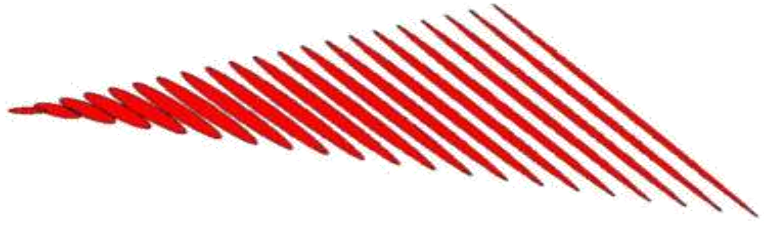

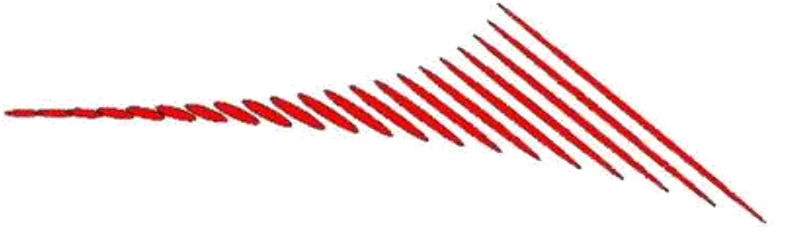

Bi-linear interpolation?

Weighted mean in general

$$\Sigma(x) = \min_{\Sigma} \sum w_i(x) \; dist(\Sigma, \Sigma_i)^2$$

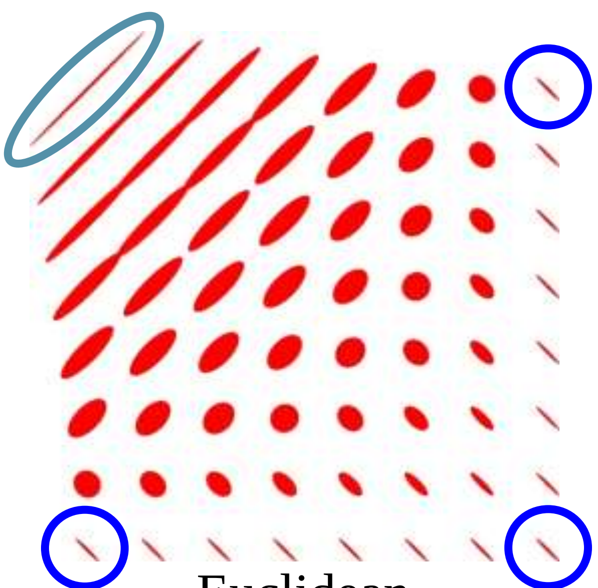

Euclidean

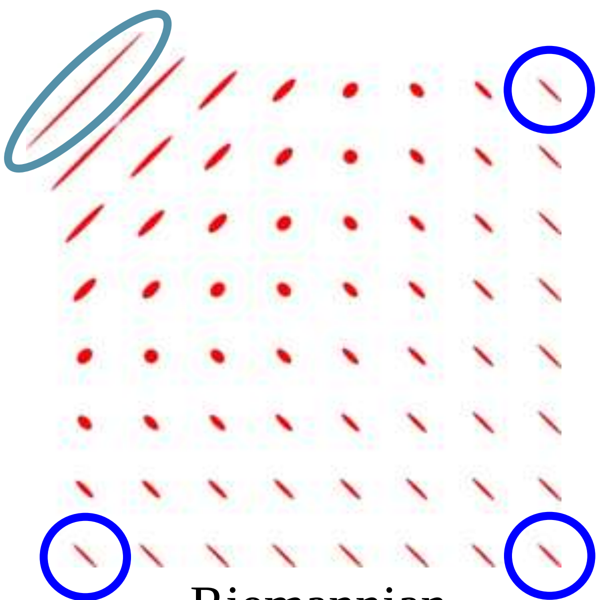

Riemannian

Gaussian filtering: Gaussian weighted mean

$$\Sigma(x) = \min \sum_{i=1}^{n} G_{\sigma}(x - x_i)\ \ dist(\Sigma, \Sigma_i)^2$$

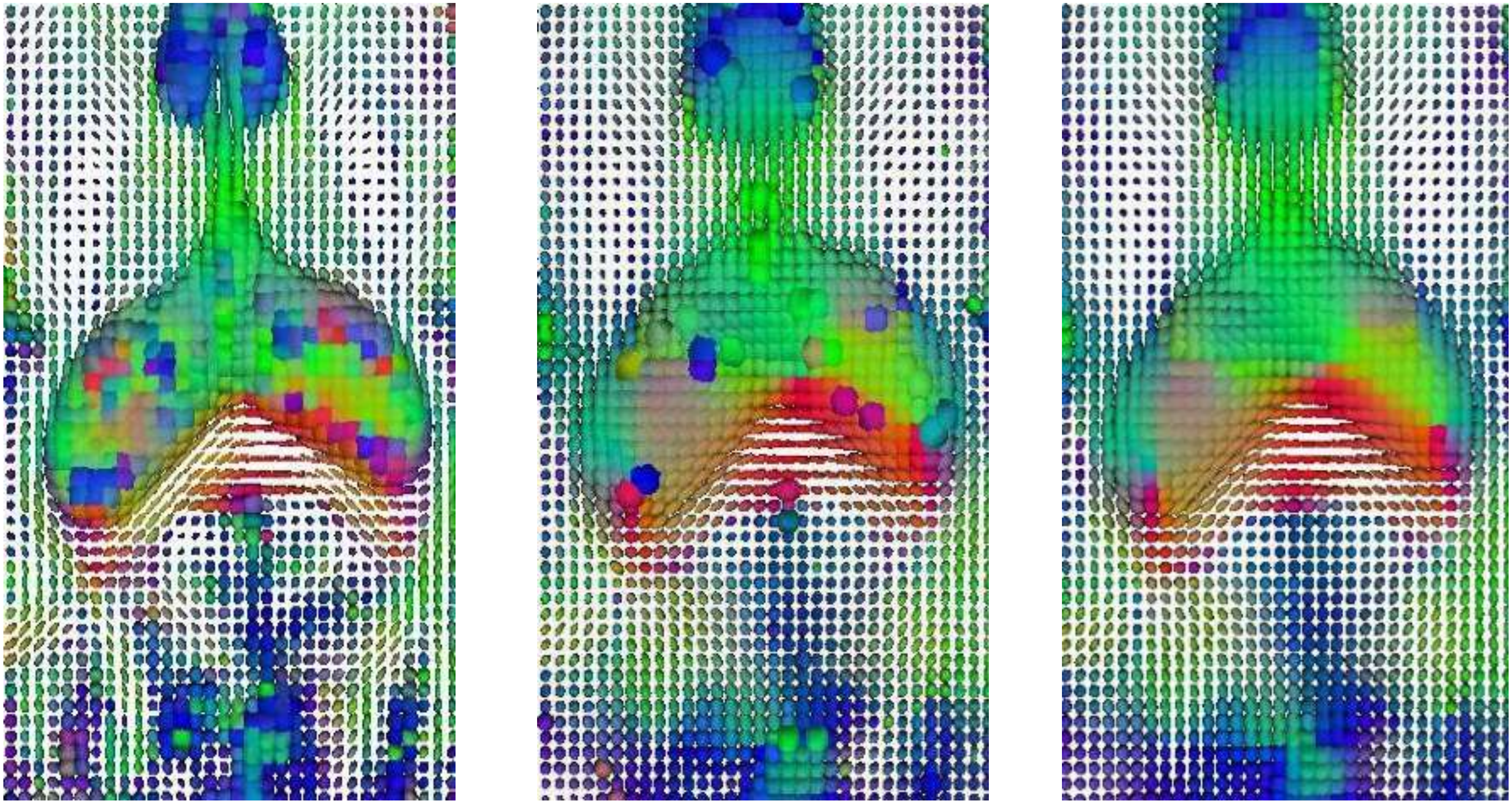

Raw | Coefficients σ=2 | Riemann σ=2

PDE for filtering and diffusion

Harmonic regularization $$C(\Sigma) = \int_{\Omega} \left\| \nabla \Sigma(x) \right\|^2_{\Sigma(x)} dx$$

- Gradient = manifold Laplacian

$$\Delta\Sigma(x) = \sum_i \partial_i^2 \Sigma - \sum_i \left(\partial_i \Sigma\right) \Sigma^{(-1)} \left(\partial_i \Sigma\right) = \sum_u \frac{\overrightarrow{\Sigma(x)\Sigma(x+u)}}{\|u\|^2} + O\left(\|u\|^2\right)$$

- Integration through geodesic marching

$$\Sigma_{t+1}(x) = \exp_{\Sigma_t(x)}\left(-\varepsilon \nabla C(\Sigma)(x)\right)$$

Anisotropic regularization

- Perona-Malik 90 / Gerig 92
- Phi functions formalism [Odyssee / Deriche]

Isotropic vs. Anisotropic Diffusion

$$C(\Sigma) = \int \left\| \nabla \Sigma(x) \right\|_{\Sigma}^{2} dx$$

$$C(\Sigma) = \int \phi\left(\left\| \nabla \Sigma(x) \right\|_{\Sigma} \right) dx$$

$$\phi(x) = \exp(-x^2 / \kappa^2)$$

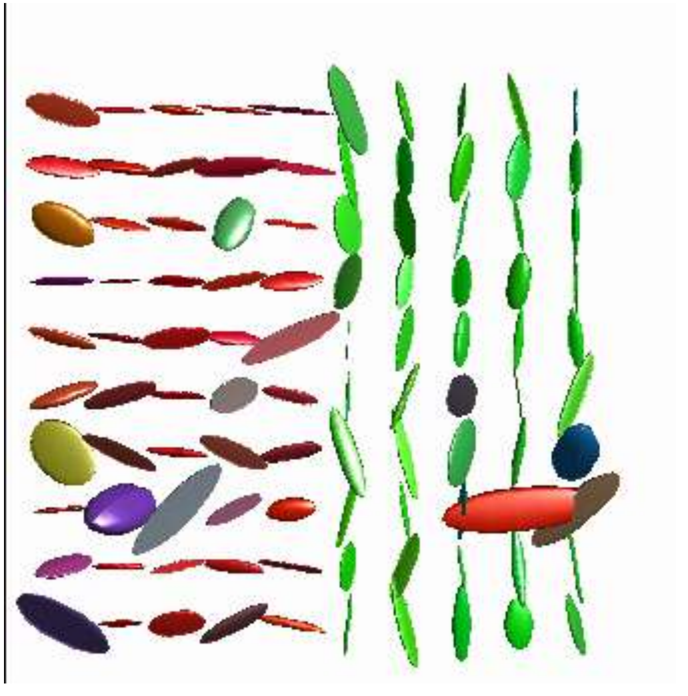

Isotropic

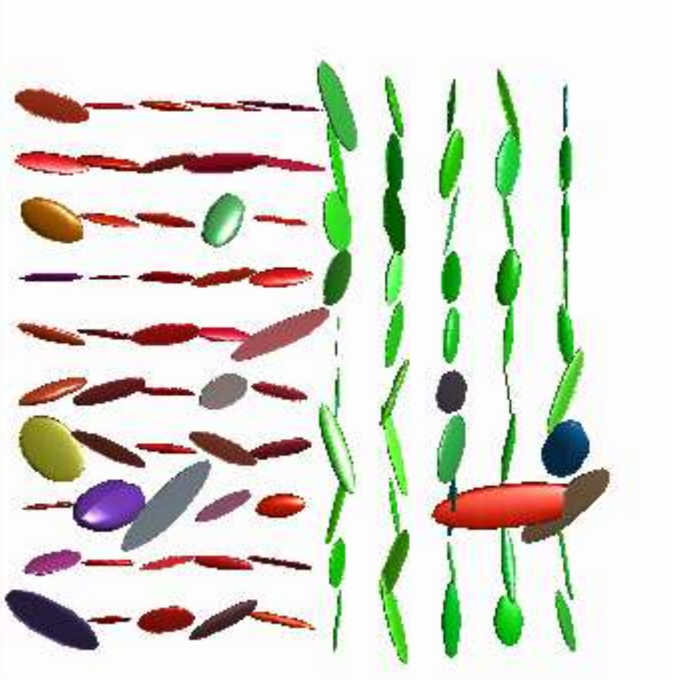

Anisotropic

Anisotropic filtering

$$\hat{\Delta}\Sigma(x) = \sum_u w\left(\left\|\partial_u \Sigma(x)\right\|_{\Sigma(x)}\right) \Delta_u \Sigma(x) \quad \text{with} \quad w(t) = \exp(-t^2/\kappa^2)$$

$$\Delta_u \Sigma(x) = \partial_u^2 \Sigma - (\partial_u \Sigma)\Sigma^{(-1)}(\partial_u \Sigma) \approx \overrightarrow{\Sigma(x)\Sigma(x+u)} / \|u\|^2$$

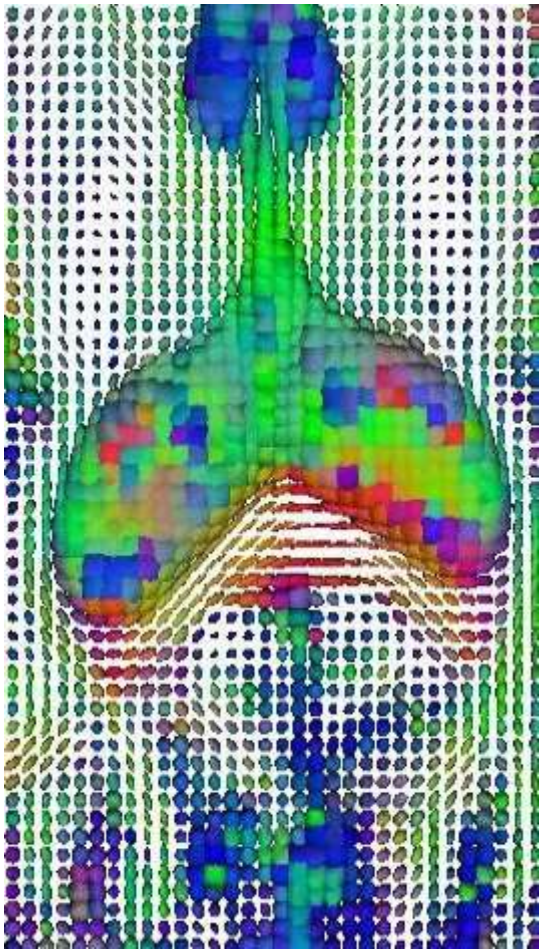

Raw

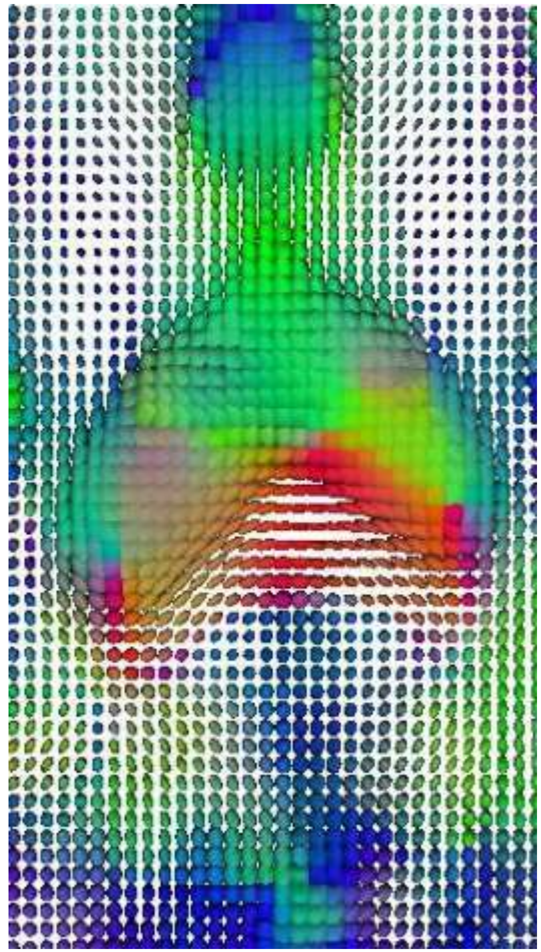

Riemann Gaussian

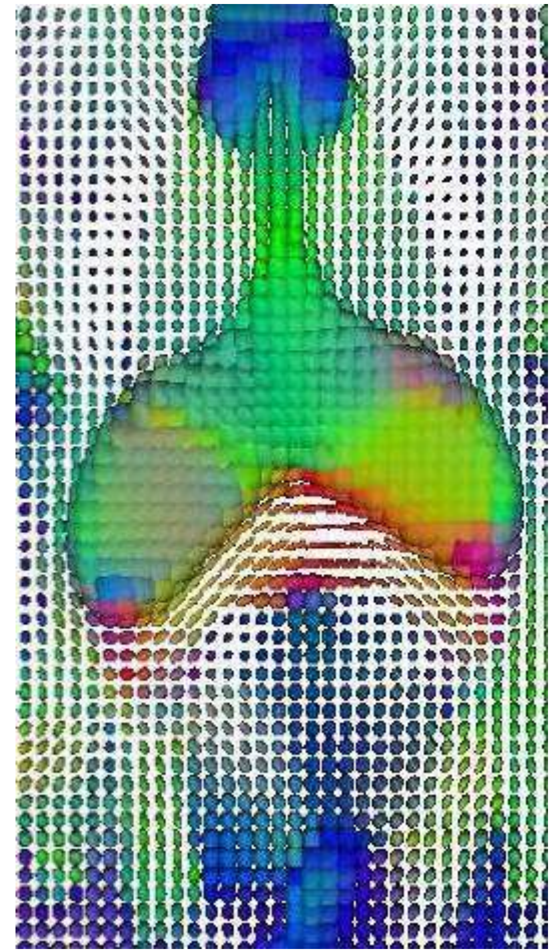

Riemann anisotropic

Extrapolation by Diffusion

$$C(\Sigma) = \frac{1}{2}\int_{\Omega}\sum_{i=1}^{n} G_{\sigma}(x - x_i)\, dist(\Sigma(x), \Sigma_i)^2\, dx + \frac{\lambda}{2}\int_{\Omega} \left\| \nabla \Sigma(x) \right\|^2_{\Sigma(x)}$$

$$\nabla C(\Sigma)(x) = -\sum_{i=1}^{n} G_{\sigma}(x - x_i)\overrightarrow{\Sigma(x)\Sigma_i} - \lambda(\Delta\Sigma)(x)$$

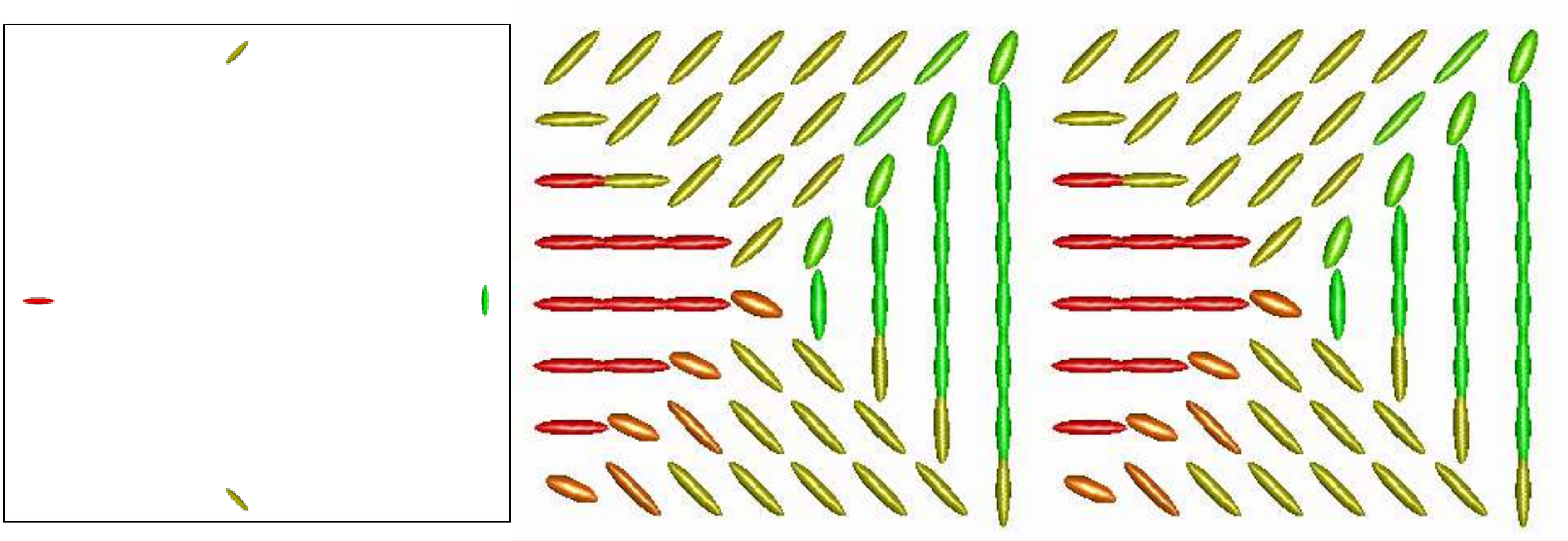

Original tensors | Diffusion λ=0.01 | Diffusion λ=∞

Roadmap

Goals and methods of Computational anatomy

Statistical computing on manifolds

A Riemannian framework for tensor computing

- Tensor image processing
  - Affine-invariant metrics
  - Log-Euclidean and other metrics
- Applications
  - Diffusion tensor images (DTI)
  - Morphometry of sulcal lines on the brain

Currents: an embedding space for curves and surfaces

Log-Euclidean statistics on image deformations

Conclusion and challenges

Log Euclidean Metric on Tensors

Exp/Log: global diffeomorphism Tensors/sym. matrices

- Vector space structure carried from the tangent space to the manifold
  - Log. product $$\Sigma_1 \otimes \Sigma_2 \equiv \exp\left(\log(\Sigma_1) + \log(\Sigma_2)\right)$$
  - Log scalar product $$\alpha \bullet \Sigma \equiv \exp\left(\alpha \log(\Sigma)\right) = \Sigma^{\alpha}$$
  - Bi-invariant metric $$\boxed{dist(\Sigma_1, \Sigma_2)^2 \equiv \left\| \log(\Sigma_1) - \log(\Sigma_2) \right\|^2}$$

Properties

- Invariance by the action of similarity transformations only
- Very simple algorithmic framework

[Arsigny, Fillard, Pennec, Ayache, MICCAI 2005, T1, p.115-122]

Riemannian Frameworks on tensors

Affine-invariant Metric (Curved space – Hadamard)

- Dot product $\langle V \mid W \rangle_\Sigma = \langle AVA^T \mid AWA^T \rangle_{A\Sigma A^T} = \langle \Sigma^{-1/2} V \Sigma^{-1/2} \mid \Sigma^{-1/2} W \Sigma^{-1/2} \rangle_{Id}$
- Geodesics $Exp_\Sigma(\overrightarrow{\Sigma\Psi}) = \Sigma^{1/2} \exp(\Sigma^{-1/2}.\overrightarrow{\Sigma\Psi}.\Sigma^{-1/2})\Sigma^{1/2}$
- Distance $\boxed{\mathrm{dist}(\Sigma,\Psi)^2 = \langle \overrightarrow{\Sigma\Psi} \mid \overrightarrow{\Sigma\Psi} \rangle_\Sigma = \left\| \log(\Sigma^{-1/2}.\Psi.\Sigma^{-1/2}) \right\|_{L_2}^2}$

[Pennec, Fillard, Ayache, IJCV 66(1), 2006, Lenglet JMIV'06, etc]

Log-Euclidean similarity invariant metric (vector space)

- Transport Euclidean structure through matrix exponential
- Dot product $\langle V \mid W \rangle_\Sigma = \langle \partial_V \log(\Sigma) \mid \partial_W \log(\Sigma) \rangle_{Id}$
- Geodesics $Exp_\Sigma(\overrightarrow{\Sigma\Psi}) = \exp(\log(\Sigma) + \partial_{\overrightarrow{\Sigma\Psi}} \log(\Sigma))$
- Distance $\boxed{\mathrm{dist}(\Sigma_1,\Sigma_2)^2 \equiv \left\| \log(\Sigma_1) - \log(\Sigma_2) \right\|^2}$

[Arsigny, Pennec, Fillard, Ayache, SIAM'06, MRM'06]

Log Euclidean vs Affine invariant

- Both means are geometric (vs arithmetic for Euclidean)
- Log Euclidean slightly more anisotropic
- Speedup ratio: 7 (aniso. filtering) to >50 (interp.)

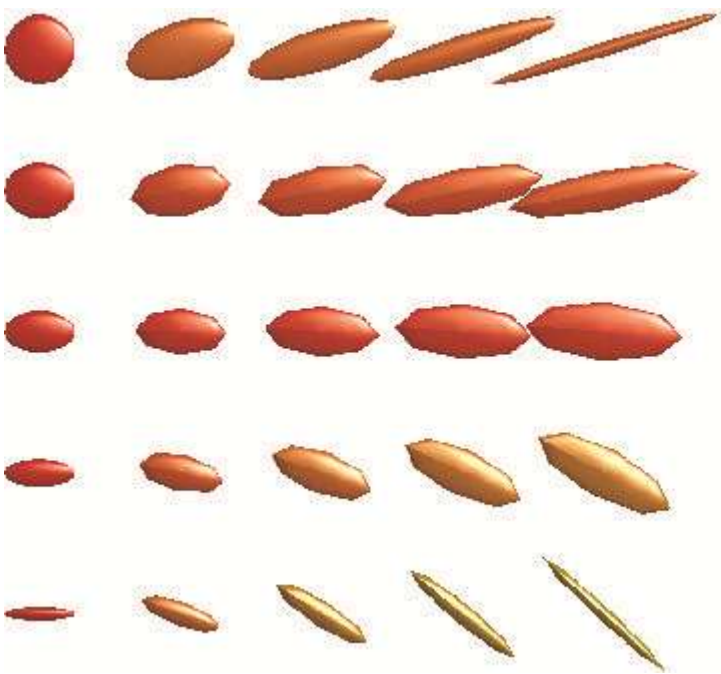

Euclidean

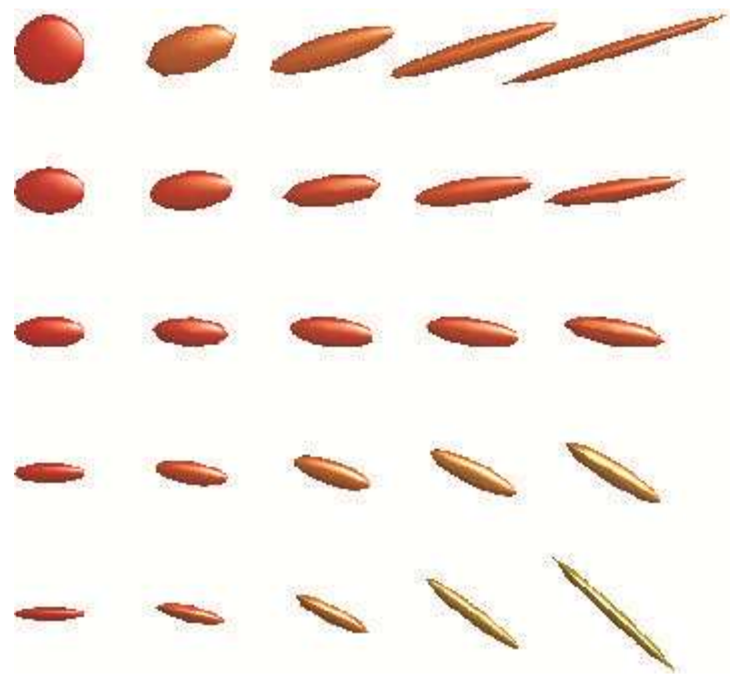

Affine invariant
Log Euclidean

[Arsigny, Fillard, Pennec, Ayache, MICCAI 2005, MRM'06]

Log Euclidean vs Affine invariant

Real DTI images: anisotropic filtering

- Both means are geometric (vs arithmetic for Euclidean)
- Log Euclidean slightly more anisotropic
  but the difference is not significant
- Speedup ratio: 7 (aniso. filtering) to >50 (interp.)

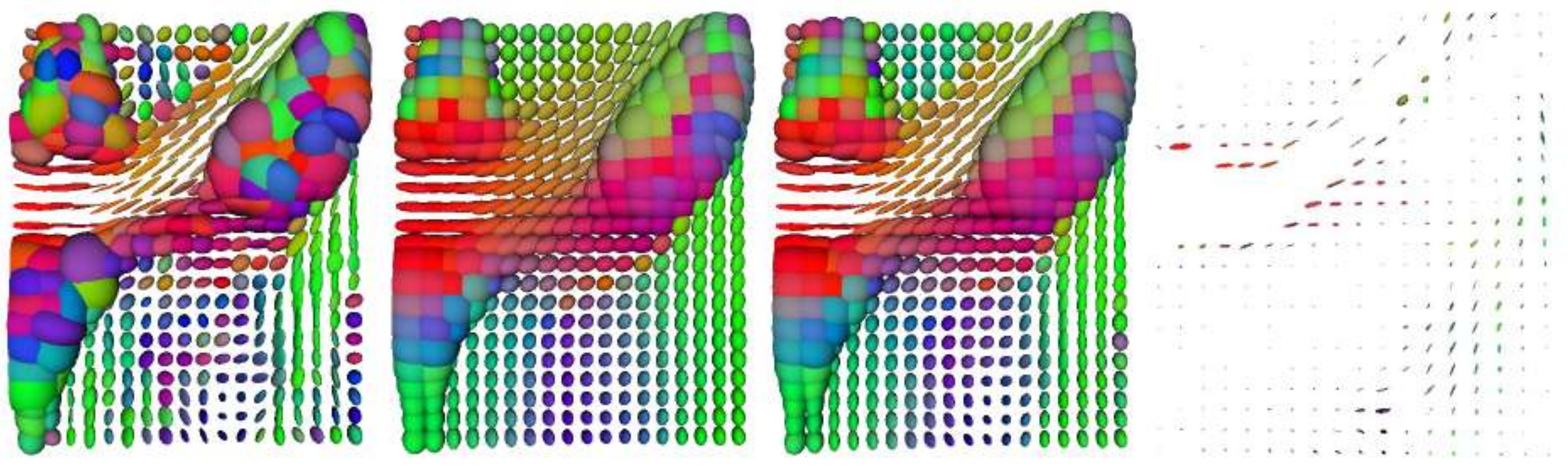

Original Euclidean Log-Euclidean Diff. LE/affine (x100)

[Arsigny, Fillard, Pennec, Ayache, MICCAI 2005, MRM'06]

Comparison of Metrics

	Euclidean	Affine Invariant	Log-Euclidean
Null/Negative eigenvalues	Reachable	Unreachable!	Unreachable!
Invariance	Rotation	Affine transforms	Similarity
Swelling effect	Yes	No	No
Computation load	Low	Important	Low

A metric for all applications?

Structure tensor (guide for diffusion)

$$\Sigma_\sigma(x) = G_\sigma * \left(\nabla I \, \nabla I^t\right)$$

Original

SNR 10% added

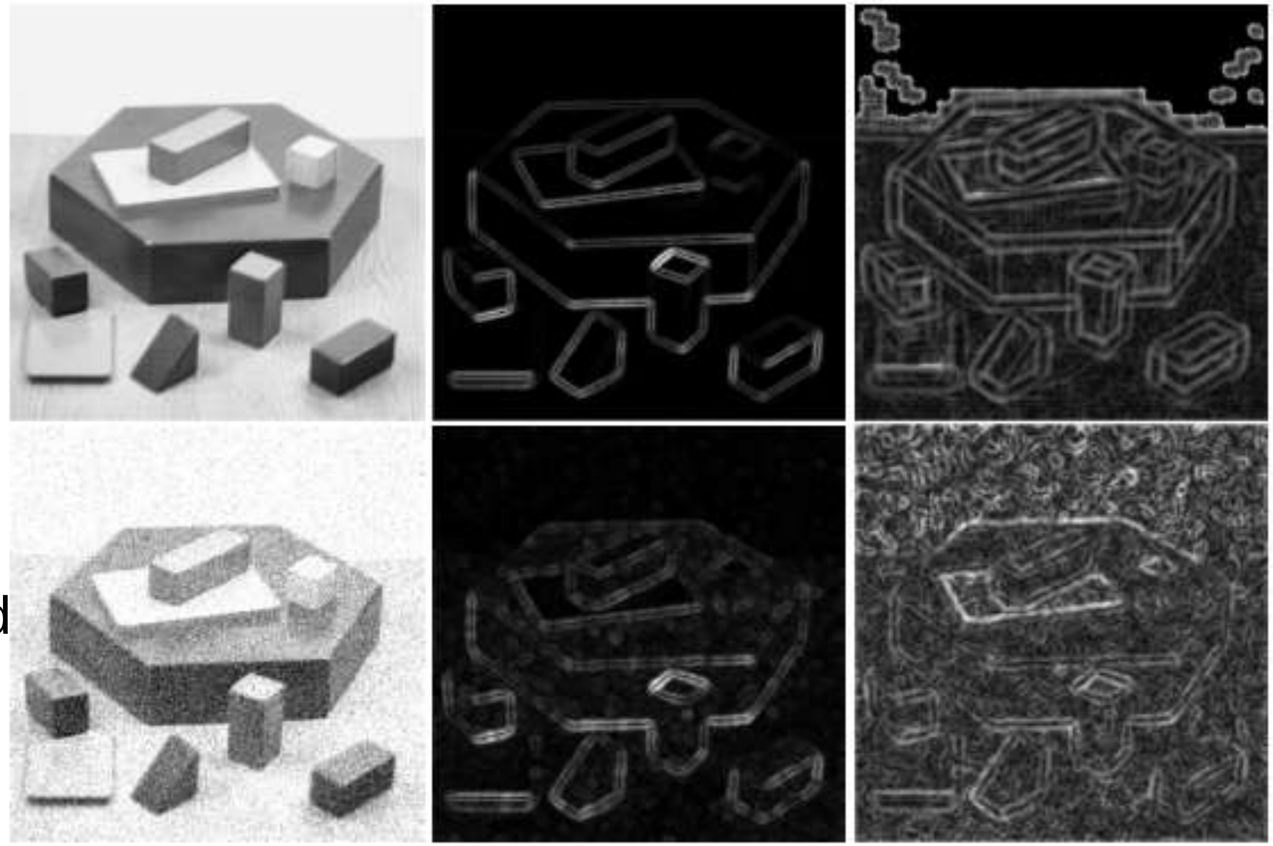

Image Euclidean grad Riemannian grad

A null eigenvalue is physically OK (perfect straight edge)

Need to change the metric?

[Fillard, Arsigny, Ayache, Pennec, DSSCV'05]

Geodesic shooting in tensors spaces

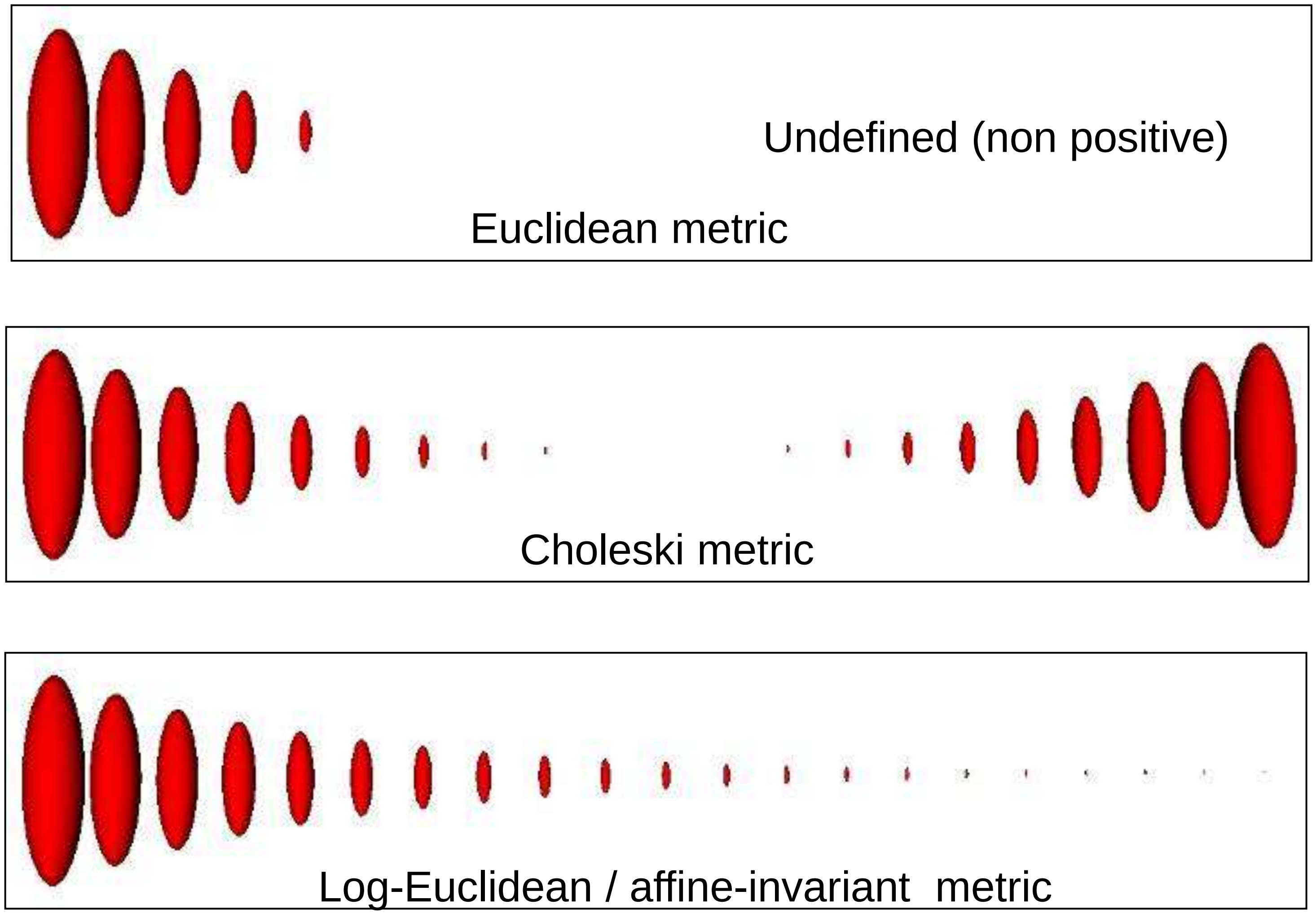

Some metrics on tensors

Log-Euclidean

- [Arsigny, MICCAI 2005 & MRM 56(2), 2006]

Square root metrics

- Cholesky [Wang Vemuri et al, IPMI'03, TMI 23(8) 2004.]
- Size and shape space [Dryden, Koloydenko & Zhou, 2008]
- Power Euclidean [Dryden & Pennec, unpublished]

Non Riemannian distances

- J-Divergence [Wang & Vemuri, TMI 24(10), 2005]
- Geodesic Loxodromes [Kindlmann et al. MICCAI 2007]

4th order tensors

- [Gosh, Descoteau & Deriche MICCAI'08]

Roadmap

Goals and methods of Computational anatomy

Statistical computing on manifolds

A Riemannian framework for tensor computing

- Tensor image processing
  - Affine-invariant metrics
  - Log-Euclidean and other metrics
- Applications
  - Diffusion tensor images (DTI)
  - Morphometry of sulcal lines on the brain

Currents: an embedding space for curves and surfaces

Log-Euclidean statistics on image deformations

Conclusion and challenges

DTI Estimation from DWI

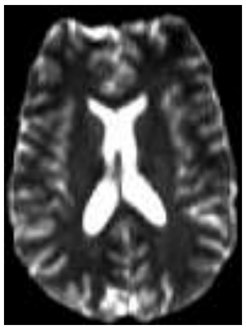

+

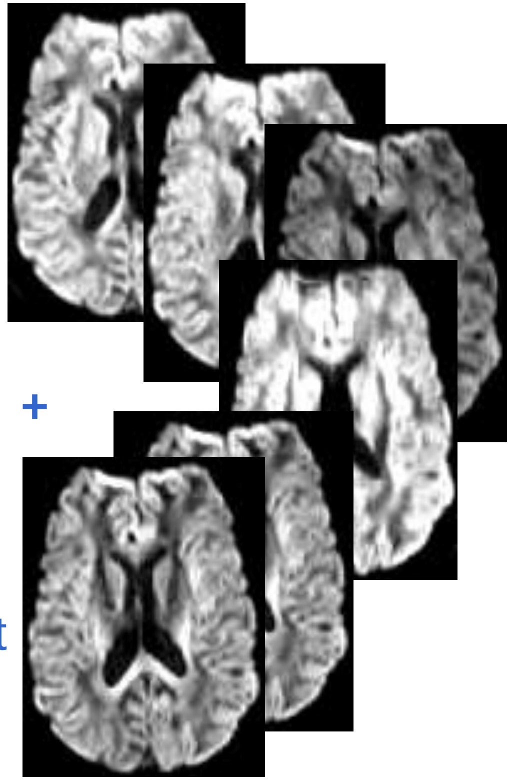

Baseline + at least 6 DWI

Stejskal & Tanner diffusion equation

$$\boxed{S_i = S_0 \exp\left(-b g_i^T D g_i\right)}$$

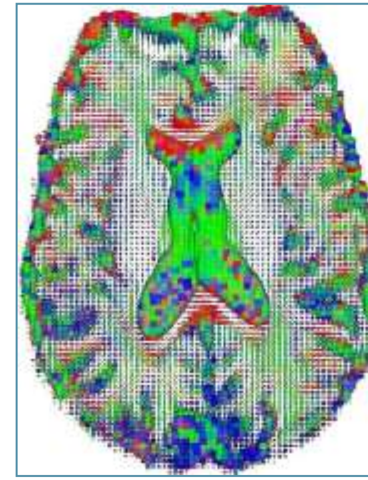

Diffusion Tensor Field

Estimation / Regularization on complex DWI:

- Anisotropic diffusion on Choleski factors [Wang & Vemuri, TMI'04]

Estimation with a Rician noise

- Smoothing DWI before estimation [Basu & Fletcher, MICCAI 2006]
- ML (MMSE) [Aja-Fernández et al, TMI 2008]
- MAP with log-Euclidean prior [Fillard et al., ISBI 2006, TMI 2007]

Noise is Gaussian in complex DW signal

- Rician = amplitude of complex Gaussian
- LSQ on Rician noise = bias for low SNRs [Sijbers, TMI 1998]

MAP Estimation with a Rician Noise Model

Maximum Likelihood estimator for Rician noise:

$$Sim(\Sigma) = -\sum_{i=1}^{N} \log\left(p\left(\hat{S}_i / S_i\right)\right) \qquad p\left(\hat{S}_i / S_i\right) = \frac{\hat{S}_i}{\sigma^2} \exp\left(-\frac{\hat{S}_i^{\,2} + S_i(\Sigma)^2}{2\sigma^2}\right) I_0\left(\frac{S_i(\Sigma)\hat{S}_i}{\sigma^2}\right)$$

Anisotropic Log-Euclidean spatial prior

$$Reg(\Sigma) = \int \Phi\left(\left\|\nabla\Sigma(x)\right\|^2_{\Sigma(x)}\right) dx$$

Gradient descent in Log-Euclidean space

$$E(\Sigma) = \underbrace{Sim(\Sigma)}_{\text{Data fidelity term = ML}} + \lambda \underbrace{Reg(\Sigma)}_{\text{Smoothing term = prior}} \qquad \Sigma_{t+1} = Exp_{\Sigma_t}(-\varepsilon.\nabla E(\Sigma_t))$$

[Fillard, Arsigny, Pennec, Ayache ISBI'06, TMI 26(11) 2007]

Rician MAP estimation with Riemannian spatial prior

$$MAP(\Sigma) = -\sum_{i=1}^{N} \int \log\left(\frac{\hat{S}_i}{\sigma^2} \exp\left(-\frac{\hat{S}_i^{\,2} + S_i(\Sigma)^2}{2\sigma^2} \right) I_0\left(\frac{S_i(\Sigma)\hat{S}_i}{\sigma^2} \right) \right).dx + \int \Phi\left(\left\| \nabla\Sigma(x) \right\|^2_{\Sigma(x)} \right).dx$$

FA

Estimated tensors

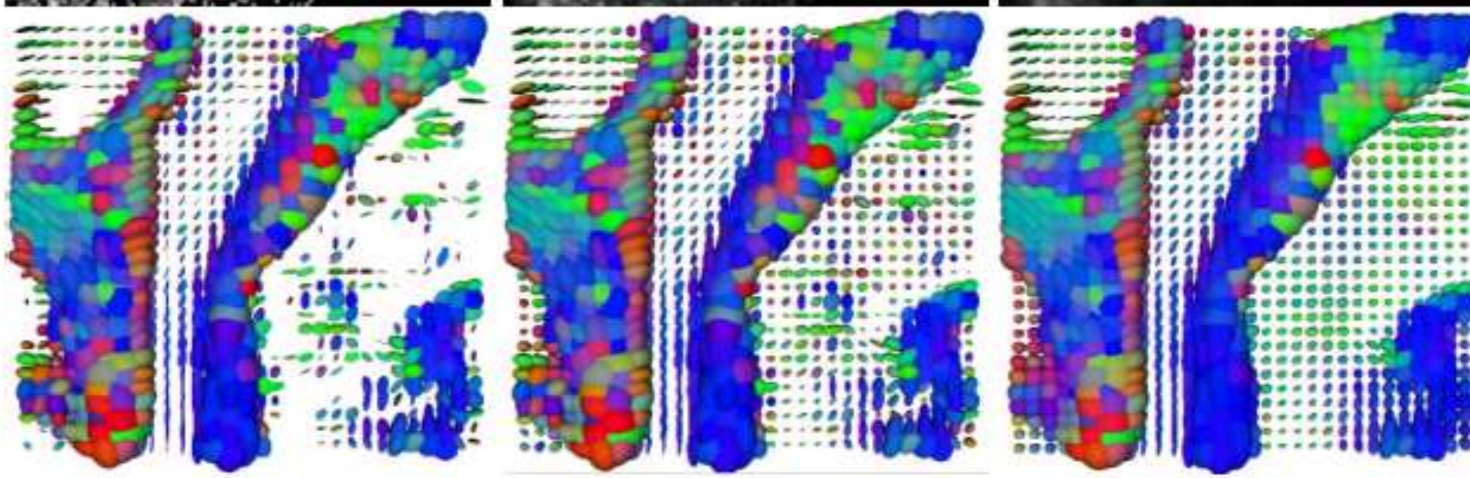

Standard ML Rician MAP Rician

[Fillard, Arsigny, Pennec, Ayache ISBI'06, TMI 26(11) 2007]

Clinical DTI of the spinal cord: fiber tracking

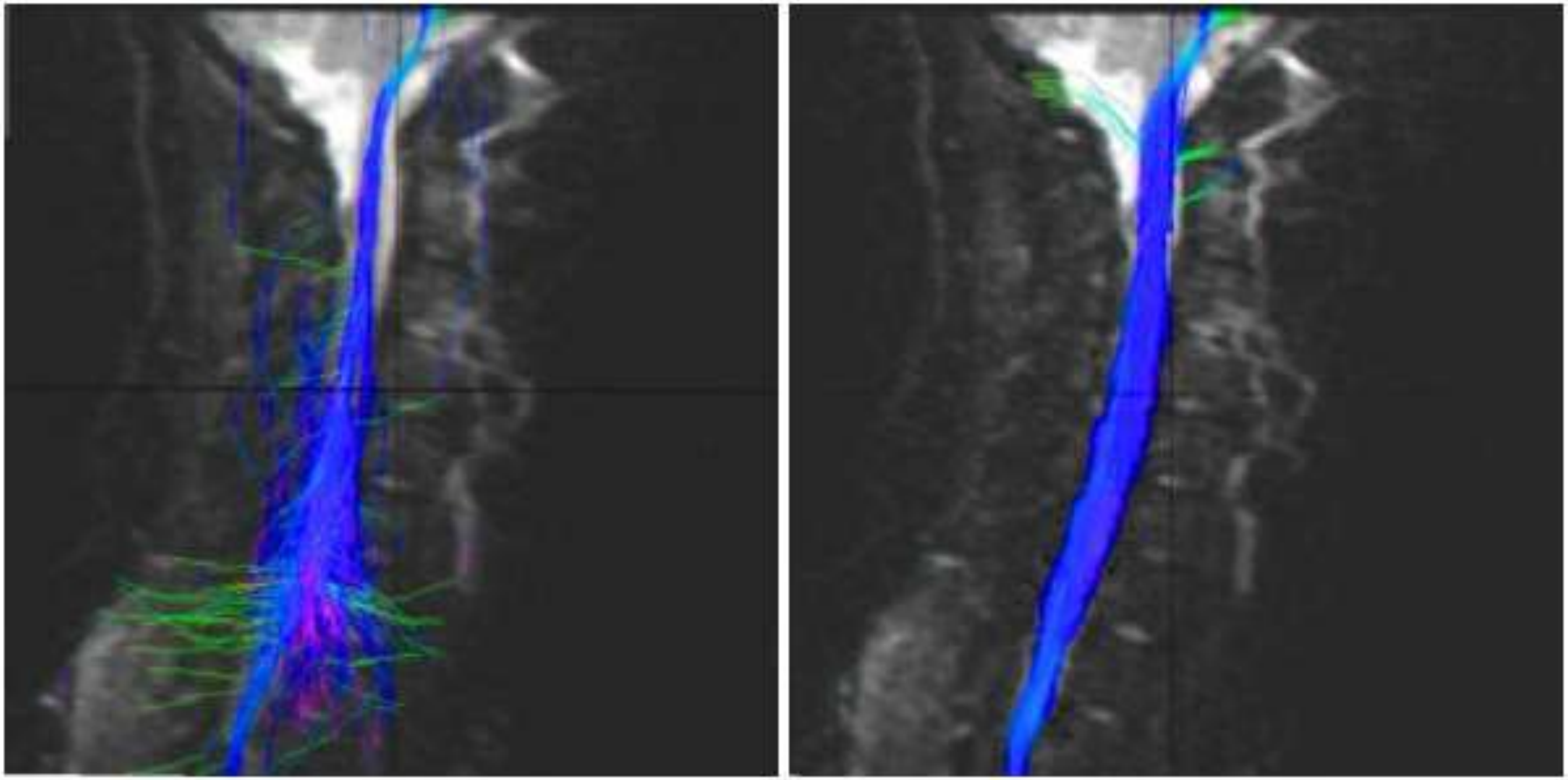

Standard MAP Rician

[Fillard, Arsigny, Pennec, Ayache ISBI'06, TMI 26(11) 2007]

Impact on fibers tracking

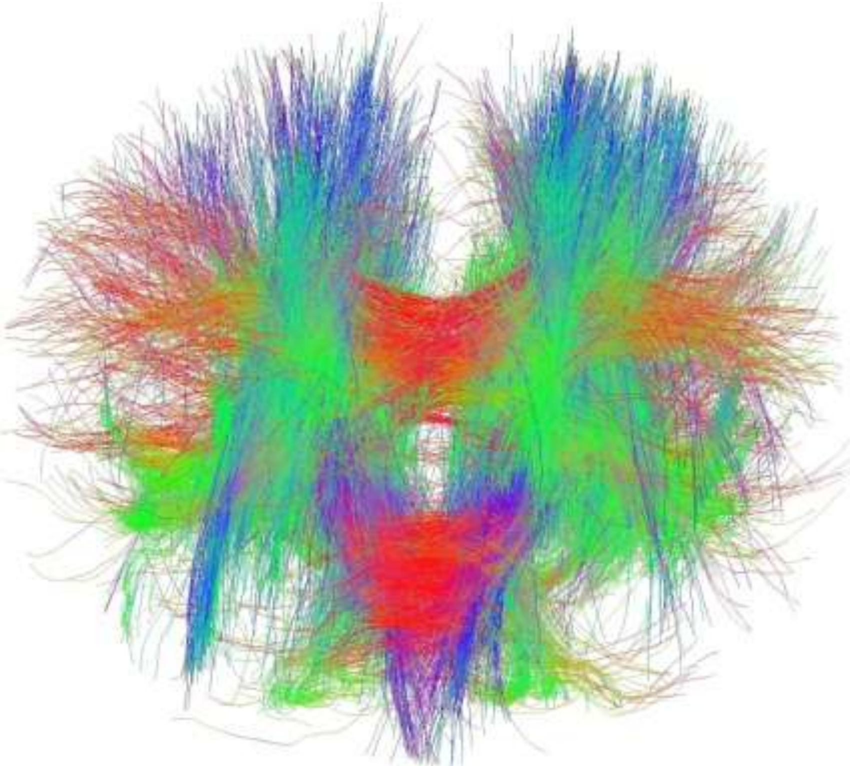

Euclidean interpolation

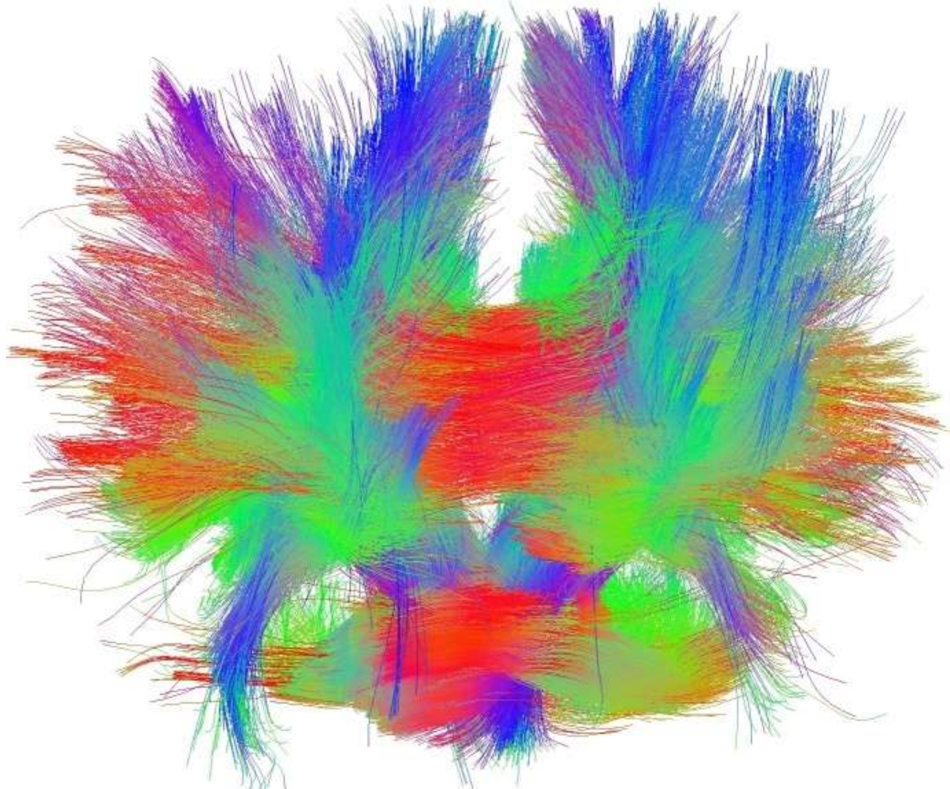

Riemannian interpolation + anisotropic filtering

[Fillard, Toussaint et al, MedINRIA: DTI Processing and Visualization Software, 2006]

From images to anatomy

- Classify fibers into tracts (anatomo-functional architecture)?
- Compare fiber tracts between subjects?

Freeware

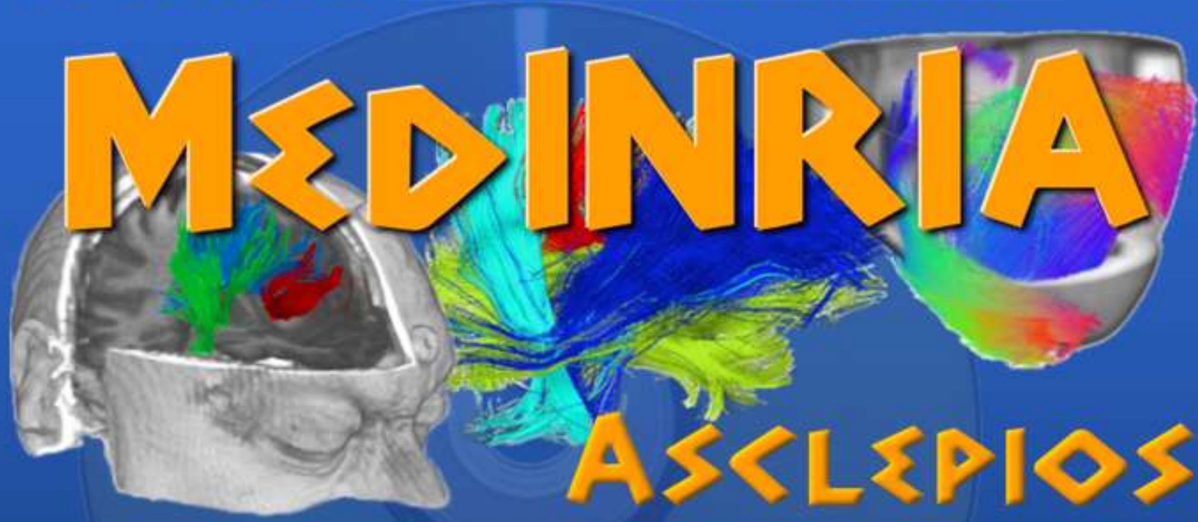

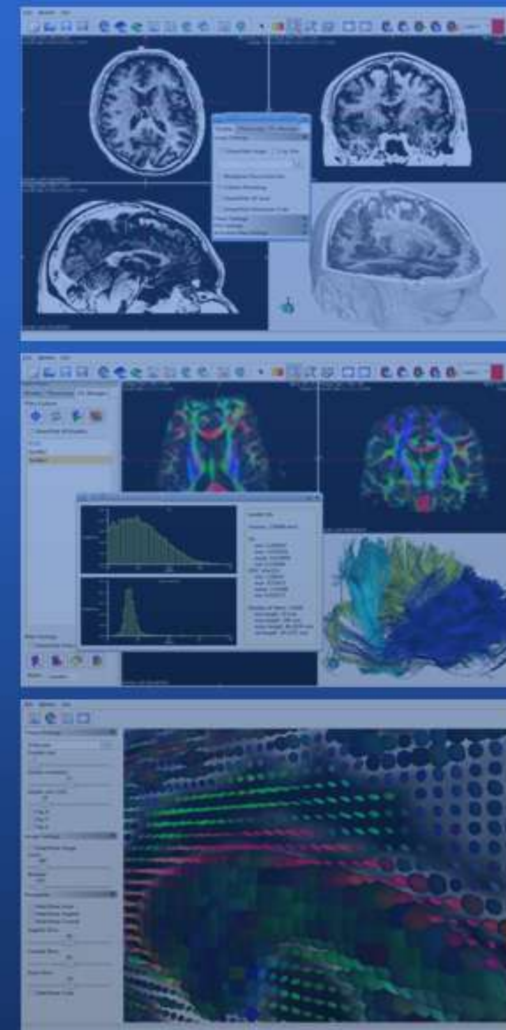

Processing and Visualization of Medical Images:

- Powered by ITK and VTK

DTI Track Module:

- Demonstration of Log-Euclidean* DTI Processing
- Interactive fiber bundling

Diffeomorphic Demons Image and DTI Registration

- Release August 2008 (next month!)

http://www.inria.fr/sophia/asclepios/software/MedINRIA/

*Patent pending

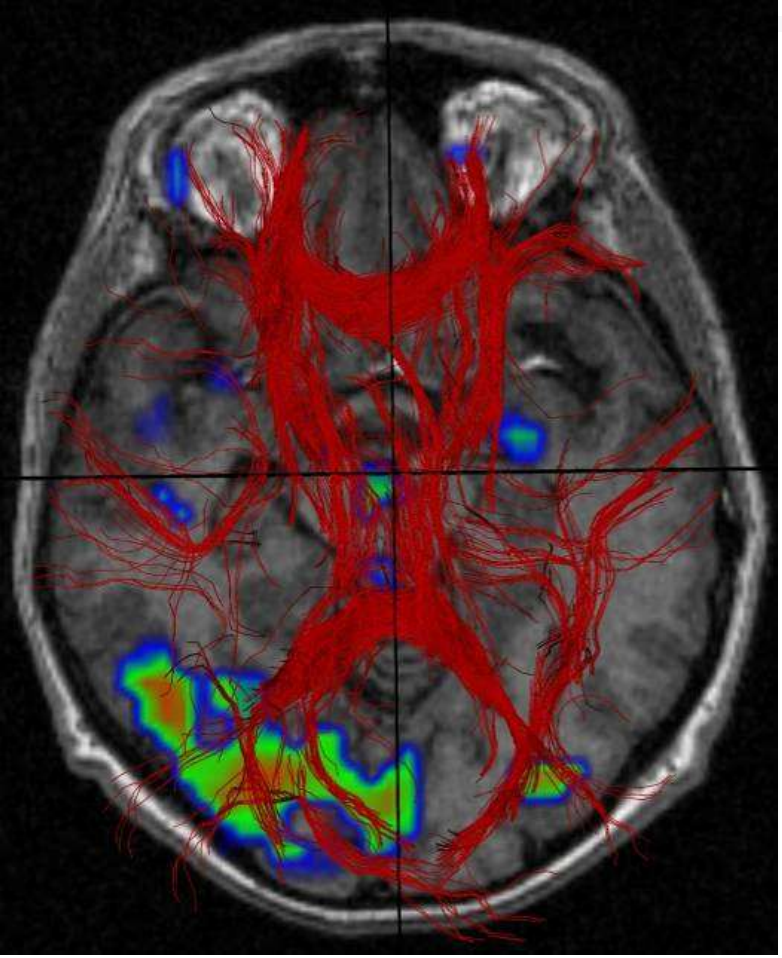

T1 + Activation map + fibers

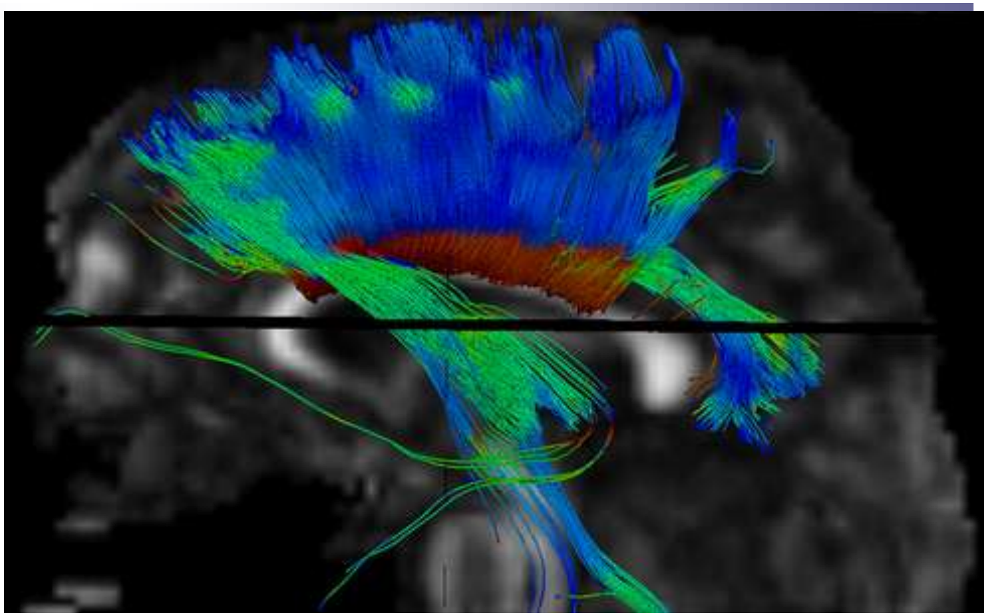

Corpus callosum + cingulum

Courtesy of P. Fillard using MedINRIA

Corticospinal tract and thalamo cortical connections

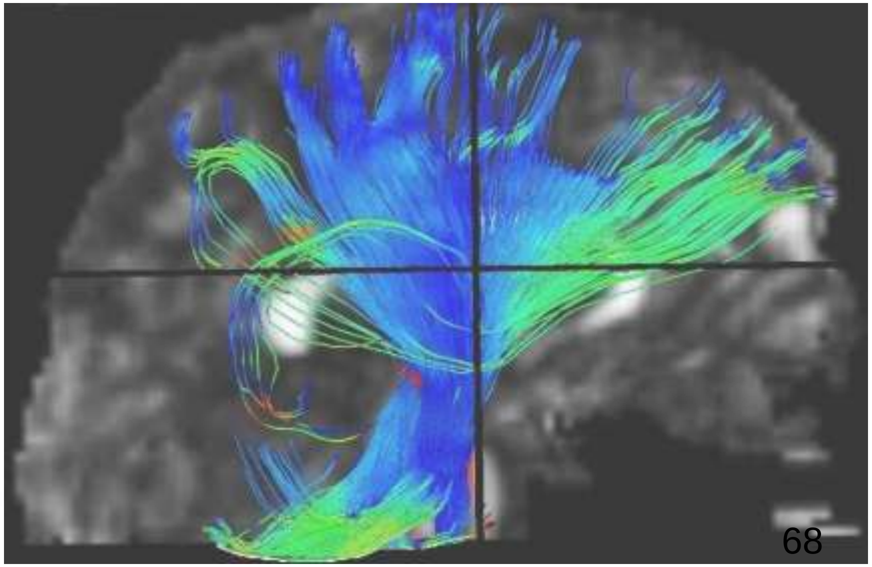

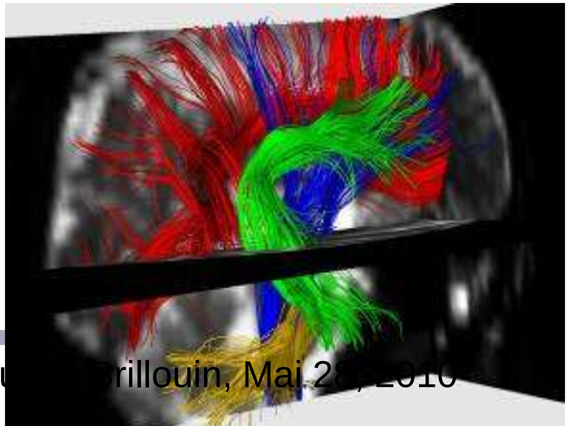

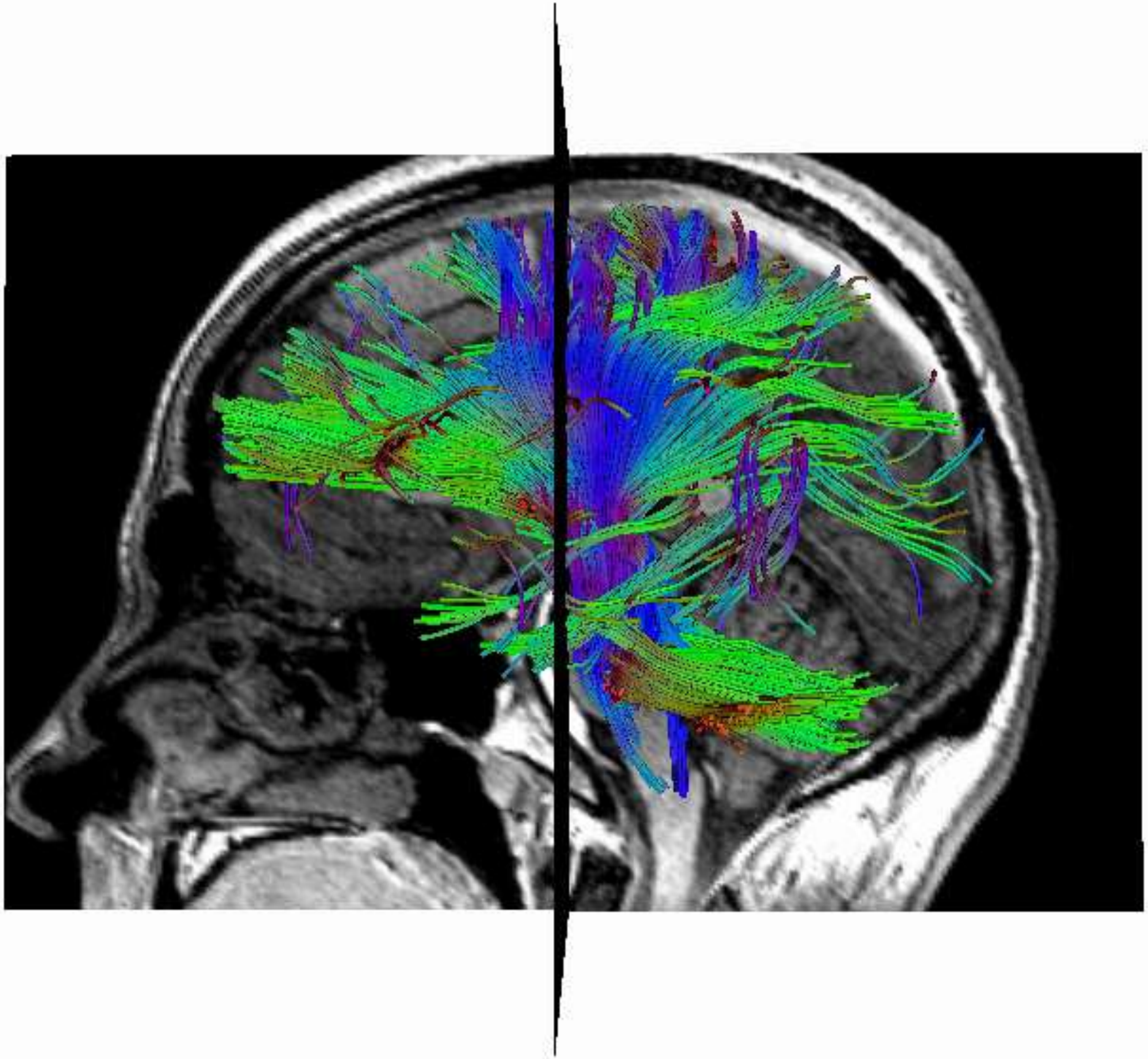

A Statistical Atlas of the Cardiac Fiber Structure

[J.M. Peyrat, et al., MICCAI'06, TMI 26(11), 2007]

Database

- 7 canine hearts from JHU
- Anatomical MRI and DTI

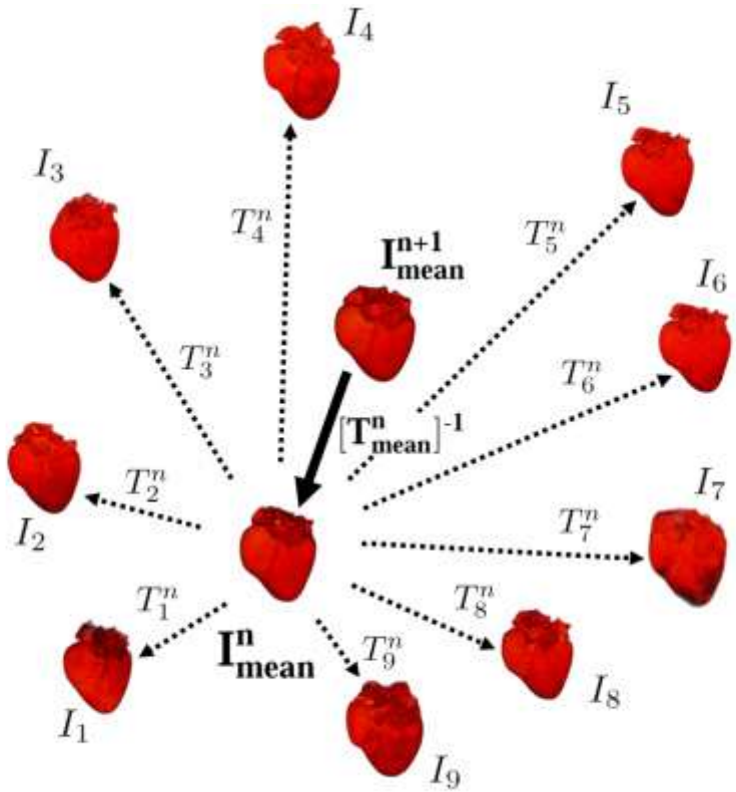

- *Average cardiac structure*
- Variability of fibers, sheets

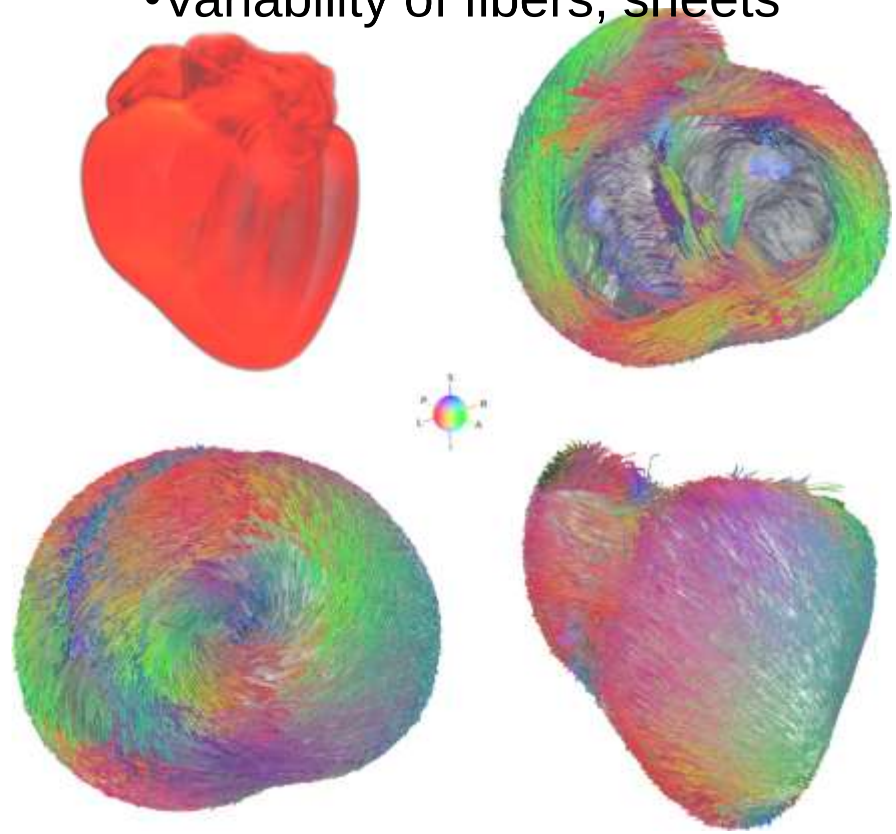

- available at http://www-sop.inria.fr/asclepios/data/heart

Roadmap

Goals and methods of Computational anatomy

Statistical computing on manifolds

A Riemannian framework for tensor computing

- Tensor image processing
  - Affine-invariant metrics
  - Log-Euclidean and other metrics
- Applications
  - Diffusion tensor images (DTI)
  - Morphometry of sulcal lines on the brain

Currents: an embedding space for curves and surfaces

Log-Euclidean statistics on image deformations

Conclusion and challenges

Methods of computational anatomy

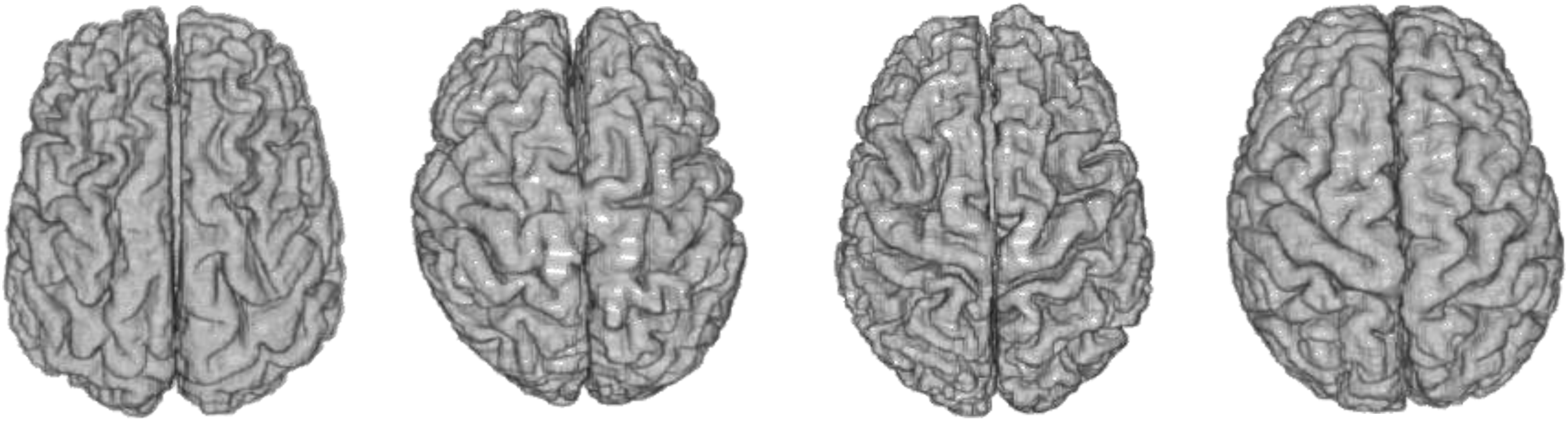

Structural variability of the cortex

Understand and model the variability of observations in the population

Use as anatomical prior to compensate for incomplete / noisy / pathological observations (personalized atlases in the clinical workflow)

Hierarchy of anatomical manifolds

- Landmarks [0D]: AC, PC [Talairach et Tournoux, Bookstein], functional landmarks
- Curves [1D]: crest lines, sulcal lines [Mangin, Barillot, Fillard…]
- Surfaces [2D]: cortex, sulcal ribbons [Thompson, Mangin, Miller…],
- Images [3D functions]: VBM, Tensors in Diffusion imaging
- Transformations: rigid, multi-affine, local deformations (TBM), diffeomorphisms [Asburner, Arsigny, Miller, Trouve, Younes…]

Morphometry of the Cortex from Sucal Lines

Associated team Brain-Atlas (2001-2008)

- LONI (UCLA) : P. Thompson et al.
- ASCLEPIOS (INRIA): V. Arsigny, N. Ayache, P. Fillard, X. Pennec

Neuroanatomical reference:

- 72 sulcal lines manually extracted and labeled
- 700 subjects

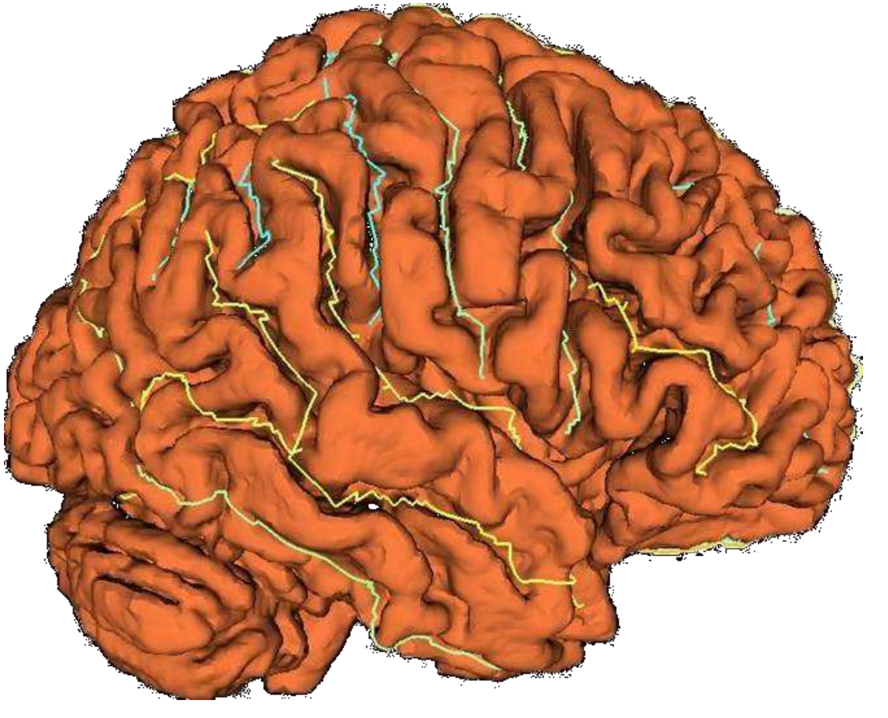

Alternative

- Automatic extraction

JF. Mangin, D. Rivière, 2003, Neurospin

Morphometry of the Cortex from Sucal Lines

1/ Mean curve: Alternated minimization of the variance on matches / position

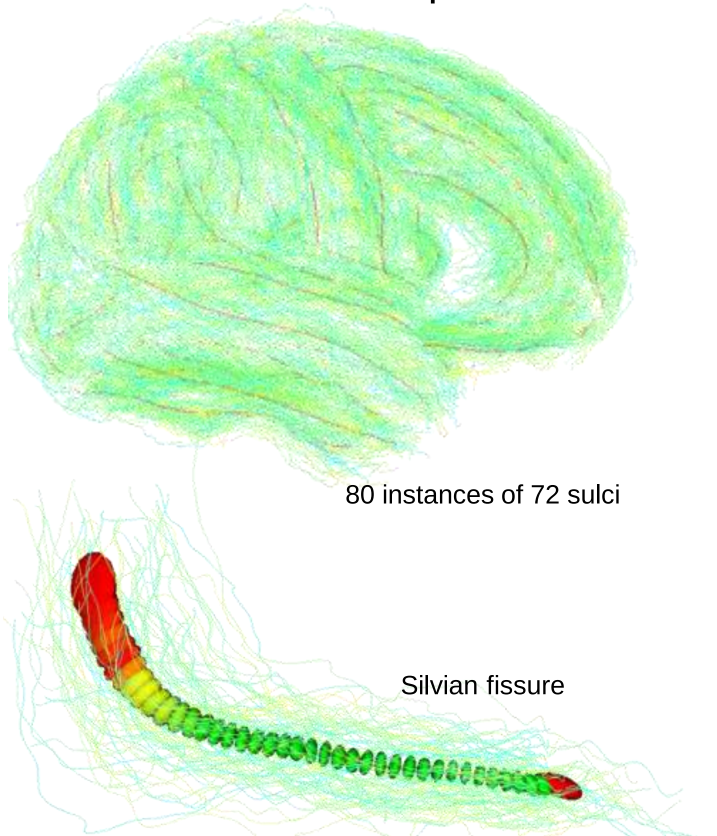

2/ Computation of the covariance tensor at each point of the mean

3/ Extrapolation to the whole volume : harmonic diffusion of tensors

$$C(\Sigma) = \frac{1}{2}\int_{\Omega}\sum_{i=1}^{n} G_{\sigma}(x - x_i)\, dist(\Sigma(x), \Sigma_i)^2\, dx + \frac{\lambda}{2}\int_{\Omega} \|\nabla \Sigma\|^2_{\Sigma(x)}$$

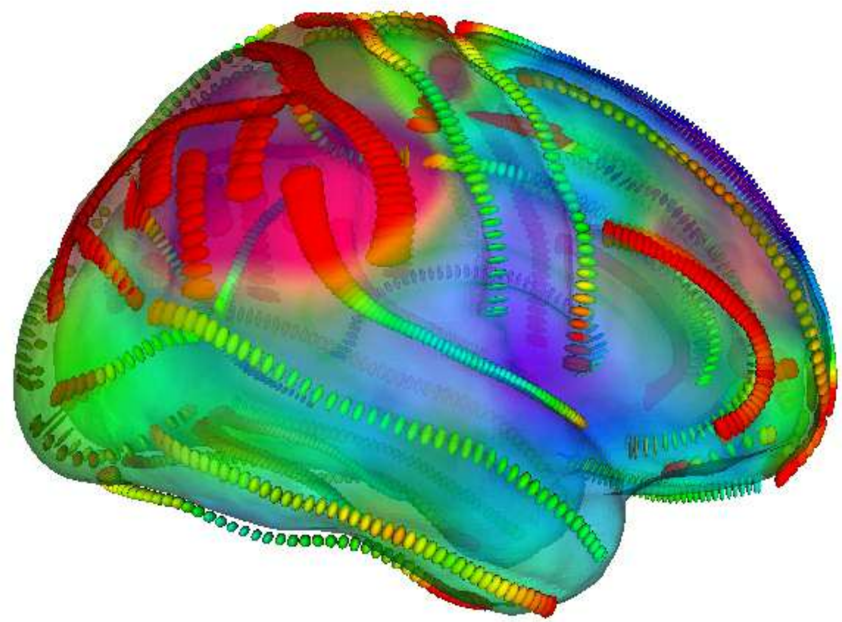

[Fillard et al., IPMI 2005, Neuroimage 34(2), 2007]

Full Brain extrapolation of the variability

$$C(\Sigma) = \frac{1}{2}\int_{\Omega}\sum_{i=1}^{n} G_{\sigma}(x - x_i)\,dist(\Sigma(x), \Sigma_i)^2\,dx + \frac{\lambda}{2}\int_{\Omega}\|\nabla\Sigma\|_{\Sigma(x)}^2$$

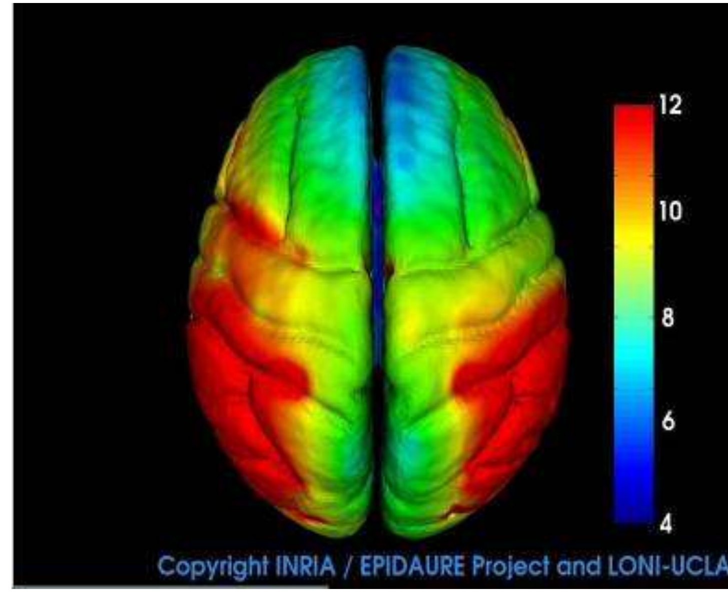

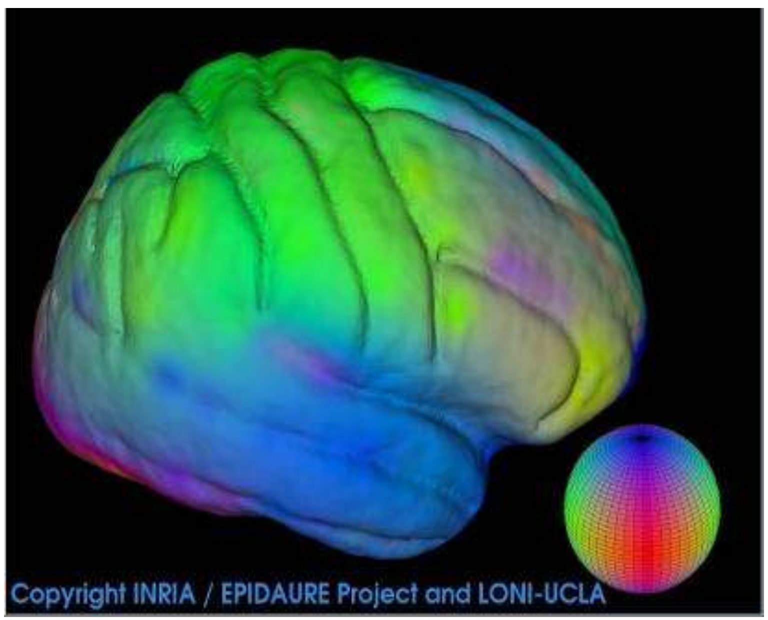

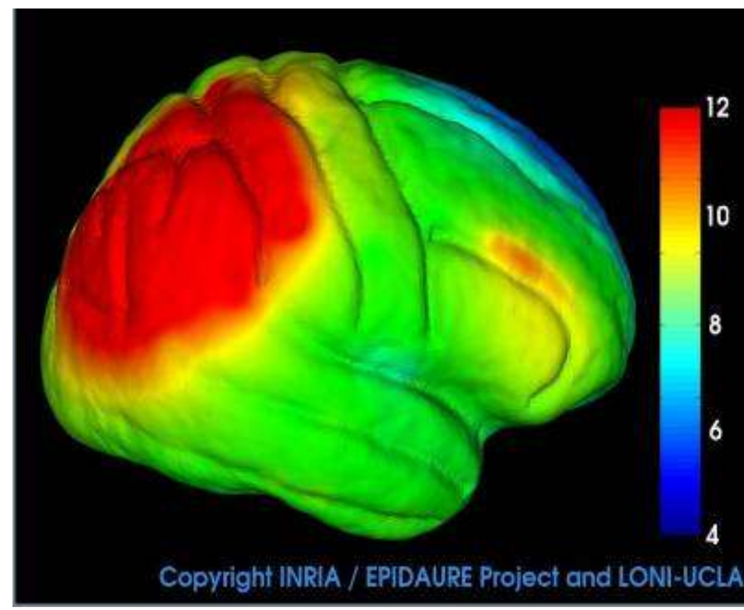

Comparison with cortical surface variability

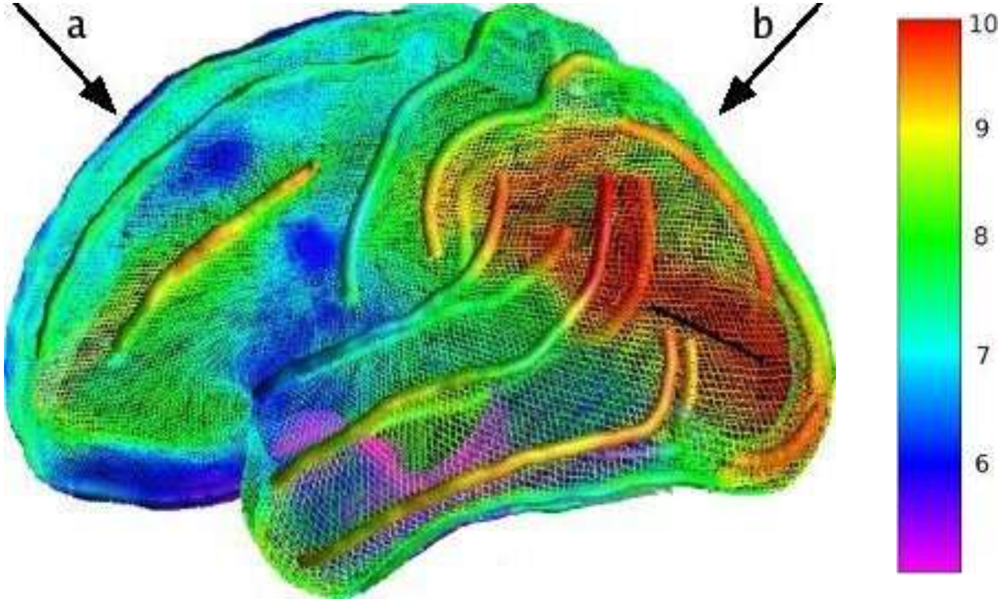

P. Thompson at al, HMIP, 2000

Average of 15 normal controls by non-linear registration of surfaces

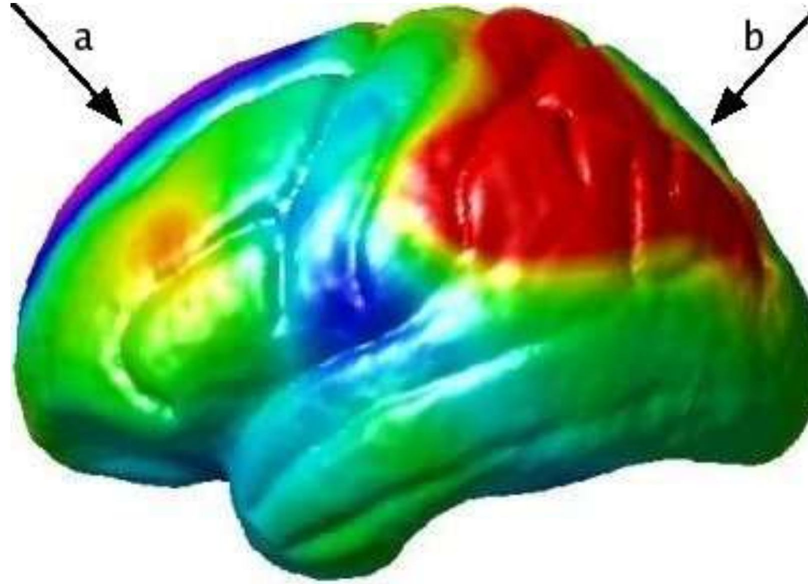

P. Fillard et al, IPMI 05

Extrapolation of our model (98 subjetcs with 72 sulci)

Consistent low variability in phylogenetical older areas

- (a) superior frontal gyrus

Consistent high variability in highly specialized and lateralized areas

- (b) temporo-parietal cortex

Asymmetry

- Maximal: Broca's area (language), parietal cortex; minimal: primary somatomotor areas

[Fillard, Arsigny, Pennec,Thompson, Ayache, IPMI 2005, NeuroImage 34(2), 2007]

Quantitative Evaluation: Leave One Sulcus Out

- Remove data from one sulcus
- Reconstruct from extrapolation of others

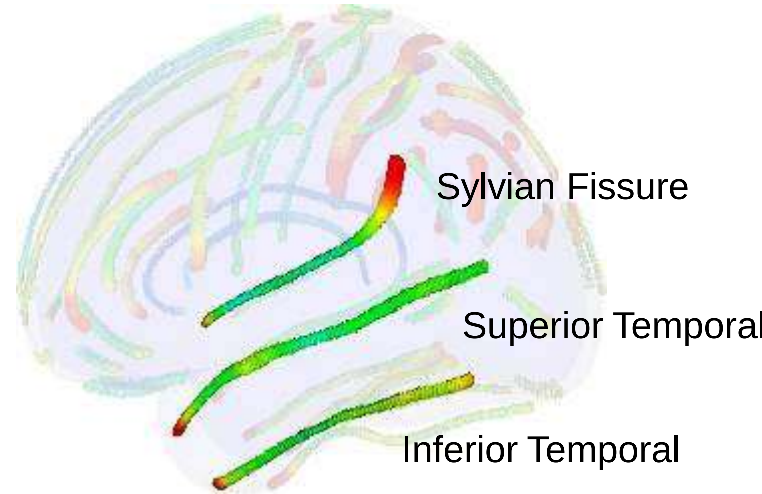

Original tensors **Leave one out reconstructions**

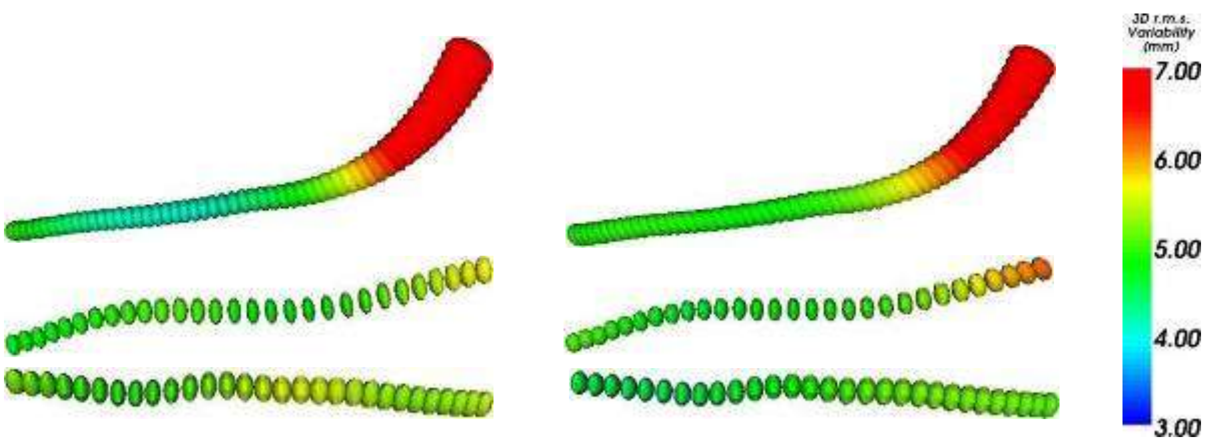

Difference of variability symmetry between groups

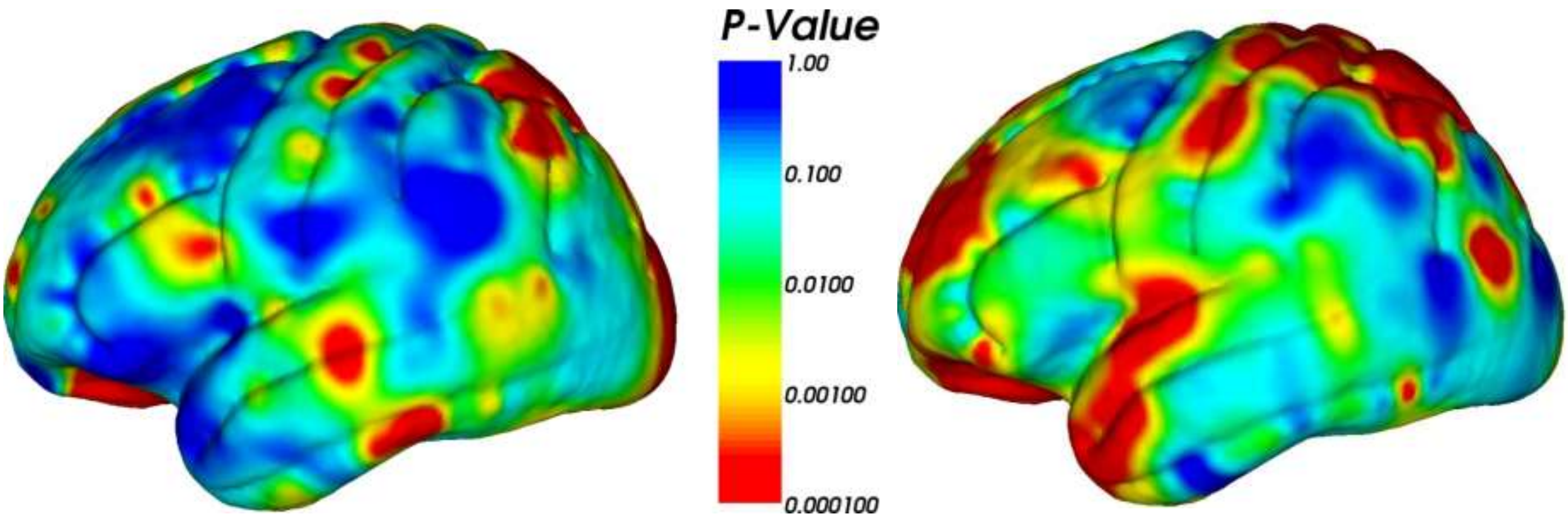

Bonferroni corrected P-value at 5% = 0.0001

Men

Women

[Fillard, Pennec,Thompson, Thompson, Evaluating Brain Anatomical Correlations via Canonical Correlation Analysis of Sulcal Lines, MICCAI Workshop on stat. Atlases, 2007]

Local and distant structural correlation

Left central sulcus

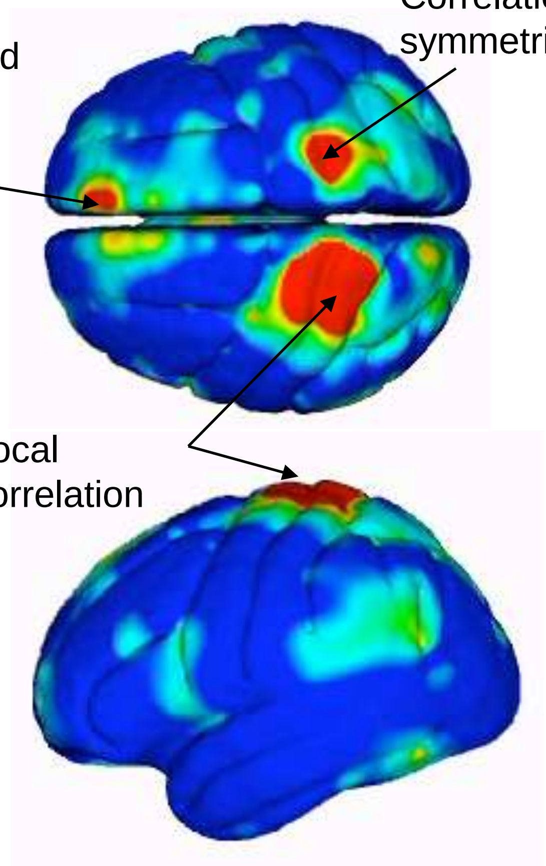

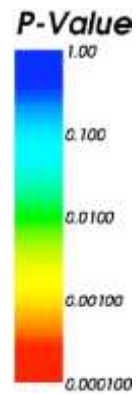

Left inferior temporal sulcus

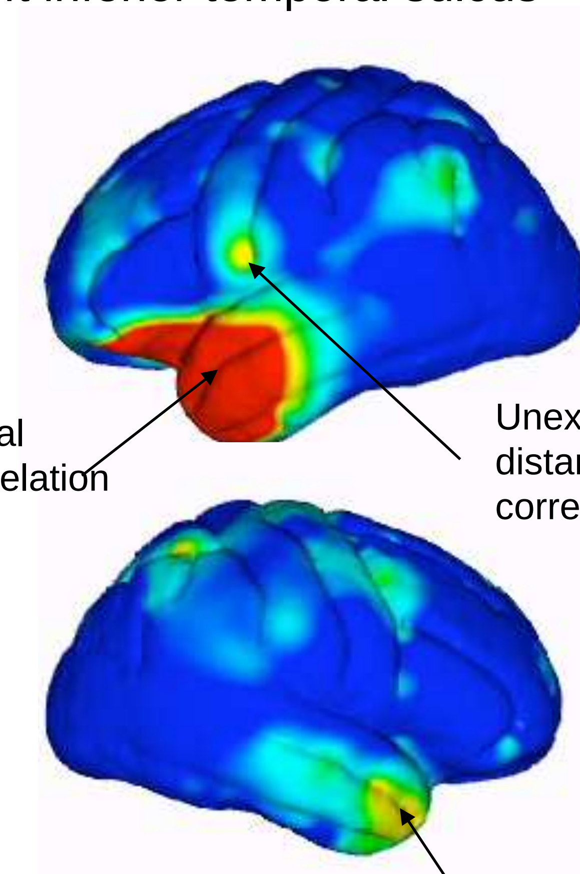

Enumeration: Modeling the Green’s function

[Fillard, Pennec,Thompson, Thompson, Evaluating Brain Anatomical Correlations via Canonical Correlation Analysis of Sulcal Lines, NeuroImage, 2009]

Roadmap

Goals and methods of Computational anatomy

Statistical computing on manifolds

A Riemannian framework for tensor computing

Currents: an embedding space for curves and surfaces

- Shapes: Forms and deformations
- Brain morphometry from curves, surfaces and tracts
- Statistical model of the right ventricle in repaired ToF
- Extension to longitudinal modeling

Log-Euclidean statistics on image deformations

Conclusion and challenges

Anatomical structures segmented in Brain Images

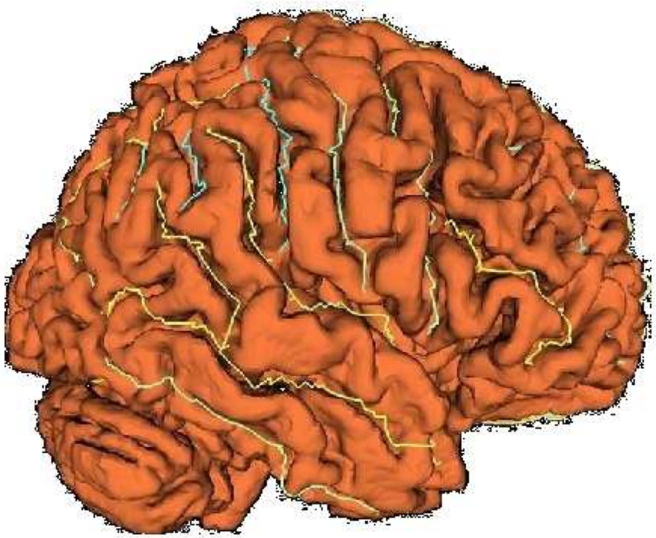

•Sulcal lines at the surface of the cortex

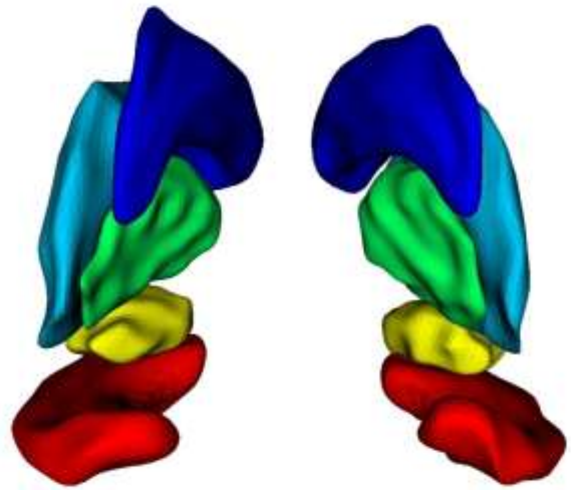

• Surface of deep brain structures

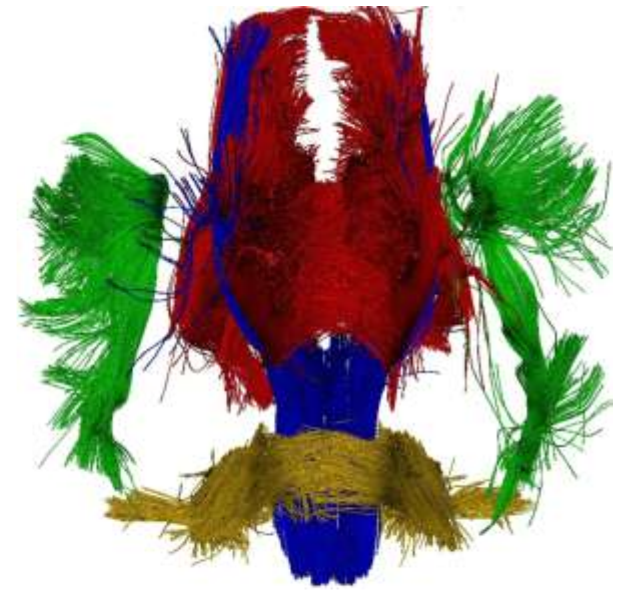

•Fiber tracts from DTI

How to measure the variability across subjects?

Consistent framework to include all objects?

Shapes: forms & deformations

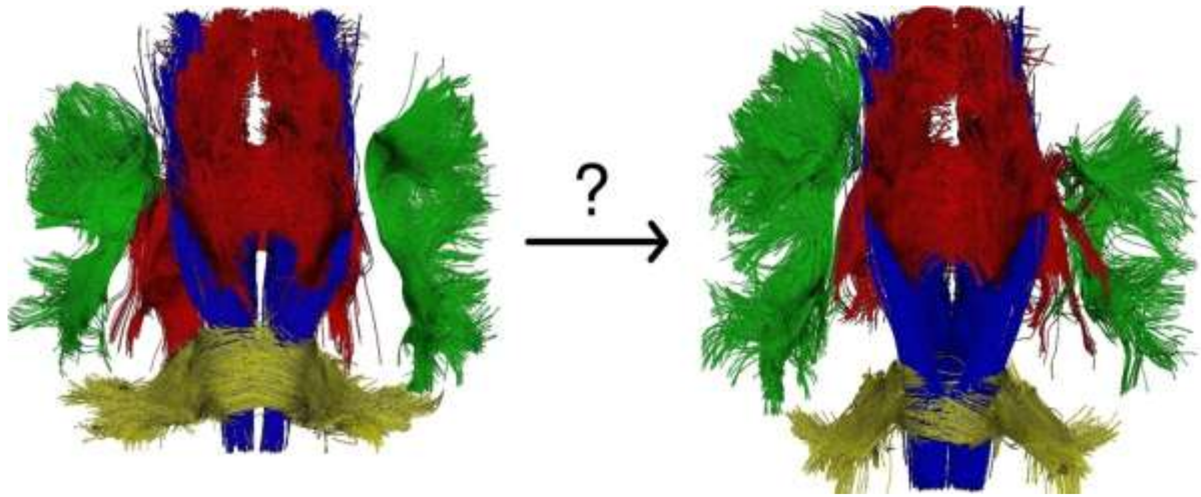

- **"Shape space" embedding [Kendall]**
  - Invariance of the metric? Shape alignement? $d(\mathcal{O}_1, \mathcal{O}_2)$ (or $\mathcal{O}_2 = \mathcal{O}_1 + \varepsilon$)
  - Deformation = nuisance factor
- **Measure of deformation [D'Arcy Thompson 1917, Grenander]**
  - Existence? $\hat{\phi} = \operatorname{argmin}\, d(\mathcal{O}_2, \phi.\mathcal{O}_1)$ (or $\mathcal{O}_2 = \hat{\phi}.\mathcal{O}_1 + \varepsilon$)
  - Residual as nuisance factor: overfitting?

Shapes: forms & deformations

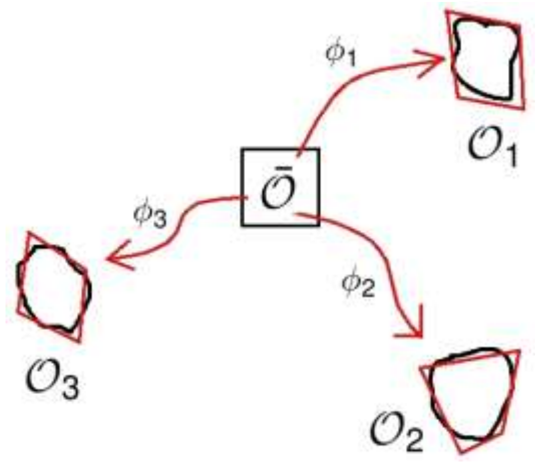

$$\mathcal{O}_i = \phi_i.\bar{\mathcal{O}} + \varepsilon_i$$

Combined approach

- Deterministic template: anatomical invariants
- Random deformations: geometrical variability
- Random residuals: “texture” variability

Generative model:

- Simulate new data: interpretation of variability
- Compare new data with the model

[Durrleman PhD 2010]

Problems and goals

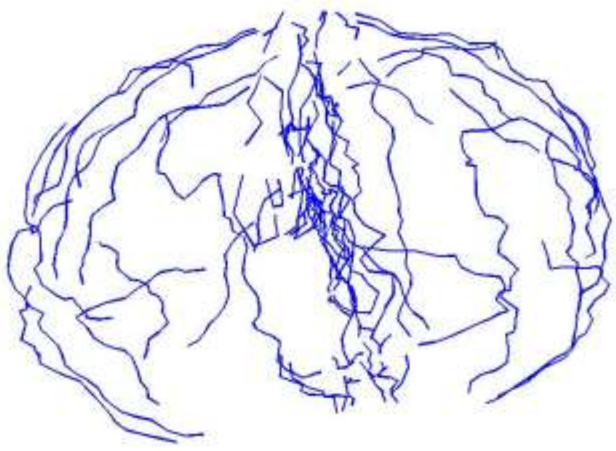
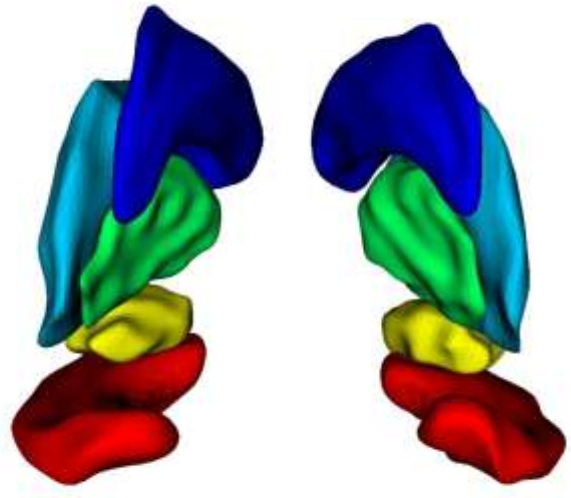
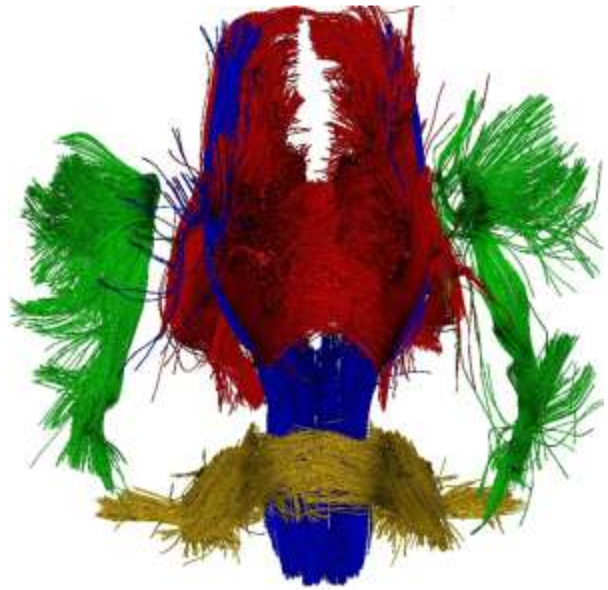

Define a metric on shapes which:

- Does not assume point correspondence
- Is generic enough (curves, surfaces, fiber bundles, etc..)
- Is compatible with deformations

Infer statistical models:

- Shape only $(\mathcal{O}_i = \bar{\mathcal{O}} + \varepsilon_i)$
- Shape and deformations $(\mathcal{O}_i = \phi_i \bar{\mathcal{O}} + \varepsilon_i)$

Currents for lines and surfaces

Matching lines / surfaces = do we really need point correspondences?

Currents = generalization of distributions (e.g. Dirac) to vectors

- Distributions are known through their action on smooth test functions
- Currents integrate smooth vector fields (e.g. $W=K\otimes L_2$ with $K=G_\sigma.Id$): they measure the flux along lines or through surfaces
- Lines and surfaces can be smooth or discrete

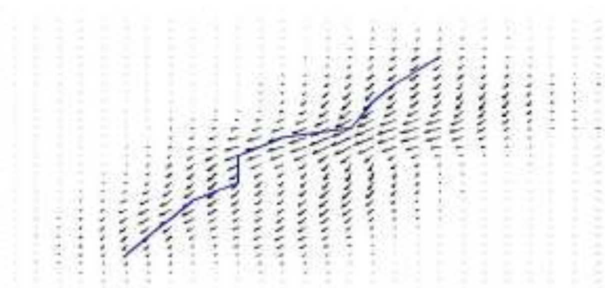

$L(\omega) = \int_L \langle \omega(x), \tau(x) \rangle \, dx$

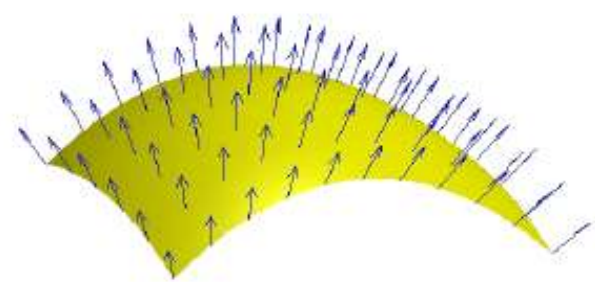

$S(\omega) = \int_S \langle \omega(x), n_x \rangle \, d\sigma(x)$

[Vaillant and Glaunes IPMI'05; Glaunes PhD'06]

Currents for lines and surfaces

Distance between currents:

- Norm of vector field maximizing the flux difference

$$d^2(L, L') = \sup_{\|\omega\|_W \leq 1} \left| L(\omega) - L'(\omega) \right|$$

- Closed form solution for RKHS

$$\langle L, L' \rangle_{W^*} \approx \sum_{i,j} t_i^{\ T}.K(x_i - x'_j).t'_j$$

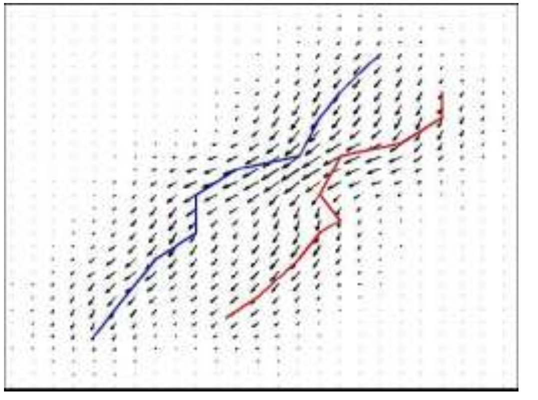

  - (+) No point correspondences needed
  - (+) No conditions on the sampling required
  - (-) "soft" distance: curvature not accounted for
  - (-) Arbitrary choice of the kernel

Algorithms on currents

- Diffeomorphic registration [Glaunes PhD'06, Durrleman MICCAI 07]
- Statistical analysis (mean, PCA) [Durrleman et al, MFCA 2008]
- Fast and stable computations thanks to approximations [Durrleman et al, MICCAI 2008 : Young investigator award]

From continuous to discrete computations

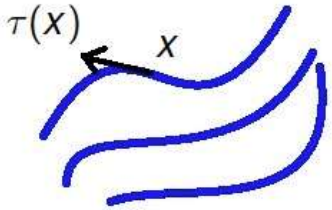

$$T = \sum_{i=1}^{\infty} \delta_{x_n}^{\tau_n} \qquad \|T\|^2 = \int_T \int_T \tau(x)^t K(x,y) \tau(y) dxdy$$

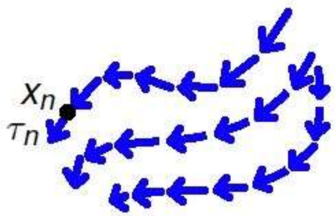

$$T \sim \sum_{i=1}^{N} \delta_{x_n}^{\tau_n} \qquad \|T\|^2 = \sum_{i=1}^{N} \sum_{j=1}^{N} \tau_i^t K(x_i, x_j) \tau_j$$

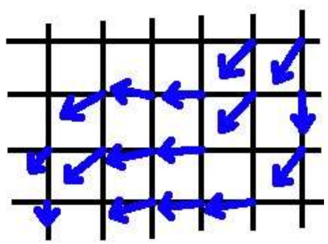

$$T \sim \sum_{i \in \Lambda} \delta_{x_n}^{\tau_n} \qquad \|T\|^2 = \boldsymbol{\tau}^t (\mathbf{K} * \boldsymbol{\tau})$$

- Projection
- Approximation using matching pursuit

	double sum	grid
complexity	$\mathcal{O}(N^2)$	$\mathcal{O}(N + N_{grid} \log(N_{grid}))$
approx. error	$\mathcal{O}(\max \lvert\tau_i\rvert)$	$\mathcal{O}(\Delta^2 / \lambda_W^2)$

[Durrleman et al, MICCAI 2008 : Young investigator award]

A common space for multiple objects

Sulcal lines at the surface of the cortex

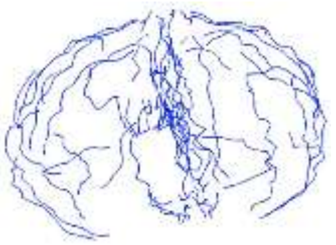

Individual lines: $\mathcal{O} = \sum_{i=1}^{70} L_i$

$$d^2(\mathcal{O}_1, \mathcal{O}_2) = \sum_{i=1}^{70} w_i \left\| L_i^1 - L_i^2 \right\|_{W*}^2$$

Surface of deep brain structures

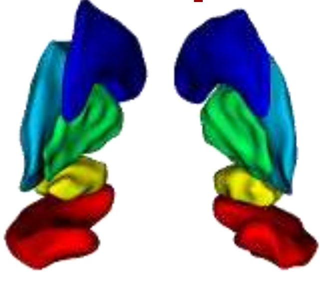

Mesh correspondence: $\mathcal{O} = \sum_{i=1}^{10} S_i$

$$d^2(\mathcal{O}_1, \mathcal{O}_2) = \sum_{i=1}^{10} w_i \left\| S_i^1 - S_i^2 \right\|_{W*}^2$$

Fiber tracts from DTI

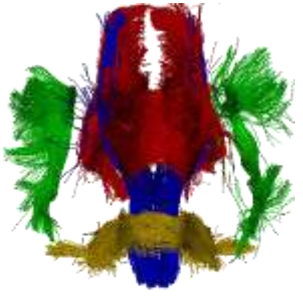

Fiber bundles correspondence: $\mathcal{O} = \sum_{i=1}^{5} F_i$

$$d^2(\mathcal{O}_1, \mathcal{O}_2) = \sum_{i=1}^{6} w_i \left\| F_i^1 - F_i^2 \right\|_{W*}^2$$

Metrics on diffeomorphisms

Space of deformations

- Transformation $y=\phi(x)$
- Curves in transformation spaces: $\phi(x,t)$
- Tangent vector = speed vector field

$$v_t(x) = \frac{d\phi(x,t)}{dt}$$

Right invariant metric

$$\|v_t\|_{\phi_t} = \left\|v_t \circ \phi_t^{-1}\right\|_{Id}$$

- Eulerian scheme
- Sobolev Norm H_k or H_∞ (RKHS) in LDDMM → diffeomorphisms
  [Miller, Trouve, Younes, Dupuis 1998 – 2009]

Geodesics determined by optimization of a time-varying vector field

- Distance

$$d^2(\phi_0, \phi_1) = \arg\min_{v_t}\left(\int_0^1 \|v_t\|_{\phi_t}^2 .dt\right)$$

- Geodesics characterized by initial momentum
- Finite dimensional parameterization of initial momentum
  (momentum support = current support points) **[Glaunes PhD'06]**

Roadmap

Goals and methods of Computational anatomy

Statistical computing on manifolds

A Riemannian framework for tensor computing

Currents: an embedding space for curves and surfaces

- Shapes: Forms and deformations
- Brain morphometry from curves, surfaces and tracts
- Statistical model of the right ventricle in repaired ToF
- Extension to longitudinal modeling

Log-Euclidean statistics on image deformations

Conclusion and challenges

Diffeomorphic matching of sulcal lines

Method

- Global space diffeomorphism (integration of time varying vector fields)
  [Trouve, Younes, Miller, etc]
- Distance between lines using currents
  [J. Glaunès, M. Vaillant: IPMI 2005]
- Statistics on diffeomorphisms:
  “Log” of deformation =
  initial vector speed / momentum

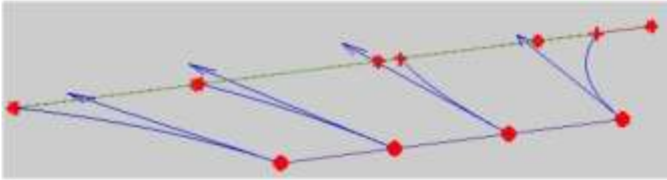

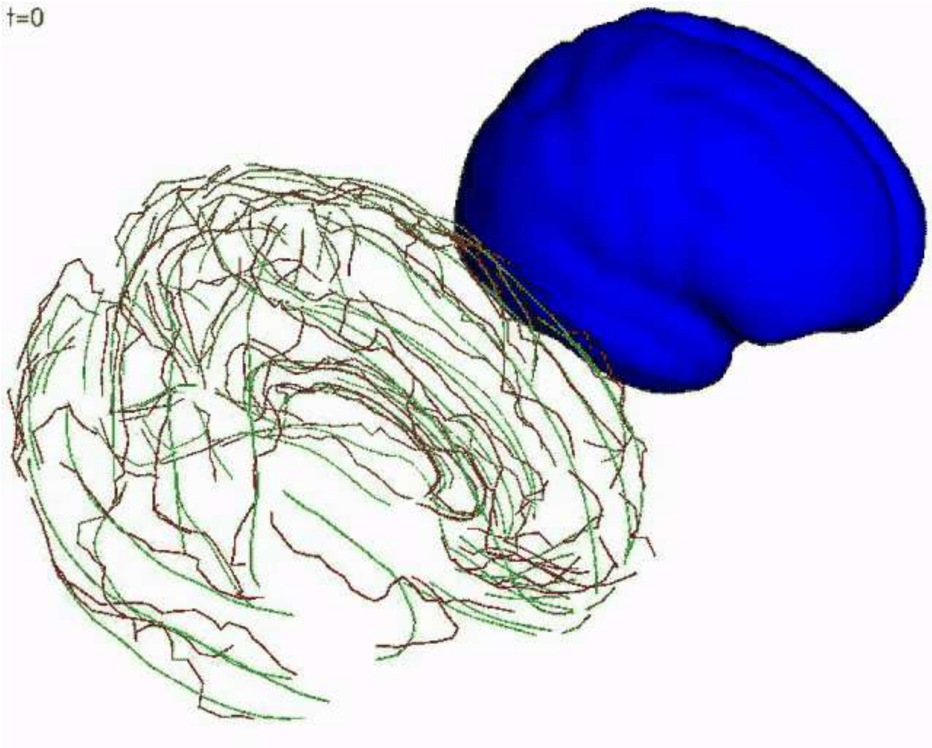

Template to subject line registration

[Durrleman, Pennec, Trouvé, Ayache, MICCAI 2007 + Medical Image Analysis, 12(5), 2008]

Brain variability from sulcal lines

Data

- 72 sulcal lines manually extracted and labeled from LONI
- Encode sampled lines as courants (points + tangents)

Statistical analysis

- Template,
- Point-wise variability
- Deformation modes

Advantages

- Generative model of deformations
- Retrieve some tangential deformation component.

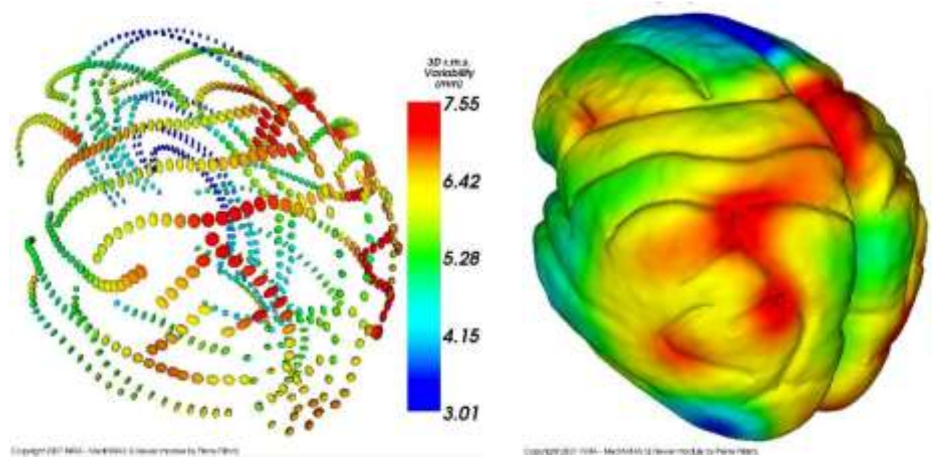

Variability at each point

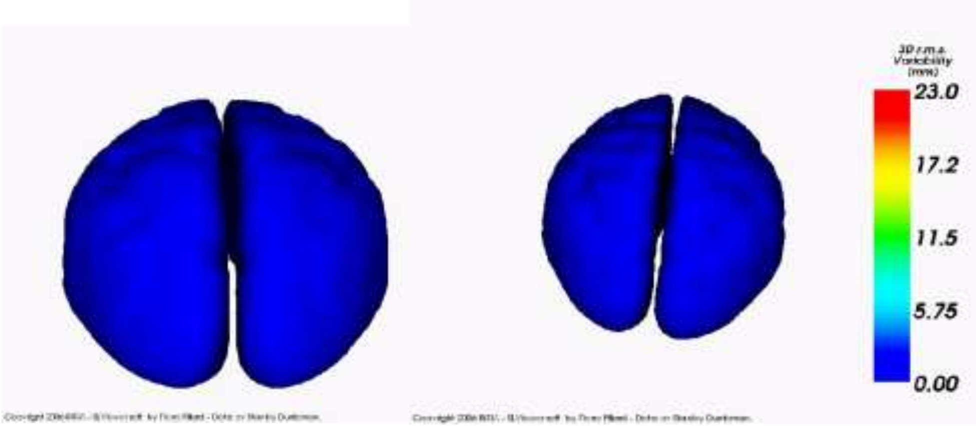

Global variability (2 PGA modes)

[Durrleman, Pennec, Trouvé, Ayache, MICCAI 2007 + Medical Image Analysis, 12(5), 2008]

Comparison of methods

The aperture problem

- Tangential variability is minimized on purpose with Fillard's method
- The global diffeomorphism performs a spatially consistent integration

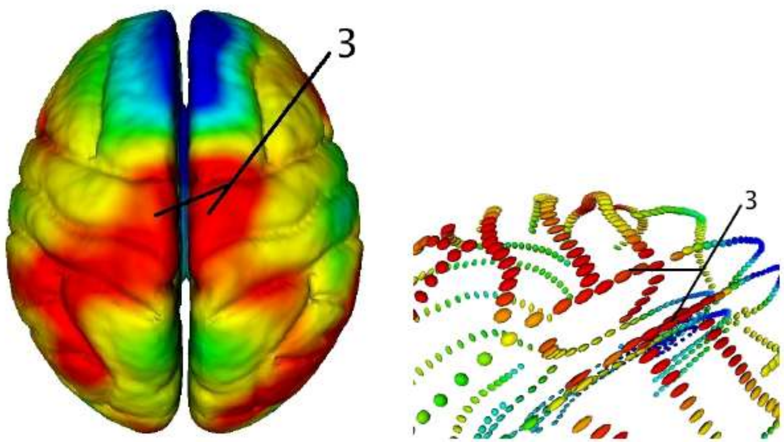

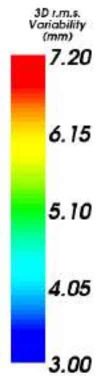

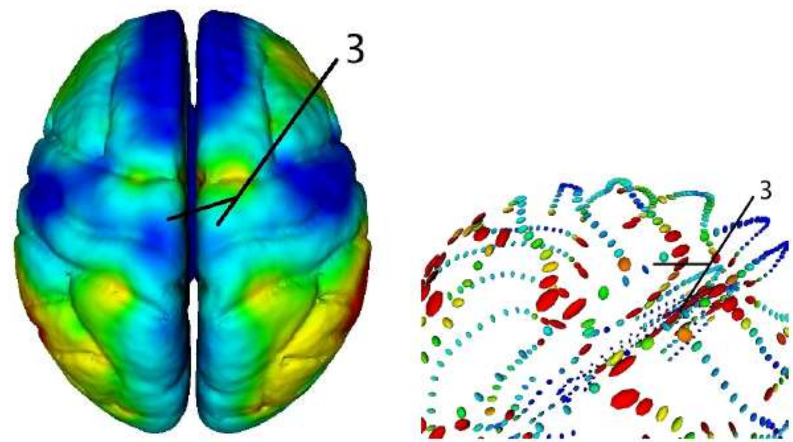

[S. Durrleman et al. MICCAI 2007]

[Fillard et al., Neuroimage 34(2), 2007]

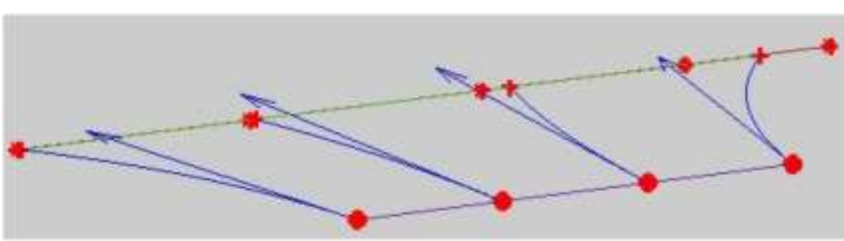

Currants

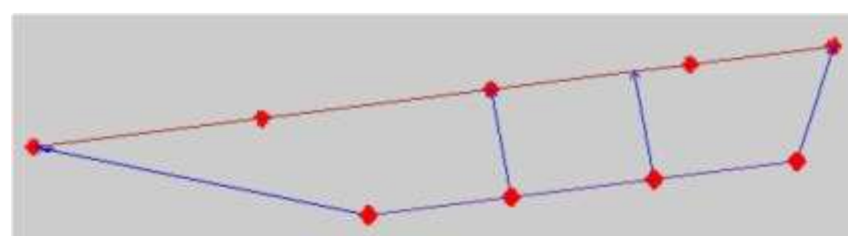

Points

Surface of deep brain structures

The Autism Research Program (UNC, Chapel Hill)

- Segmentation protocols: www.psychiatry.unc.edu/autismresearch/mri/roiprotocols.htm
- H. Hazlett, M. Poe, G. Gerig, R. Smith, J. Provenzale, A. Ross, J. H. Gilmore, and J. Piven, “Magnetic resonance imaging and head circumference study of brain size in autism,” The Archives of General Psychiatry, vol. 62, pp. 1366–1376, December 2005.
- K. Gorczowski, M. Styner, J-Y. Jeong, J. S. Marron, Joseph Piven, H. Hazlett, S. Pizer and G. Gerig, Statistical Shape Analysis of Multi-Object Complexes, CVPR, 2007

A longitudinal pediatric database:

- Left/right meshes of 5 brain structures
  Caudate, Putamen, Globus Pallidus, Amygdala, Hippocampus
- Time points at age 2 and 4
- Autistic vs healthy controls:

#subjects	Autistics	Controls	Unknown
with 2 time points	**23**	**6**	**4**
with scan only at age 2	27	8	6
with scan only at age 4	1	4	1

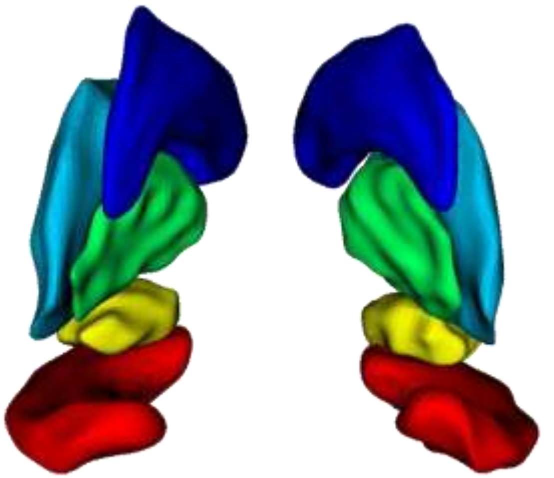

From surfaces to currents

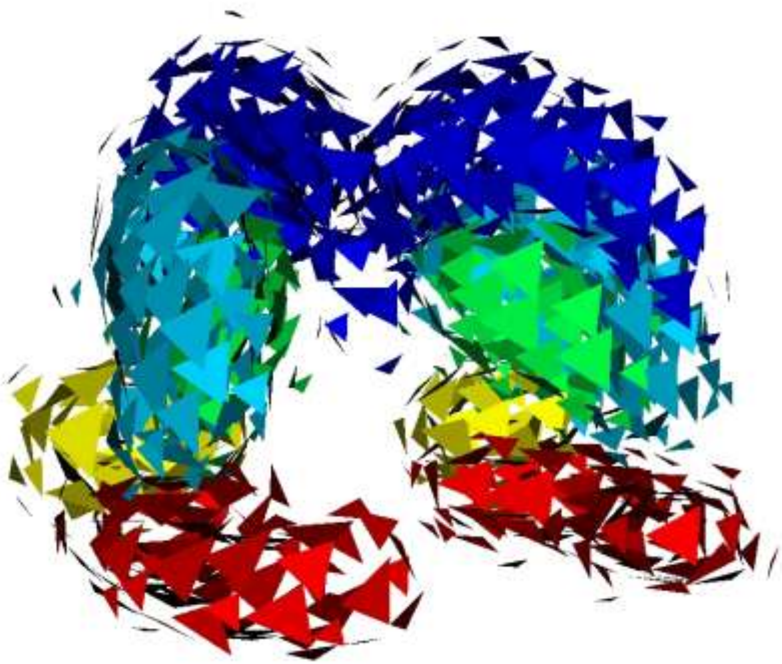

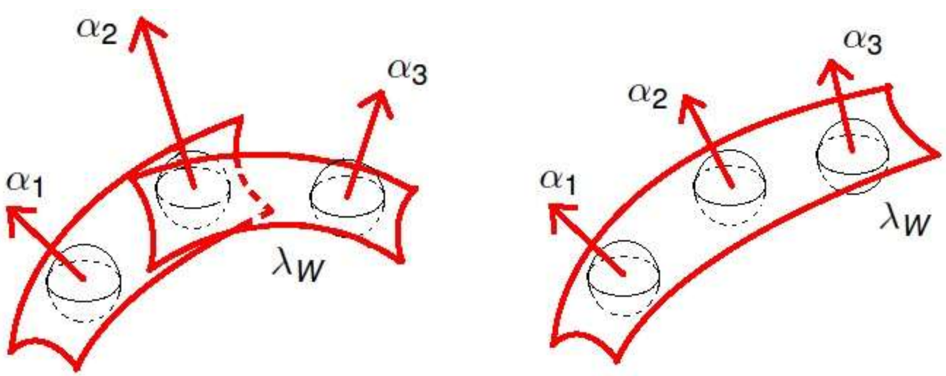

Scale on currents: $\lambda_W = 10mm$

Approx. error < 5% variance

Data storage:

Mesh: 8 Mb

Approx: 1.2 Kb

Time to register the mean of:

	3 subj	50 subj
original data	10h	∞
with approx.	5min	5min

Magnitude of momenta encodes area

Surfaces registration

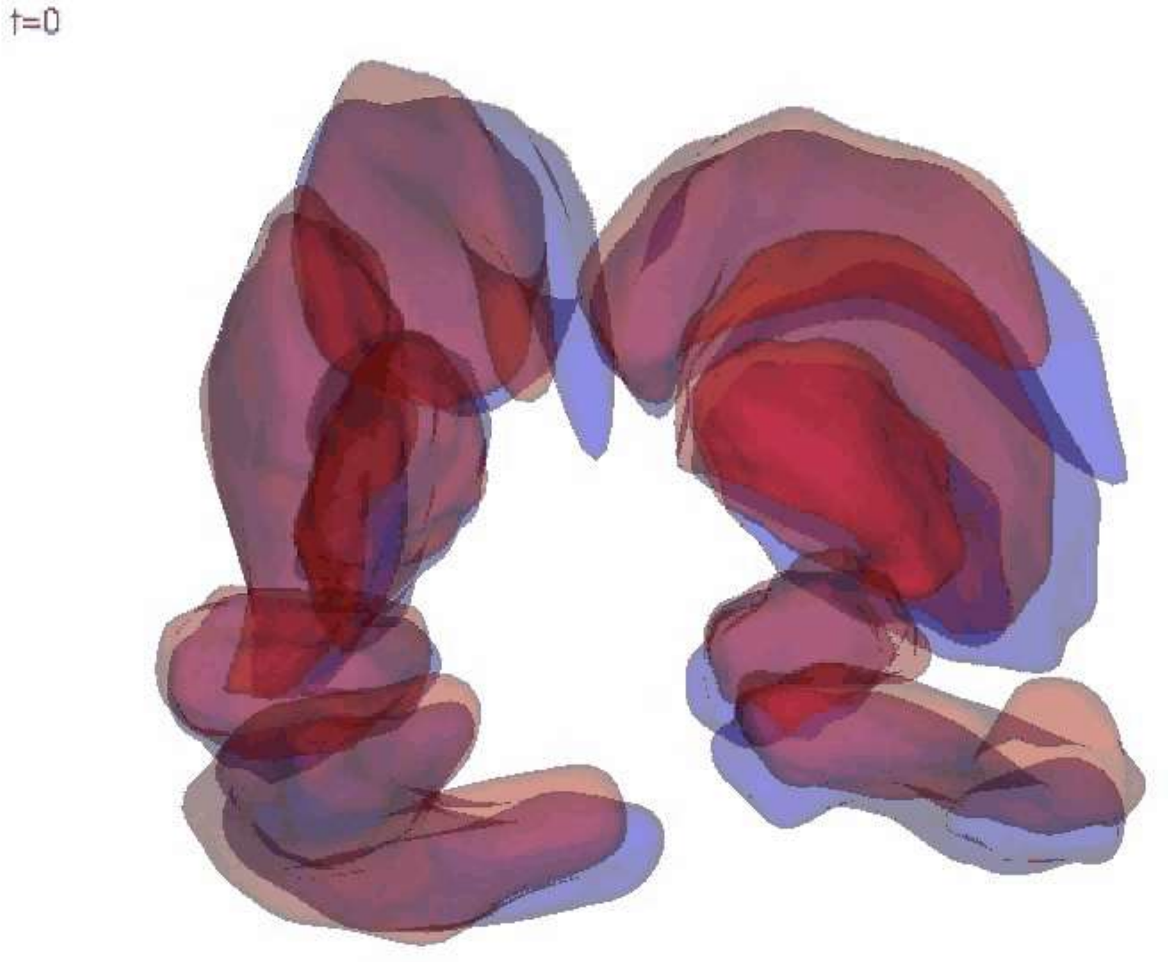

Statistical analysis of Populations

•Autistics

•Controls

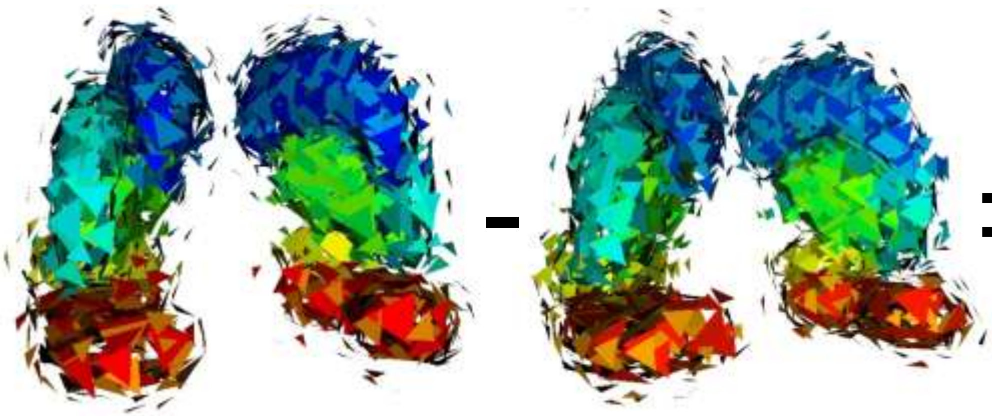

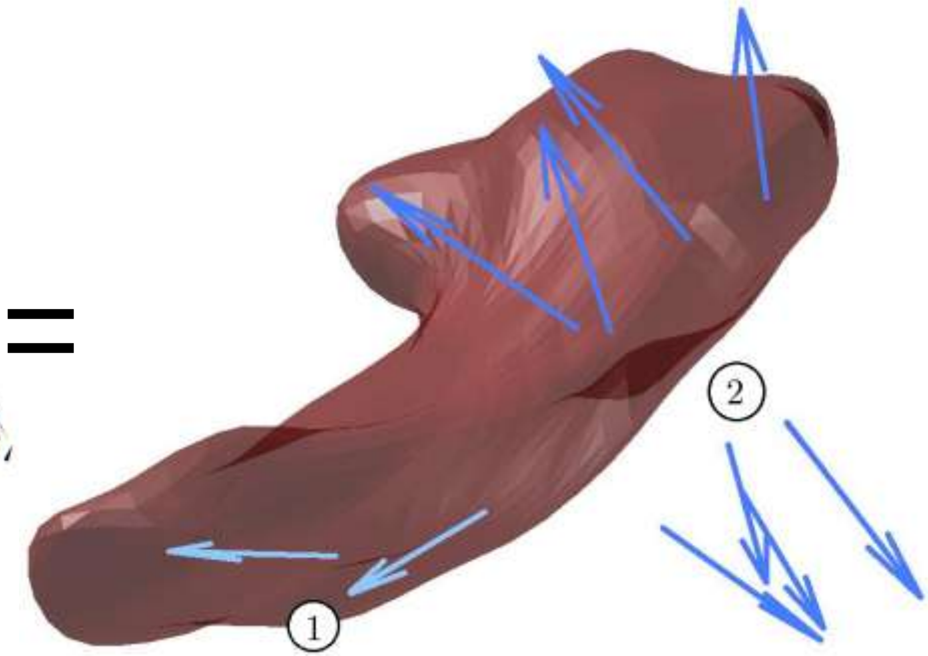

Curvature (1) + thickening (2) of hippocampus

[Durrleman, Pennec, Trouvé, Ayache, MICCAI 2008 + Medical Image Analysis, 13(5), 2009]

Vary data: from lines to fiber tracts

5 tracts on 5 subjects

- Corpus callosum
- Corticospinal
- Corticobulbar
- Arcuate left
- Arcuate right

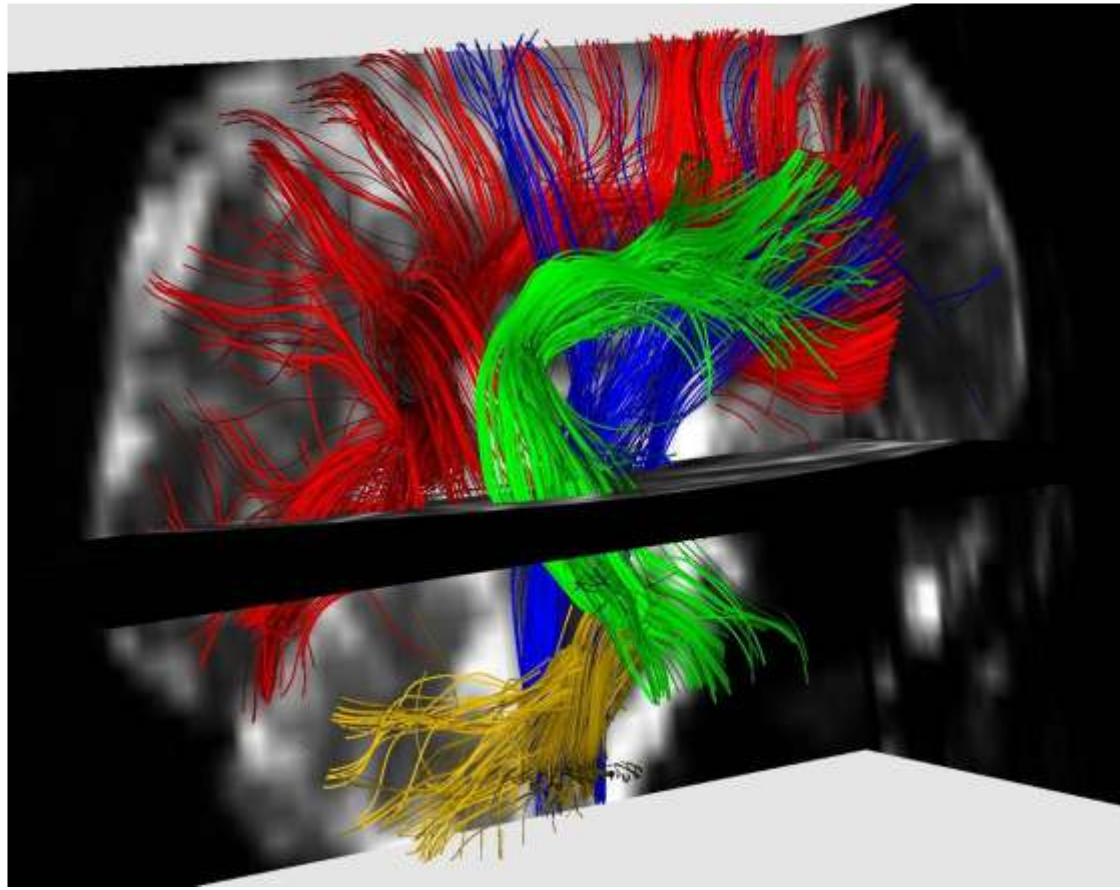

• Reconstruction of fibers biases the correspondences along fibers

• No one-to-one correspondences between fibers of different subjects

The mathematical object “Fiber tract”?

- Lines represented by singular currents
- Tract = fuzzy set of lines = continuous current

Diffeomorphic registration of Fiber tracts

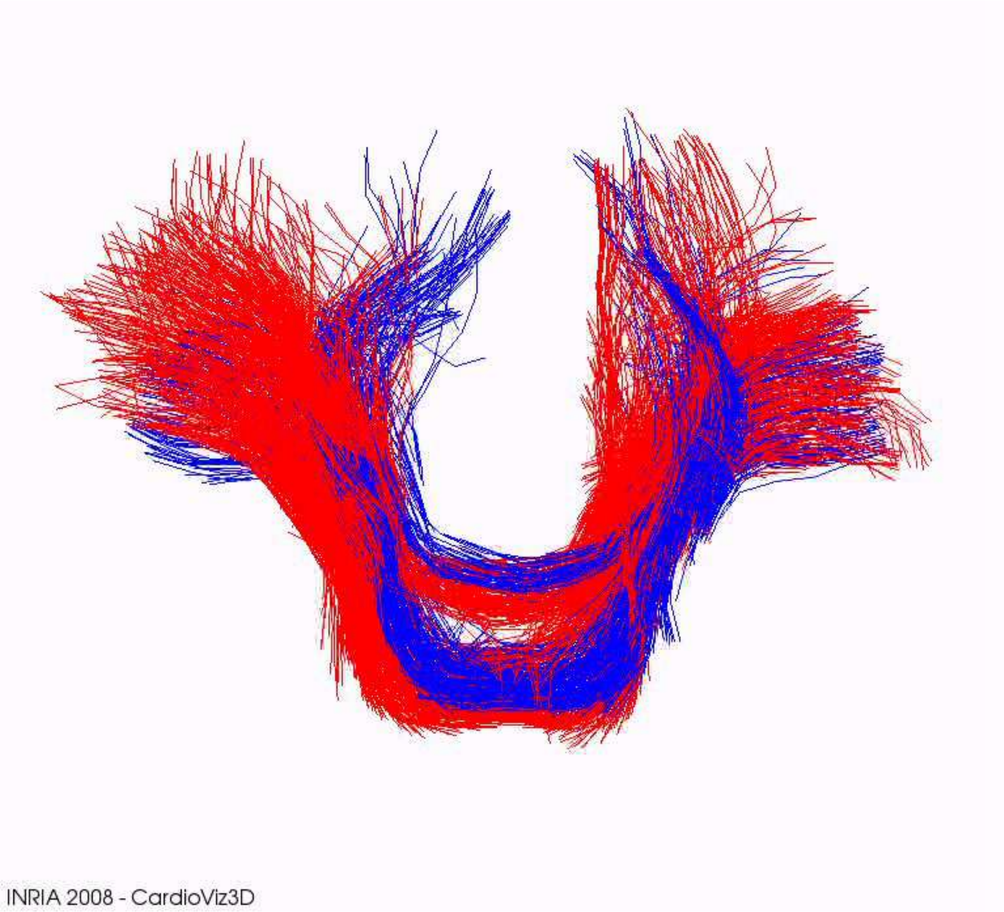

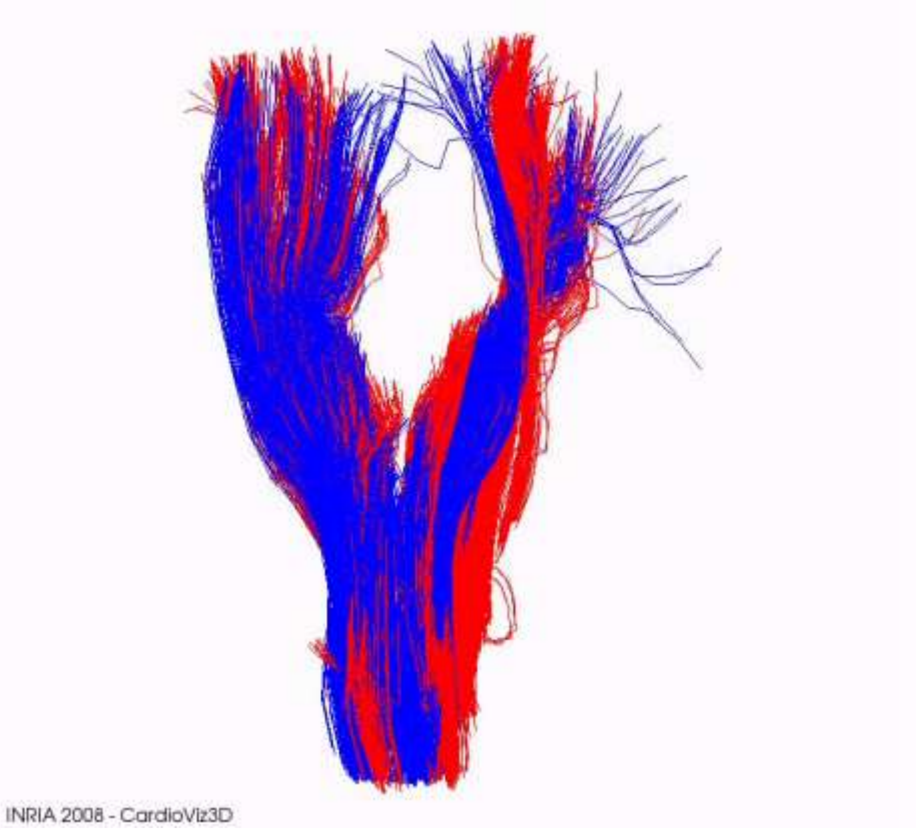

Cortico-bulbar tract

Cortico-spinal tract

[Durrleman, Fillard, Pennec, Trouvé, Ayache. A Statistical Model of White Matter Fiber Bundles based on Currents. In Proc. of IPMI'09, LNCS, 2009]

Statistical analysis:
Template, deformation and texture modes

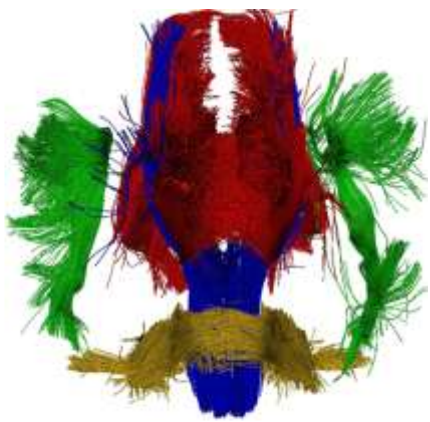

One subject

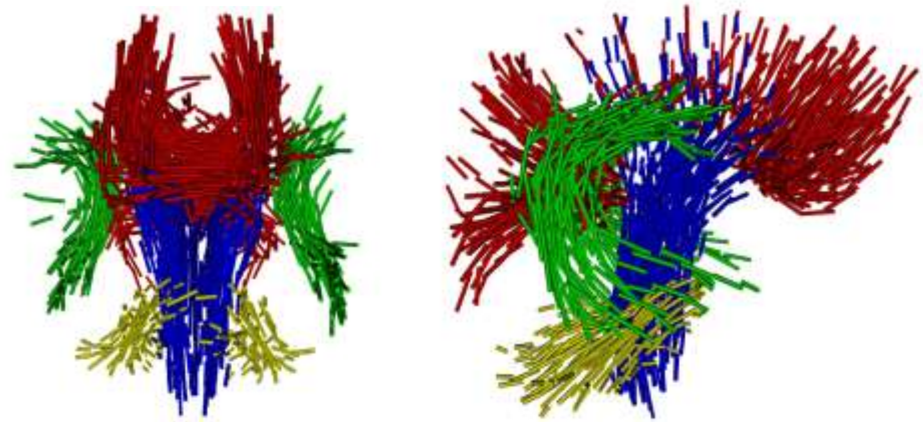

Template (occipital and lateral views)

Cortico-bulbar
tract

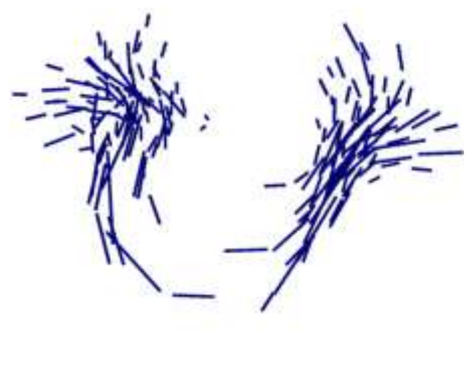

1st deformation mode (template +/- σ)

1st mode of residues (template +/- σ)

[Durrleman et al., IPMI 2009]

Roadmap

Goals and methods of Computational anatomy

Statistical computing on manifolds

A Riemannian framework for tensor computing

Currents: an embedding space for curves and surfaces

- Shapes: Forms and deformations
- Brain morphometry from curves, surfaces and tracts
- Statistical model of the right ventricle in repaired ToF
- Extension to longitudinal modeling

Log-Euclidean statistics on image deformations

Conclusion and challenges

Repaired Tetralogy of Fallot

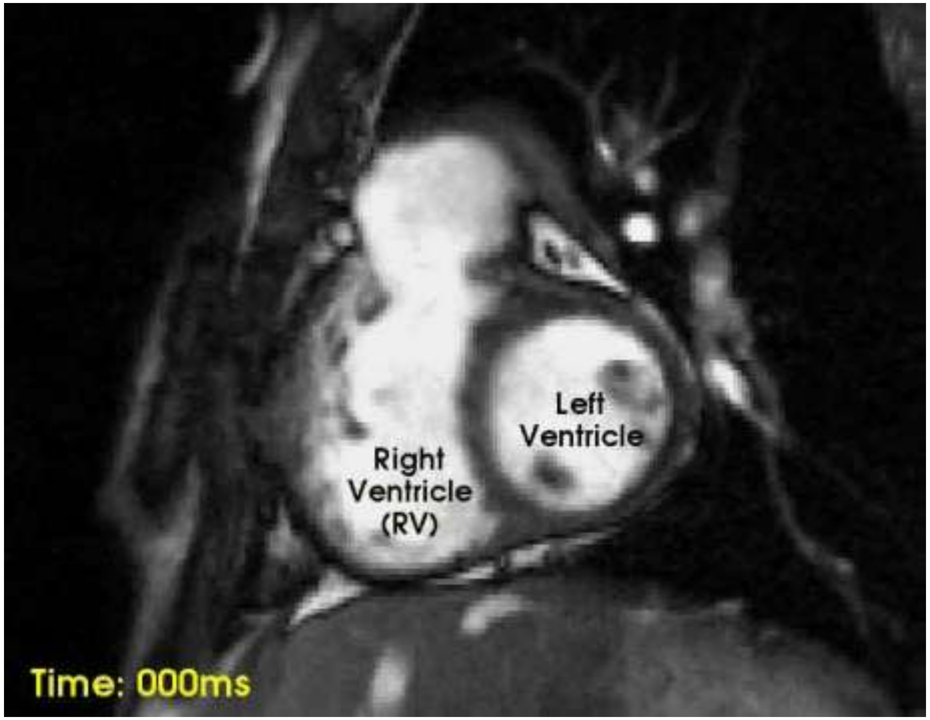

- *Severe Congenital Heart Disease*
- *Occurs 1 of 2500 (Hoffman, JACC 02)*
- *Surgical repair in infancy*
- *After repair: chronic pulmonary valve regurgitations and extremely dilated right ventricle (RV).*

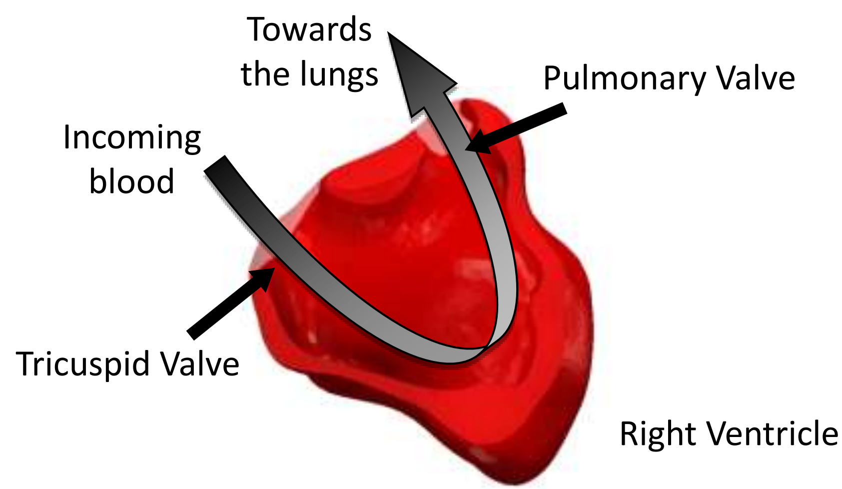

Valve replacement: Increase life expectancy, but limited valve lifespan

When is the best timing for valve replacement?

Life expectancy 40 years

Statistical Model of Right Ventricle in Tetralogy of Fallot

Problem and goal

- ToF: serious congenital cyanotic heart defect (blue baby syndrome)
- After repair: chronic pulmonary valve regurgitations and extremely dilated right ventricle (RV).
- → determine clinical variables that are predictors of the RV shape remodeling to determine best timing for implanting new valves.

Method

- Estimate mean and modes of the end-diastolic RV shape
- Find modes that are significantly correlated to clinical variables (body surface area, tricuspid and pulmonary valve regurgitations).
- Create a generative model though canonical correlation analysis

[Mansi et al, in Proc. of MICCAI 2009]

Atlas and Deformations Joint Estimation

Method:

- Estimate mean and modes of the end-diastolic RV shape
- Find modes that are significantly correlated to clinical variables (body surface area, tricuspid and pulmonary valve regurgitations).
- Create a generative model though canonical correlation analysis

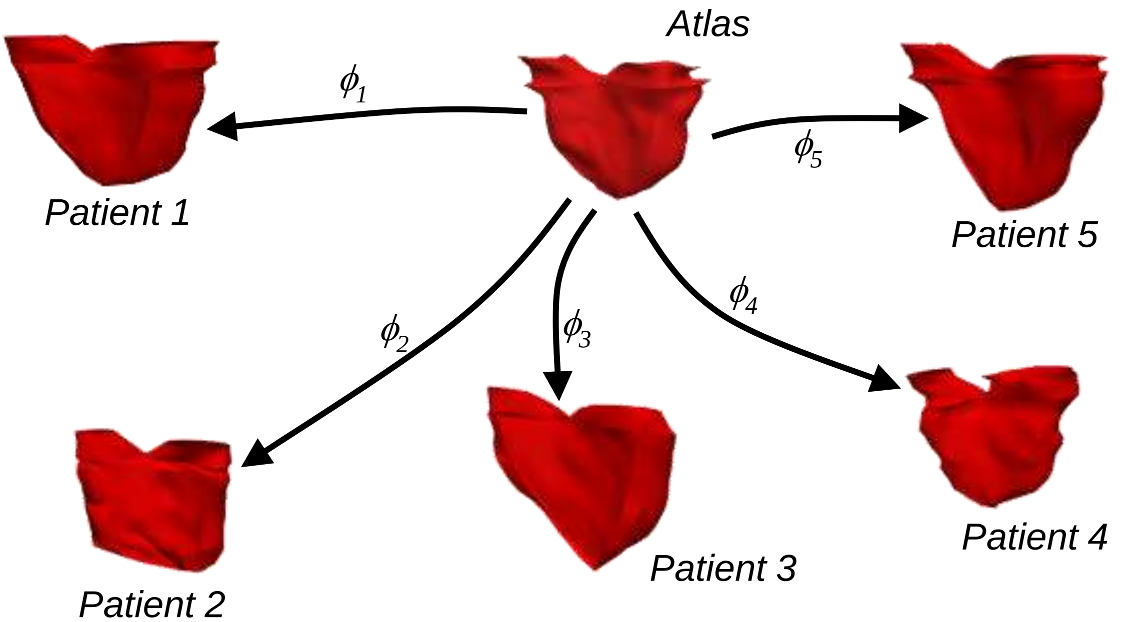

[Mansi et al, in Proc. of MICCAI 2009]

Atlas and Deformations Joint Estimation

Method:

- Estimate mean and modes of the end-diastolic RV shape
- Find modes that are significantly correlated to clinical variables (body surface area, tricuspid and pulmonary valve regurgitations).
- Create a generative model though canonical correlation analysis

Average RV anatomy of 18 ToF patients

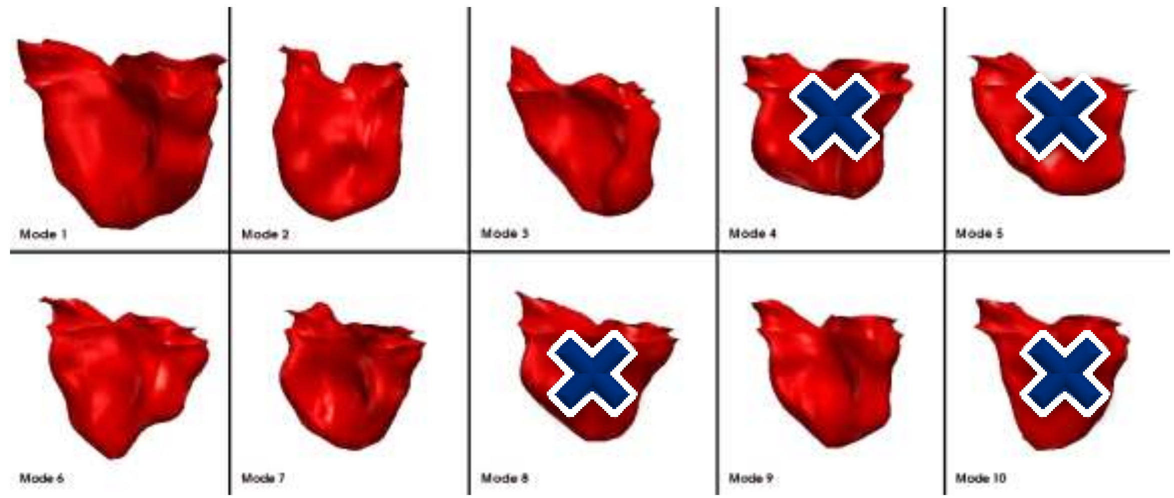

10 Deformation Modes = 90% of spectral energy

6 modes significantly correlated to BSA

[Mansi et al, in Proc. of MICCAI 2009]

Statistical Model of Right Ventricle in Tetralogy of Fallot

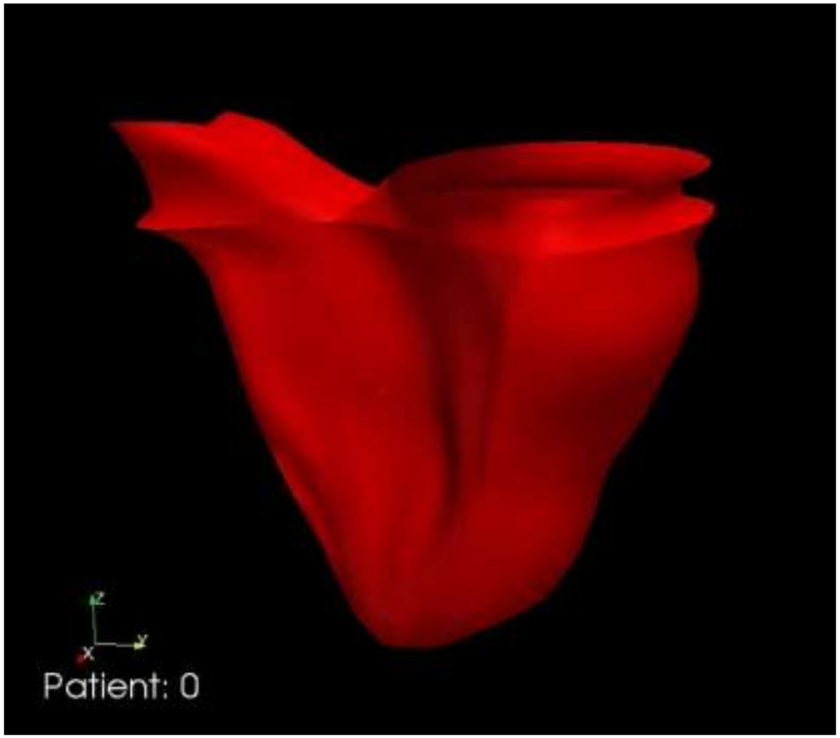

Shape of RV in 18 patients

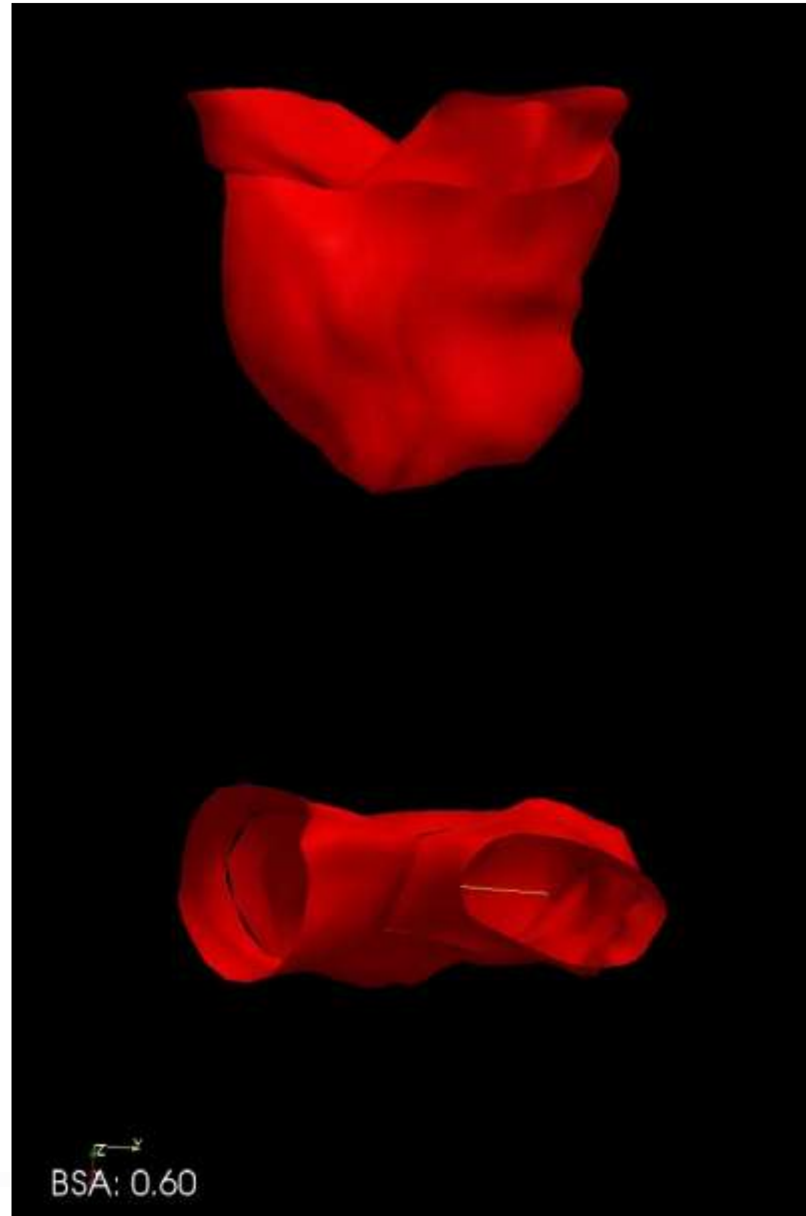

Predicted remodeling effect

Clinical Interpretation by a Cardiologist

Volume increases → Valve annuli deform → Pulmonary stenosis reduces → RV pressure decreases → Septum pushed inwards → RV free-wall outwards

(Lurz et al., Eur. Heart. J. 09)

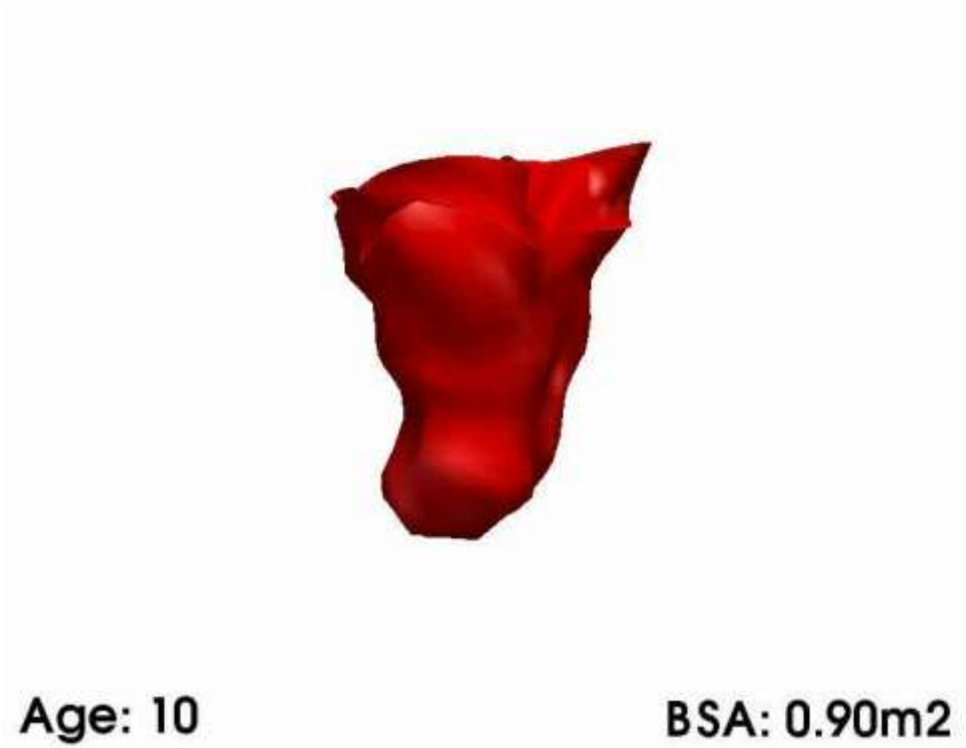

[Mansi et al, in Proc. of MICCAI 2009]

Modes Explaining Pathological Anatomy

Pair-wise Wilconxon test — Can this mode differentiate regurgitation severity?

Pulmonary regurgitations: modes 2 *($p<0.1$)*

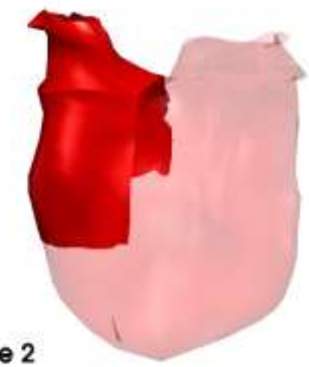

Mode 2

Tricuspid regurgitations: modes 3 *($p < 0.1$)*

Mode 3

These modes may capture the pathological features of heart growth in ToF

[Mansi et al, in Proc. of MICCAI 2009]

Roadmap

Goals and methods of Computational anatomy

Statistical computing on manifolds

A Riemannian framework for tensor computing

Currents: an embedding space for curves and surfaces

- Shapes: Forms and deformations
- Brain morphometry from curves, surfaces and tracts
- Statistical model of the right ventricle in repaired ToF
- Extension to longitudinal modeling

Log-Euclidean statistics on image deformations

Conclusion and challenges

Longitudinal evolution in populations

Spatiotemporal variability:

- Morphological changes
- Change of growth speed
- Issue: data evenly distributed in time

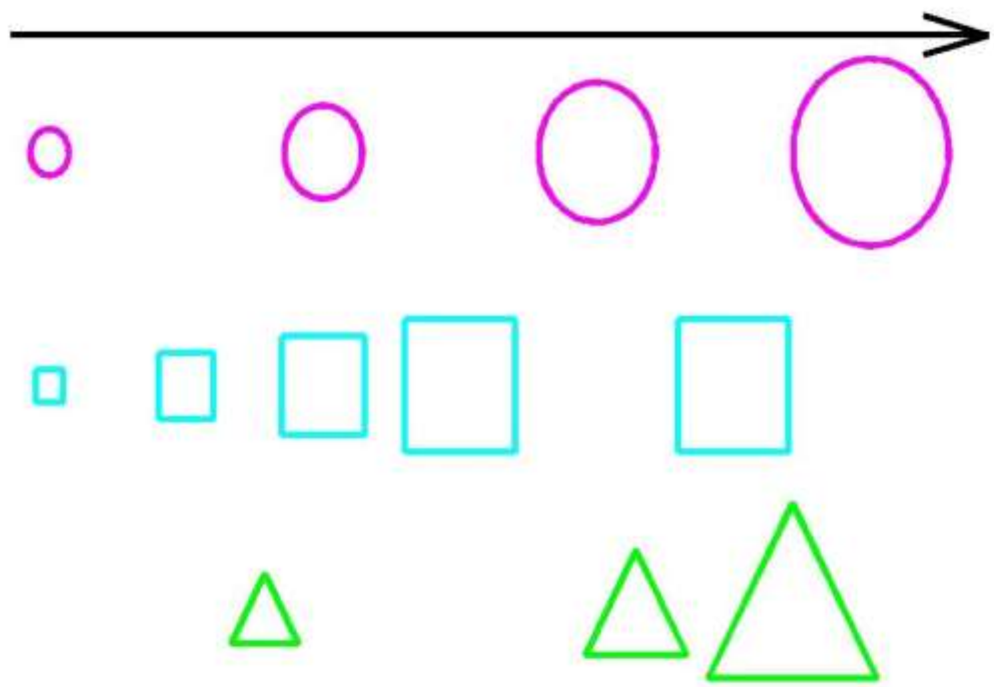

Longitudinal evolution in populations

Strategy:

1. Regression model for shape evolution
2. Spatiotemporal registration
3. Spatiotemporal atlas estimation

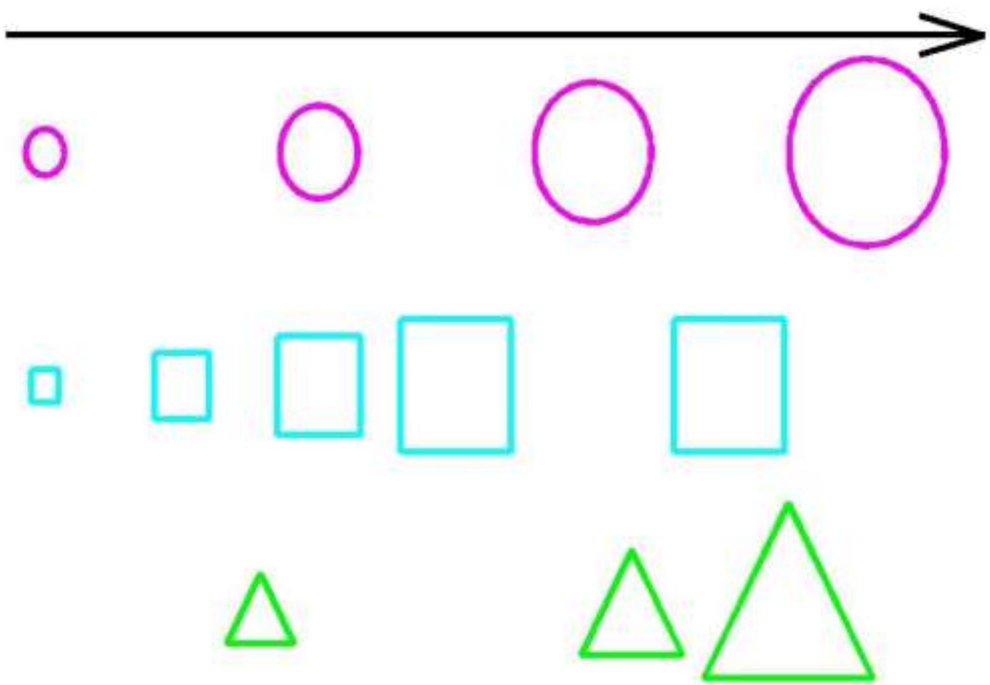

Spatiotemporal Atlas Estimation in Longitudinal Data

1/ Regression

- Given observations at different times
- Compute shape at all time (time regularization kernel)

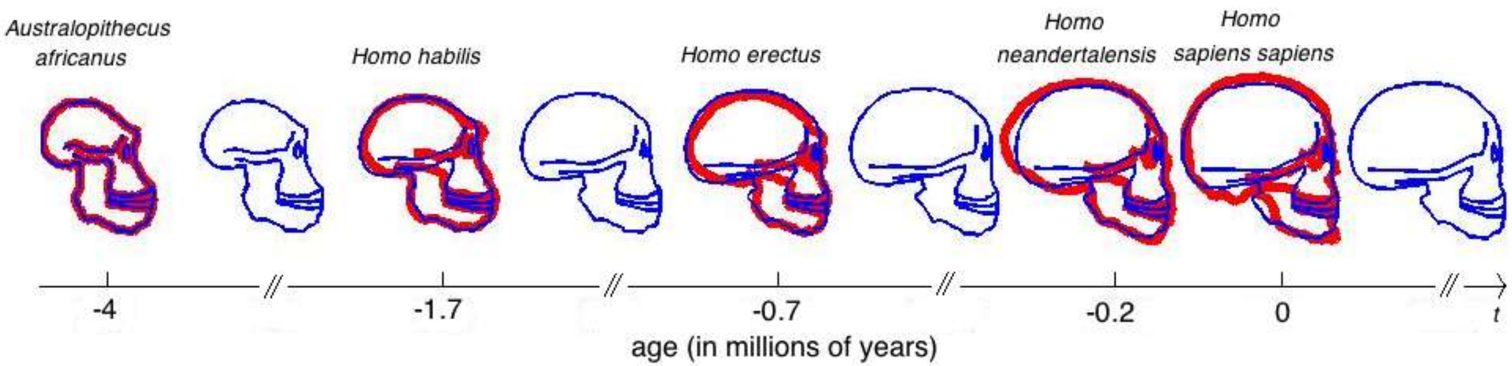

$$\min_{Def} \sum_i \mathrm{dist}^2(\mathrm{Obs}_{t_i}, \mathrm{Def}(t_i) * \mathrm{Baseline}) + \mathrm{Reg}(\mathrm{Def})$$

[Durrleman et al, in Proc. of MICCAI 2009]

Spatiotemporal Atlas Estimation in Longitudinal Data

1/ Regression

- Given observations at different times
- Compute shape at all time (time regularization kernel)

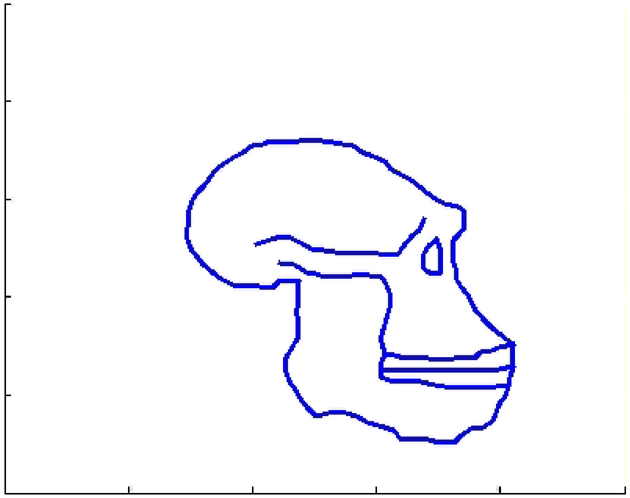

$$\min_{Def} \sum_i \mathrm{dist}^2(\mathrm{Obs}_{t_i}, \mathrm{Def}(t_i) * \mathrm{Baseline}) + \mathrm{Reg}(\mathrm{Def})$$

[Durrleman et al, in Proc. of MICCAI 2009]

Spatiotemporal Atlas Estimation in Longitudinal Data

2/ Asymmetric spatio-temporal registration

- Find the space deformation (static 3D diffeo $\phi(x)$)
- Find the time warp (1D diffeo $\psi(t)$)
- That best match two evolving shape (Def(t)*Baseline)

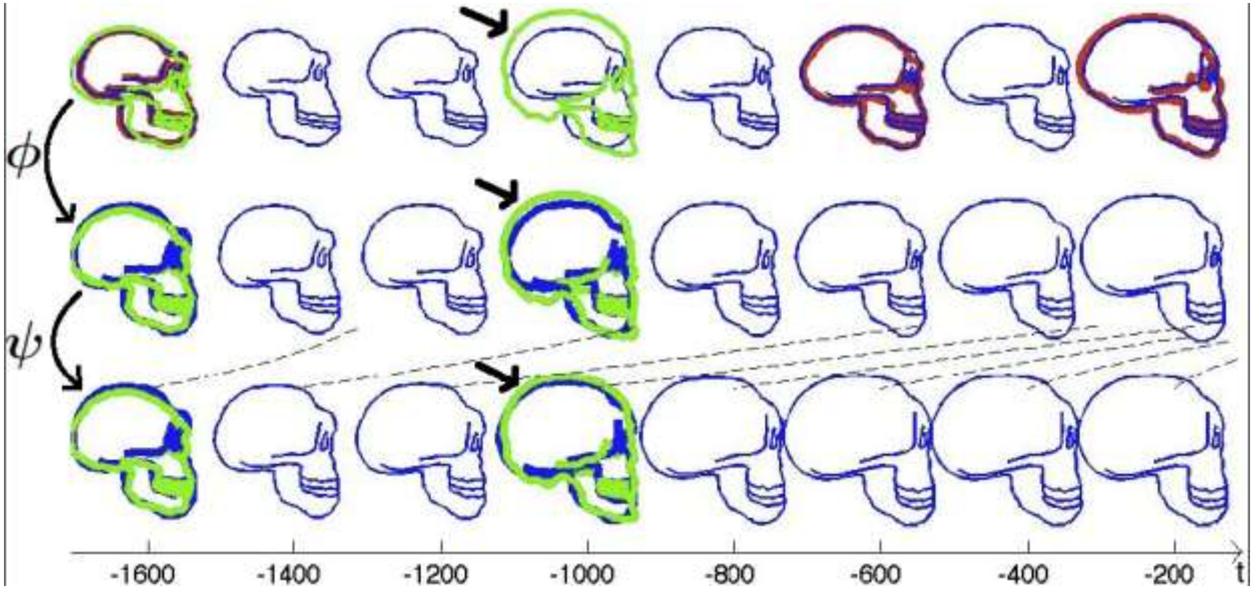

$$\min_{Def} \sum_i \mathrm{dist}^2(\mathrm{Obs}_{t_i}, \phi * (\mathrm{Def}(\psi(t_i)) * \mathrm{Baseline})\ ) + \mathrm{Reg}(\mathrm{Def(t)}) + \mathrm{Reg}(\phi)$$

3/ Spatiotemporal Atlas Estimation

- Find the typical scenario (Def(t)*Baseline)
  - The template (Baseline)
  - And its mean evolution (Def(t))
- That best matches each subject k modulo
  - A space deformation (change of coordinates = 3D diffeo $\phi_k(x)$)
  - A time warp (1D diffeo $\psi_k(t)$)

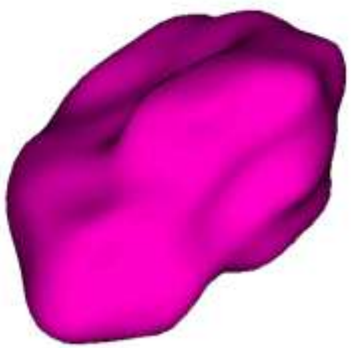

- 2 scans:
  - initial: age 2-3 years
  - follow-up: age 4-5 years
- 12 subjects:
  - 4 autistics
  - 4 developmental delay
  - 4 controls

$$\min_{Def} \sum_k \sum_{t_i} \mathrm{dist}^2(\mathrm{Obs}_{k,t_i}, \phi_k * (\mathrm{Def}(\psi_k(t_i)) * \mathrm{Baseline})) + \mathrm{Reg}(\mathrm{Def(t)}) + \sum_k \mathrm{Reg}(\phi_k)$$

Brain Development of Children

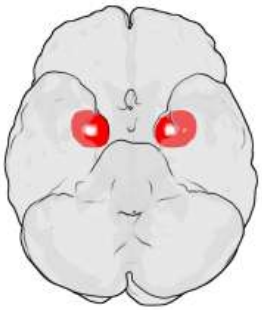

- Brain Amygdala

- *With SCI Institute, Utah*

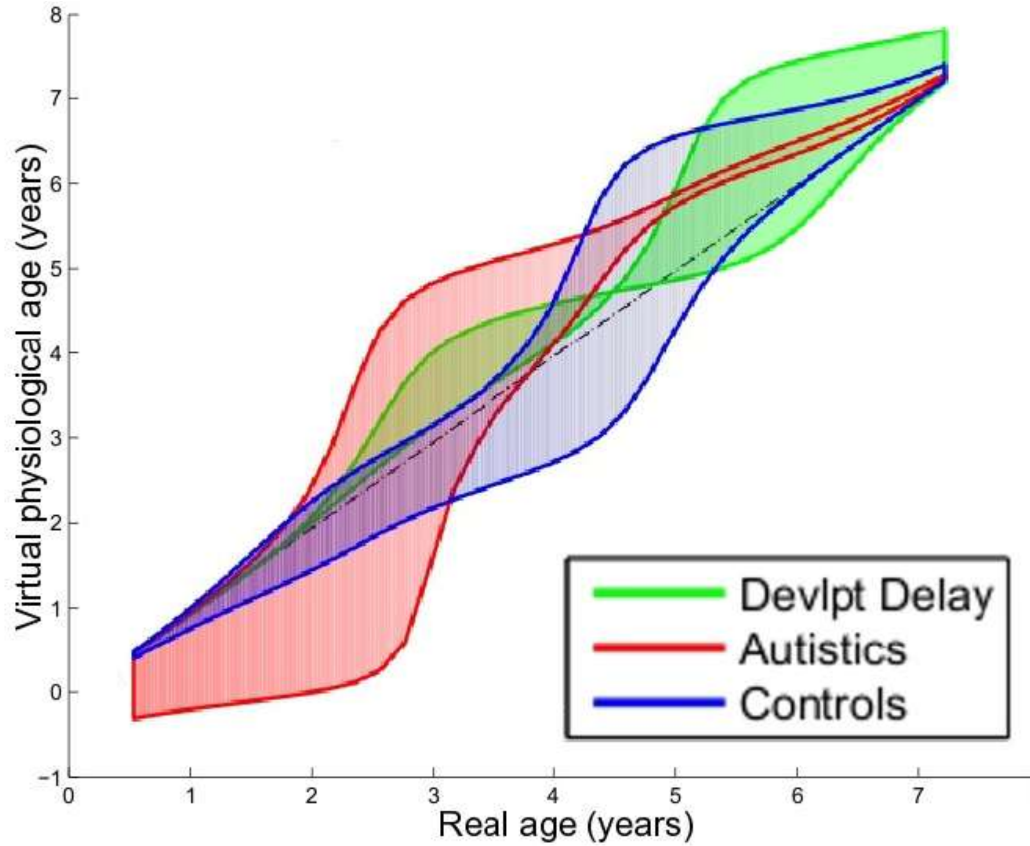

Mean scenario of evolution from 0.5 to 7 years (12 subjects with 2 time-points)

- **[S Durrleman, X Pennec, A Trouvé, G Gerig, and N Ayache. Spatiotemporal Atlas Estimation for Developmental Delay Detection in Longitudinal Datasets, MICCAI 2009]**

MICCAI 2010 WORKSHOP (www.miccai2010.org)

Spatio-Temporal Image Analysis for Longitudinal and Time-Series Image Data

www.sci.utah.edu/~gerig/MICCAI2010-SpatioTemporal

Organizers:

- Guido Gerig, University of Utah
- Thomas Fletcher, University of Utah
- Xavier Pennec, INRIA Sophia Antipolis

Important Dates:

- June 8th, 2010 — Full paper submissions
- July 13th, 2010 — Notification of acceptance
- August 18th, 2010 — Camera ready papers due
- Sept. 24 — Workshop

Roadmap

Goals and methods of Computational anatomy

Statistical computing on manifolds

A Riemannian framework for tensor computing

Currents: an embedding space for curves and surfaces

Log-Euclidean Statistics on image deformations

- The “log-Euclidean framework” for registration
- Longitudinal measures of changes

Conclusion and challenges

Statistics on which deformations feature?

Global statistics on displacement field or B-spline parameters

- [Rueckert et al., TMI, 03], [Charpiat et al., ICCV'05],
- [P. Fillard, stats on sulcal lines]
- Simple vector statistics, but inconsistency with group properties

Space of "initial momentum" [Quantity of motion instead of speed]

- [Vaillant et al., NeuroImage, 04, Durrleman et al, MICCAI'07]
- Based on left-invariant metrics on diffeos [Trouvé, Younes et al.]
- Needs theoretically a finite number of point measures
- Computationally intensive for images

An alternative: log-Euclidean statistics on diffeomorphisms?

- [Arsigny, MICCAI'07]
- [Bossa, MICCAI'07, Vercauteren MICCAI'07, Ashburner NeuroImage 2007]
- Mathematical problems but efficient numerical methods!

Local statistics on local deformation (mechanical properties)

- Gradient of transformation, strain tensor
- Riemannian elasticity [Pennec, MICCAI'05, MFCA'06]
- TBM [N. Lepore & C. Brun, MICCAI'06 & 07, ISBI'08, Neuroimage09]

Log-Euclidean Framework

Log-Euclidean processing of tensors

[Arsigny et al, MRM’06, SIAM’6]

- Idea: one-to-one correspondence of tensors with symmetric matrices, via the matrix logarithm.
- Simple processing of tensors via their logarithm (vector space)!
- Consistency with group structure (e.g., inversion-invariance)
- Very close to the affine invariant metric

Log-Euclidean processing of linear transformations

[Arsigny et al, WBIR’06, Commowick, ISBI’06, Alexa et al, SIGGRAPH’02]

- Idea: linearize geometrical transformations close enough to identity via matrix logarithm [restriction to data whose logarithm is well-defined]
- Simply process transformations via their logarithm (vector space)!
- E.g., fuse local linear transformations into global invertible deformations.

Use the group exp/log to map the group to its Lie Algebra

Examples: Polyaffine Transformations

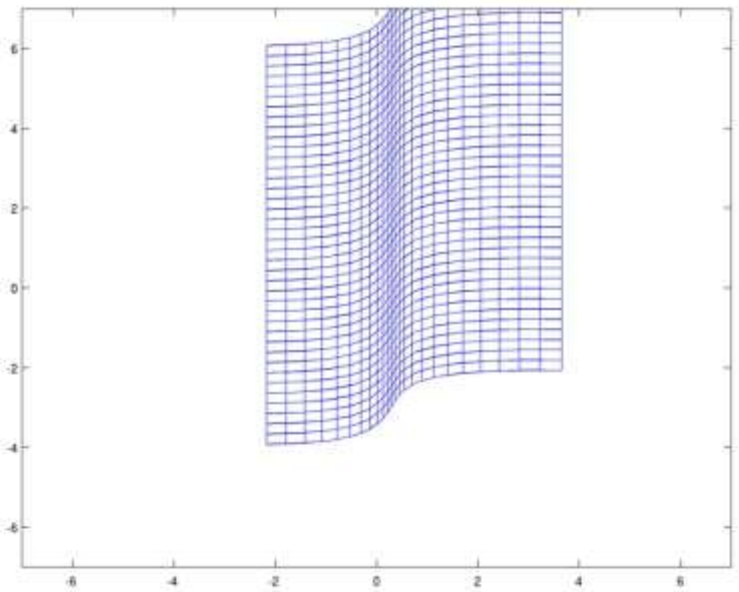

Fusing two translations

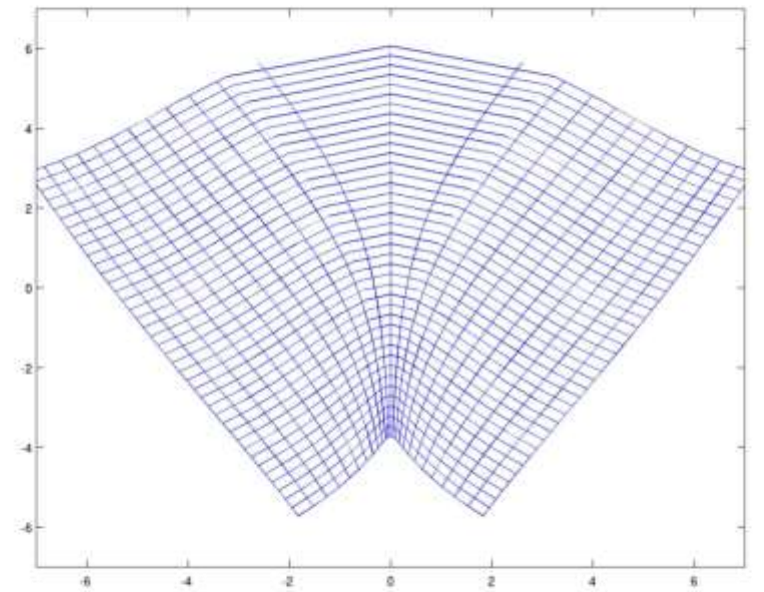

Fusing two rotations

[Arsigny, Pennec, Ayache, Medical Image Analysis, 9(6):507-523, Dec. 2005]
[Arsigny et al WBIR’06]

Generalization to Diffeomorphisms

- Diffeomorphisms belong to an infinite-dimensional Lie groups.
- Logarithm of a diffeomorphism is **a smooth static vector field**.
- Exponential of a smooth vector field V(x): integration during 1 unit of time of the ODE dx/dt = V(x).

Correspondence between Vector fields and Diffeomorphisms

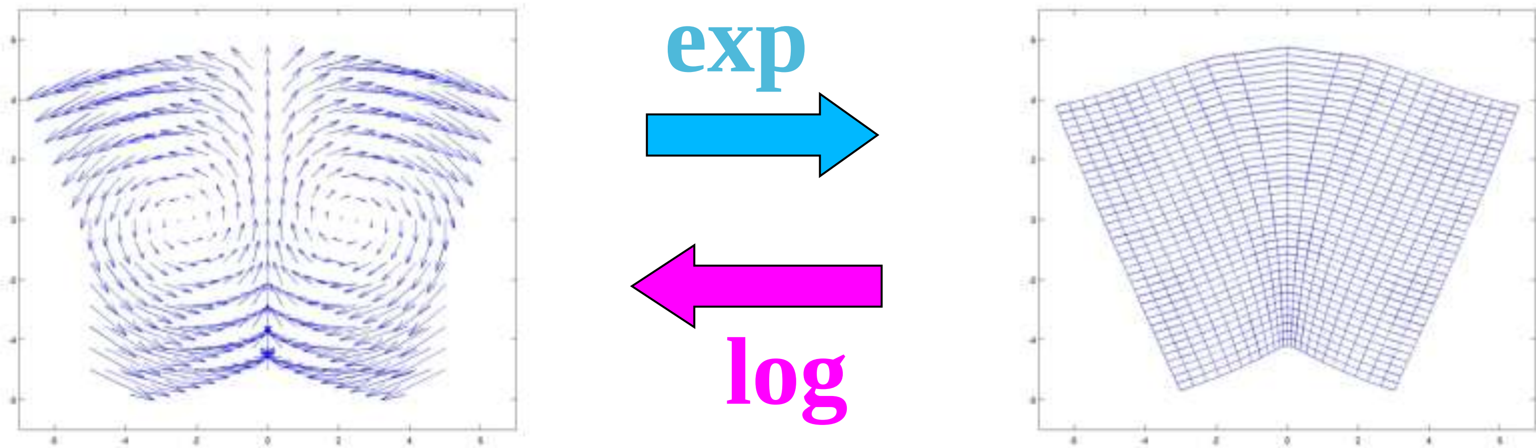

Vector field *Diffeomorphism*

[Arsigny et al MICCAI'06]

Generalization to Diffeomorphisms

Mathematical problems

- Is the exponential locally diffeomorphic?

$$\partial_V \exp(0) = V, \; i.e. \simeq D\exp(0) = Id.$$

- Infinite-dimensional case: not sufficient.
- For general diffeomorphisms (very large space): false.
- For Banach-Lie groups: true.
- Trouvé's construction is close to a Banach-Lie group: maybe!

But efficient numerical methods!

- Idea: take advantage of algebraic properties of exp and log.
  - exp(t.V) is a one-parameter subgroup.
  - In particular: exp(V)=exp(V/2) o exp(V/2)

→ Direct generalization of numerical matrix algorithms.

Exponential & diffeomorphisms:

Flows of Vector Fields

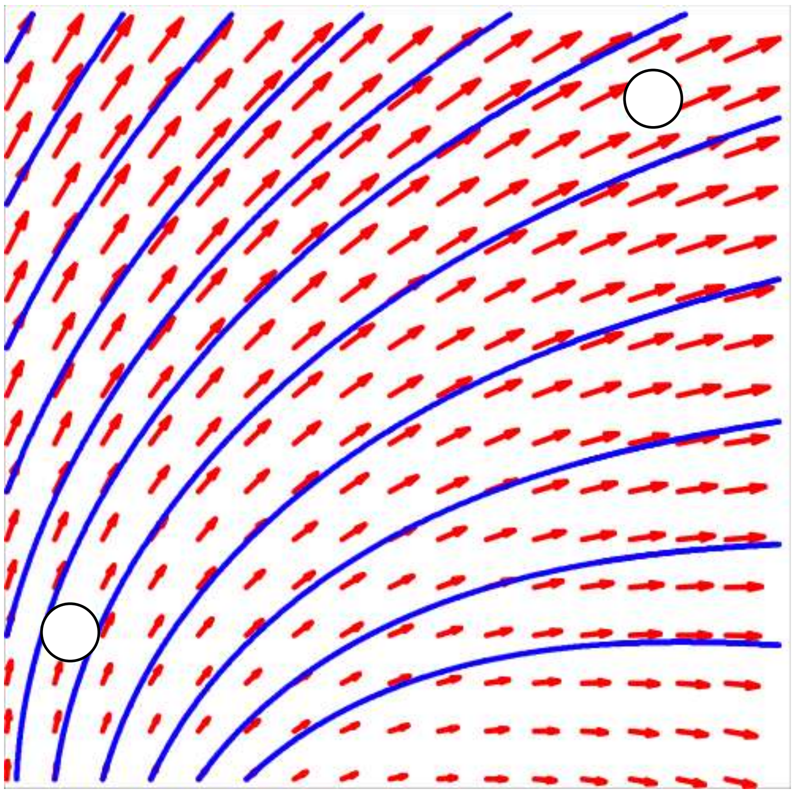

$$\frac{\partial x}{\partial t} = v(x)$$
$$x(0) = x_0$$
$$x(1) = \int_0^1 v(x(t))dt$$
$$\triangleq \exp(v)$$

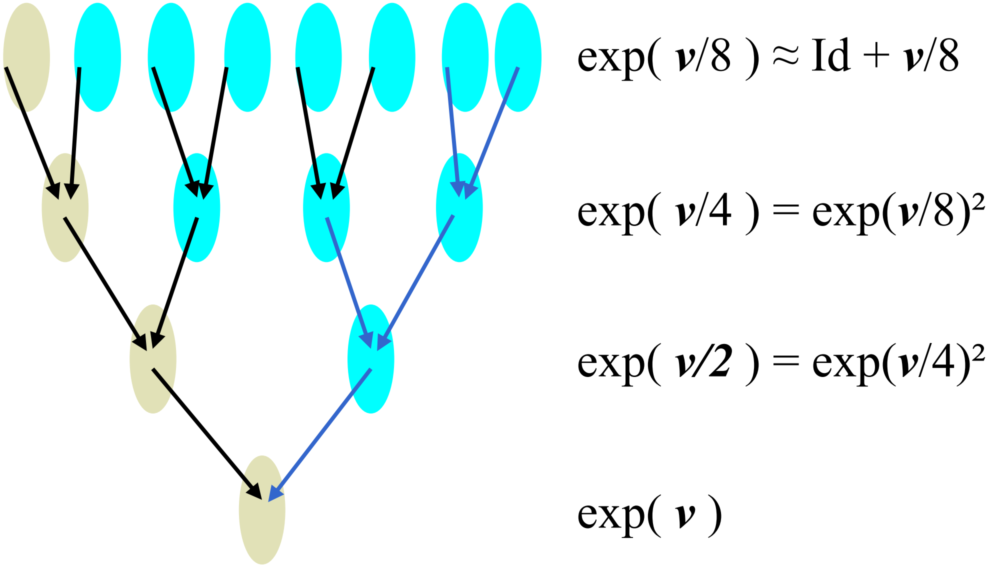

V. Arsigny, O. Commowick, X. Pennec, N. Ayache. A Log-Euclidean Framework for Statistics on Diffeomorphisms. In Proc. of MICCAI'06, LNCS 4190, pages 924-931, 2-4 October 2006.

Scaling and Squaring Method

Fusion of two rotations (N=6).

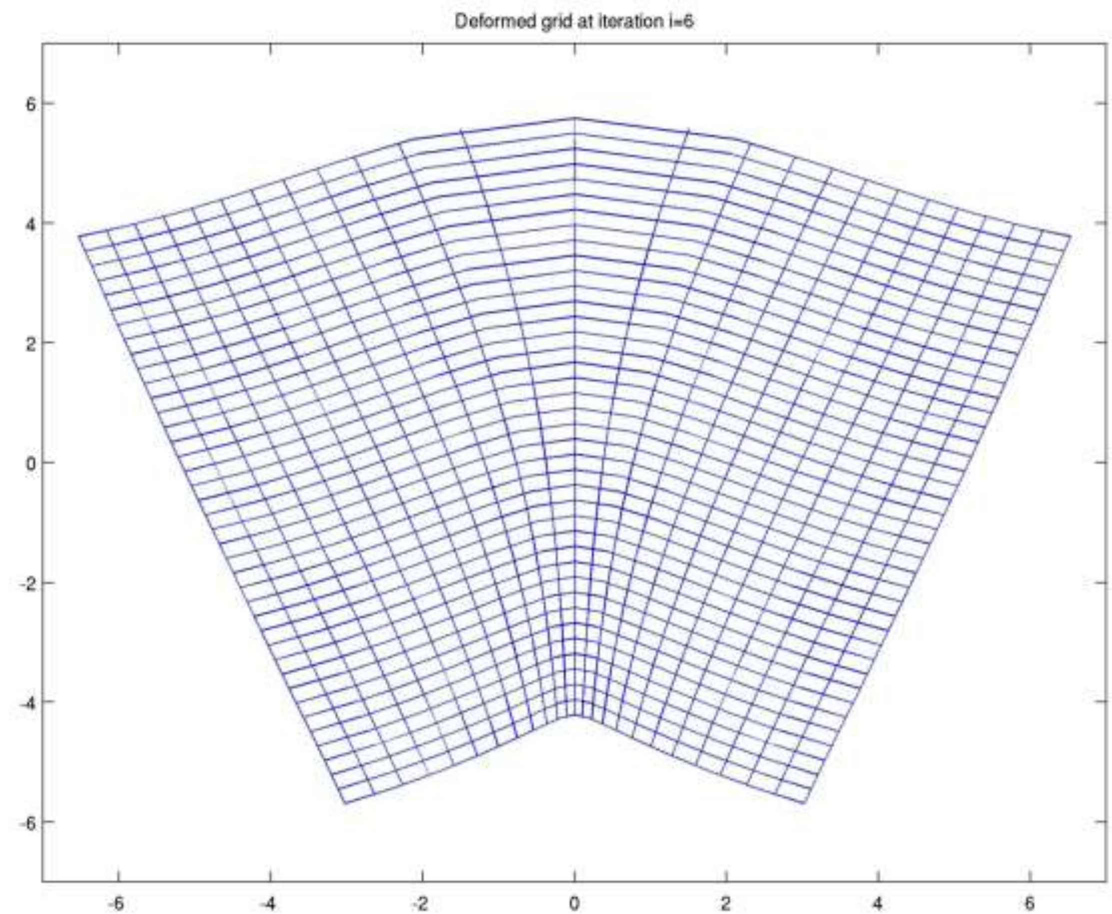

Inverse Scaling and Squaring

Matrix case

1) Choose normalization 2^N
2) Compute recursively N square roots.
3) Multiply by 2^N final matrix.

Diffeomorphism case

1) Choose normalization 2^N
2) Compute recursively N square roots (gradient descent).
3) Multiply by 2^N final displacements

- Numerical precision so far: 3% on average
- Sensitive to high frequencies (high pass filter)
- Very slow (square root solved by least squares)

→Compute the “log” directly in the registration algorithm?

The Demons Framework

Efficient energy minimization

$$E(C,U,\dot{U}) = \boxed{E_S(I,J,C)} + \boxed{\sigma \int \| C-U \|^2} + \boxed{\lambda \int \| \nabla U \|^2}$$

similarity *Auxiliary* *Elastic-like Regularity*

Alternate Minimization

- on C, Correspondance Field (image forces)
  Gauss-Newton gradient descent: normalized optical flow
- on U, Deformation Field (regularization)
  Quadratic norm → convolution (Gaussian)
- **Interest**: fast computation

• J.P. Thirion: Image Matching as a diffusion process: an analogy with Maxwell's demons. Medical Image Analysis 2(3), 242-260, 1998.
• P. Cachier E. Bardinet, E. Dormont, X. Pennec and N. A.: Iconic Feature Based Nonrigid Registration: the PASHA Algorithm, Comp. Vision and Image Understanding (CVIU), 89 (2-3), 272-298, 2003.

Log-Domain Demons

Idea: [Arsigny MICCAI 2006, Bossa MICCAI 2007]

- Parameterize the deformation by its logarithm
- Time varying (LDDMM) replaced by stationary vector fields
- Efficient scaling and squaring methods to integrate autonomous ODEs

Geodesic gradient descent

- Compute gradient (or 2[nd] order update) of Sim(I, J $\circ\ \phi$)
- Replace $\phi \leftarrow \phi \circ (\mathrm{Id}+\mathbf{u})$ by $\phi = \exp(\mathbf{v}) \leftarrow \exp(\mathbf{v}) \circ \exp(\mathbf{u})$

Approximation with BCH formula

- $\exp(\boldsymbol{v}) \circ \exp(\varepsilon \boldsymbol{u}) = \exp(\boldsymbol{v} + \varepsilon \boldsymbol{u} + [\boldsymbol{v},\varepsilon \boldsymbol{u}]/2 + [\boldsymbol{v},[\boldsymbol{v},\varepsilon \boldsymbol{u}]]/12 + \ldots)$
  - Lie bracket $[\boldsymbol{v},\boldsymbol{u}](\mathrm{p}) = \mathrm{Jac}(\boldsymbol{v})(\mathrm{p}).\boldsymbol{u}(\mathrm{p}) - \mathrm{Jac}(\boldsymbol{u})(\mathrm{p}).\boldsymbol{v}(\mathrm{p})$

T Vercauteren, X Pennec, A Perchant, and N Ayache. *Symmetric Log-Domain Diffeomorphic Registration: A Demons-based Approach*, MICCAI 2008

Symmetric Log-Domain Demons

Use easy inverse: $\phi^{-1} = \exp(-v)$

Iteration

- Given images I_0, I_1 and current transformation $\phi = \exp(\boldsymbol{v})$
- Forward and backward demons forces

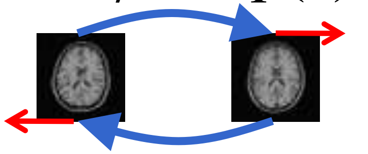

- Symmetric update: $\boldsymbol{v} \leftarrow \frac{1}{2}\left(Z(\boldsymbol{v},\boldsymbol{u}^{\text{forw}}) - Z(-\boldsymbol{v},\boldsymbol{u}^{\text{back}})\right)$
- Regularize (Gaussian): $\boldsymbol{v} \leftarrow K_{\text{diff}} * \boldsymbol{v}$

Symmetry helps the convergence

- Clearly shown in Klein study

Open-source ITK implementation

- http://hdl.handle.net/10380/3060

T Vercauteren, X Pennec, A Perchant, and N Ayache. *Symmetric Log-Domain Diffeomorphic Registration: A Demons-based Approach*, MICCAI 2008

DT-REFinD: Diffusion Tensor Registration with Exact Finite-Strain Differential

[Thomas Yeo, et al. DTI Registration with Exact Finite-Strain Differential. ISBI'08, TMI 28(12):1914-1928 2010]

- Tensor metric: Log-Euclidean (Arsigny ’06)
- Tensor reorientation: Finite strain with exact differential

DTI Diffeomorphic Demons loop: [Vercauteren MICCAI’07]

- Iterated one parameter diffeomorphisms

  $$E(c, \phi) = \| F - M \circ c \|^2/\sigma_i^2 + \mathrm{dist}(c, \phi)^2 /\sigma_x^2 + \mathrm{Reg}(\phi) /\sigma_T^2$$

  - Compute demons force u by optimizing: $\mathrm{Sim}(F, M, \phi \circ \exp(\boldsymbol{u})) + \|\boldsymbol{u}\|^2$
  - Exponential update: $\phi \leftarrow \phi \circ \exp(\boldsymbol{u})$
  - Gaussian smoothing: $\phi \leftarrow K * \phi$

Fast and accurate

- 15 minutes,128x128x60, Xeon 3.2GHz
- Better tensor alignment

DT-REFinD: Diffusion Tensor Registration with Exact Finite-Strain Differential

Moving Image *M* | Target Image *F* | Approx. Grad (dR=0) | Exact Gradient

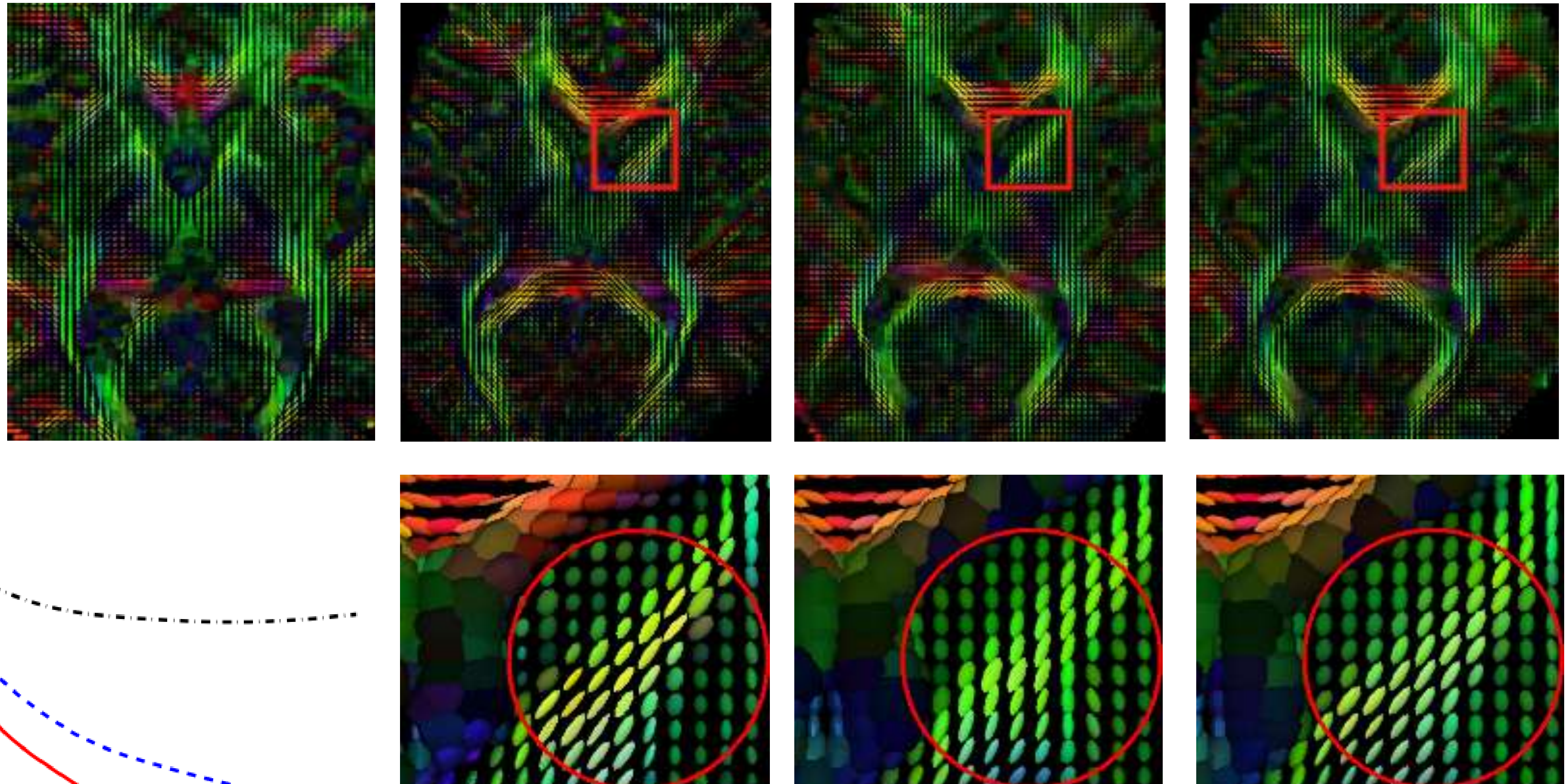

Image similarity

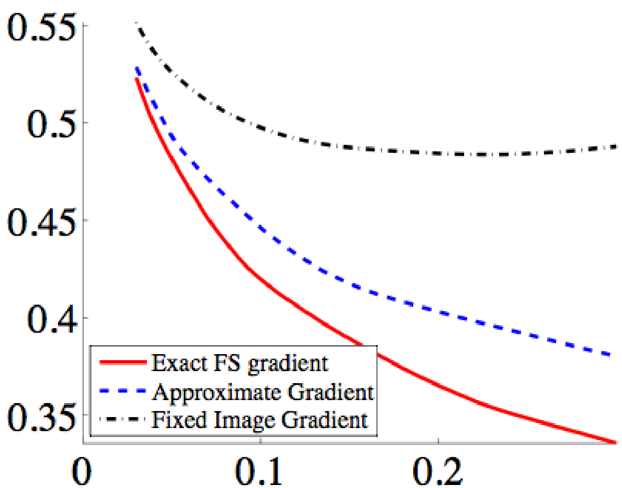

Harmonic Energy

15 minutes,128x128x60, Xeon 3.2GHz

DTI data courtesy of Denis Ducreux, MD,
Bicêtre Hospital, Paris, France

Log-domain DTI registration

Statistics on DTI image log-deformations:

- 30 Subjects in MNI space
- All pairwise registrations
- Null mean (inverse consistency)
- 4, 16, 32 and 64 modes account for 25%, 60%, 75% and 80% of variance

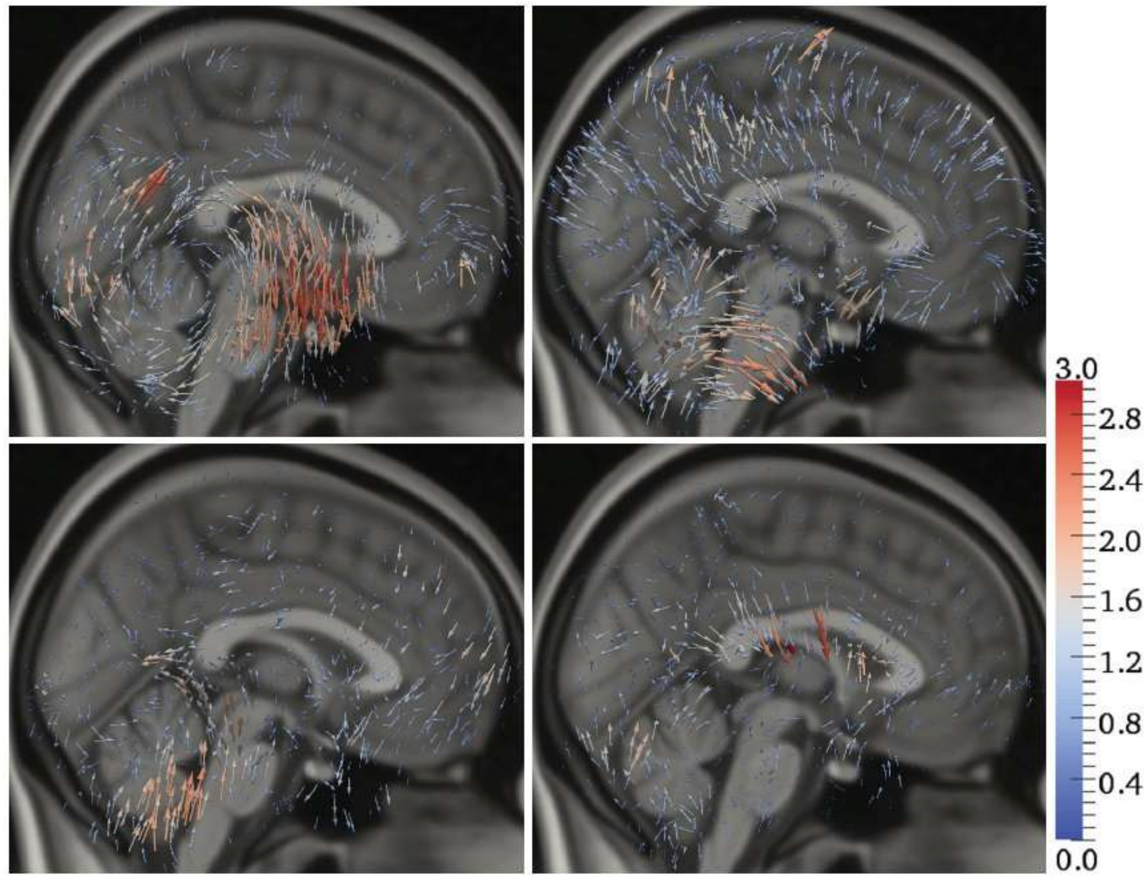

- Current work: reuse these modes to better constrain T1 registration

[A. Sweet and X. Pennec. Log-Domain Diffeomorphic Registration of Diffusion Tensor Images. In Workshop on Biomedical Image Registration 2010, 2010.]

Log-Euclidean framework for diffeomorphisms

Conclusions

- Log-Euclidean framework for diffeomorphisms: algorithmically simple in spite of infinite dimensions.
- Very suitable for registration
- Compatible with “inverse-consistency”
- Vector statistics directly generalized to diffeomorphisms.

Questions

- What are the diffeomorphisms that we cannot reach?
- Is this space a BCH Lie-group?
- Can we obtain bi-invariance in addition?
- Is there an underlying information-geometric structure?

Roadmap

Goals and methods of Computational anatomy

Statistical computing on manifolds

A Riemannian framework for tensor computing

Currents: an embedding space for curves and surfaces

Log-Euclidean Statistics on image deformations

- The "log-Euclidean framework" for registration
- Measuring longitudinal changes

Conclusion and challenges

Individual Measure of Temporal Evolution

Signal changes (Voxel-based morphometry)

- Detect apparent changes of the signal
  - Lesion evolution (e.g. SEP)
- Adapted to functional imaging

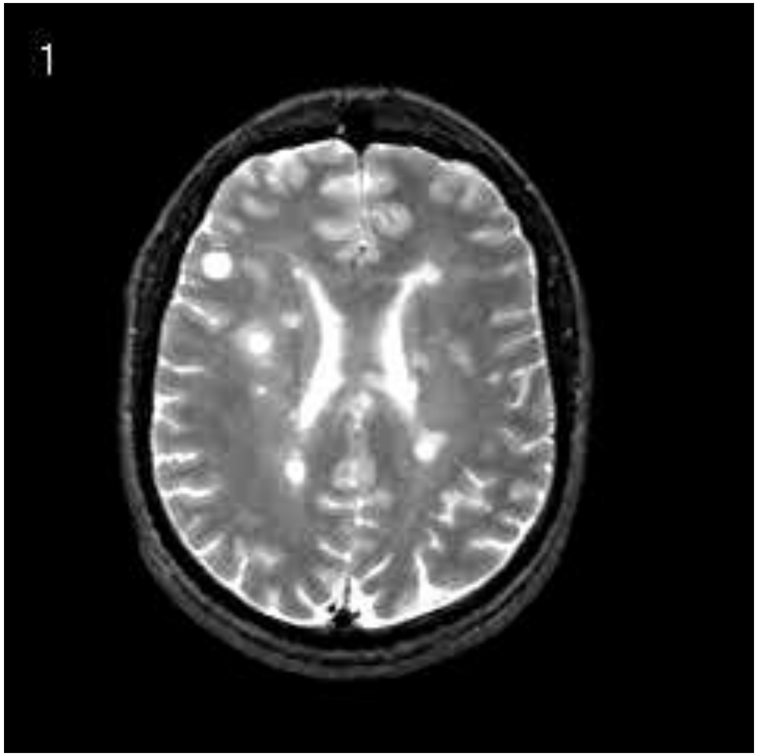

Individual Measure of Temporal Evolution

Signal changes (Voxel-based morphometry)

- Detect apparent changes of the signal
  - Lesion evolution (e.g. SEP)

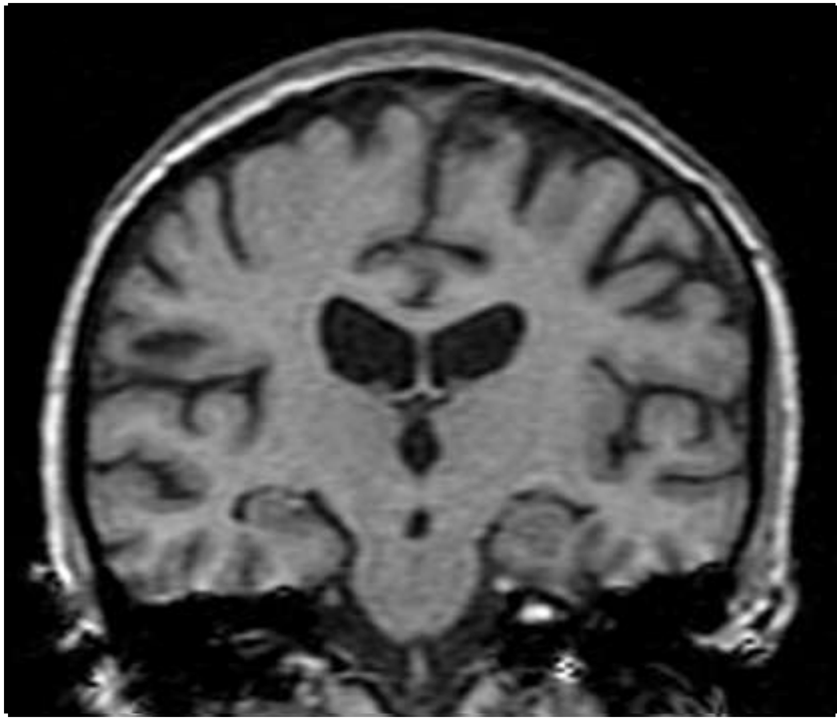

- Adapted to functional imaging

- Indirect for anatomical shape changes (e.g. brain atrophy for Alzheimer’s Disease)

Longitudinal measures in images?

Geometry changes (Deformation-based morphometry)

- Measure the physical or apparent deformation found by deformable registration

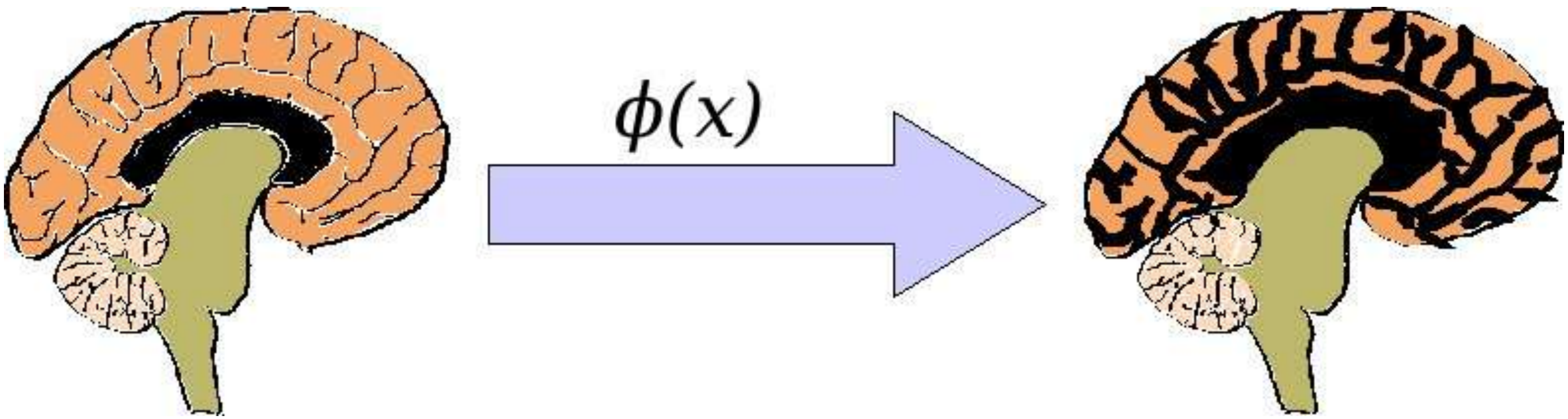

Quantification of apparent deformations for Multiple Sclerosis

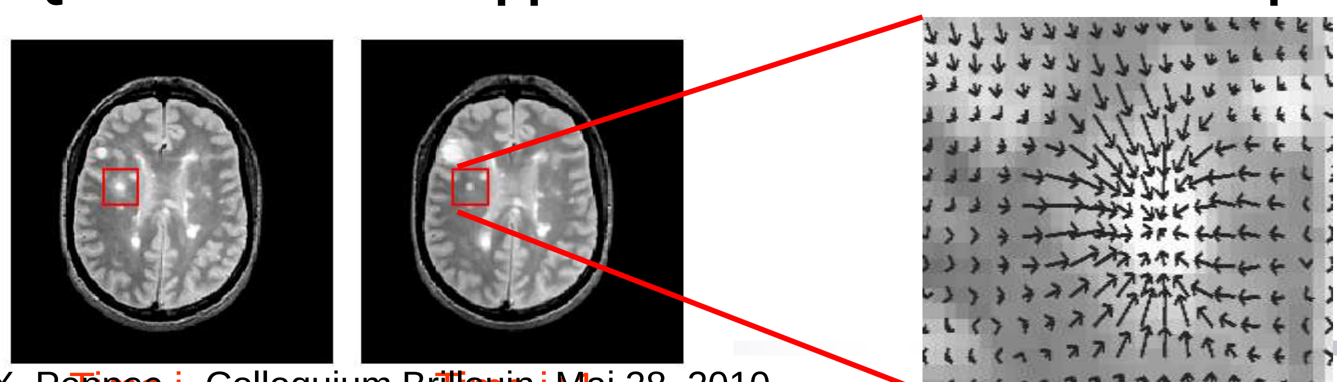

[D. Rey, G. Dugas-Phocion, G. Malandain (Asclepios) In collaboration with C. Lebrun, S. Chanalet (CHU Pasteur, Nice)]

Atrophy estimation for Alzheimer

Alzheimer's Disease Neuroimaging Initiative (ADNI)

- 200 NORMAL 3 years
- 400 MCI 3 years
- 200 AD 2 years
- Visits every 6 month
- 57 sites

Data collected

- Clinical, blood, LP
- Cognitive Tests
- **Anatomical images:1.5T MRI** (25% 3T)
- Functional images: FDG-PET (50%), PiB-PET (approx 100)

Atrophy estimation for Alzheimer

Established markers of anatomical changes (Slides from M. W. Wiener)

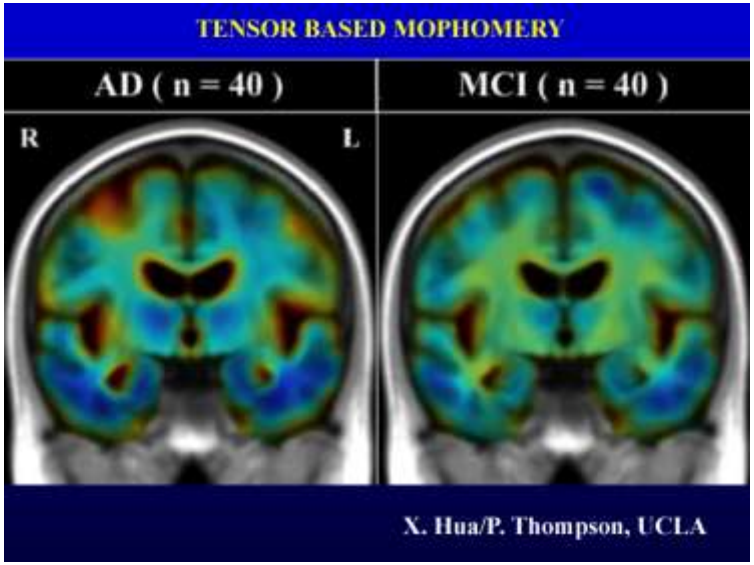

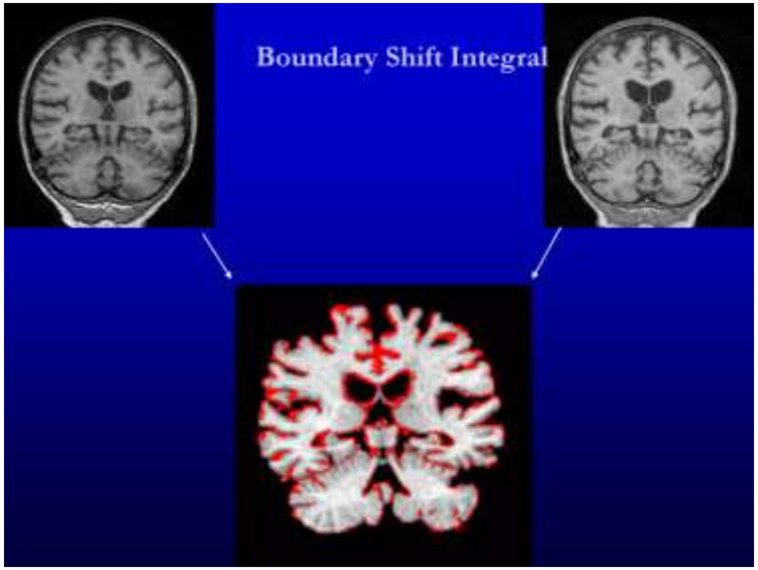

Local: TBM (Paul Thompson, UCLA)

Local volume change: Jacobian (determinant of spatial derivatives matrix)

Global: BSI / KNBSI (N. Fox, UCL)

Intensity flux through brain surface

SIENA (S.M. Smith, Oxford)

percentage brain volume change

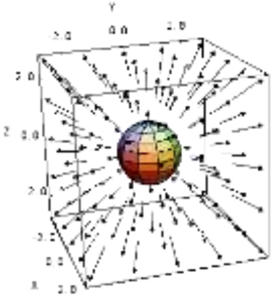

PhD Marco Lorenzi collaboration with G. Frisoni (IRCCS Fatebenefratelli, Brescia)

- Combine consistently local (voxel) and global (regions / brain)
- Improve detection / localization power

Consistent measures at the voxel and regional level

Properties of the velocity fields

- Integrate Jac(ϕ) (~ TBI) → Volume change
- Integrate log(Jac(ϕ)) → Flux-like (~ BSI)

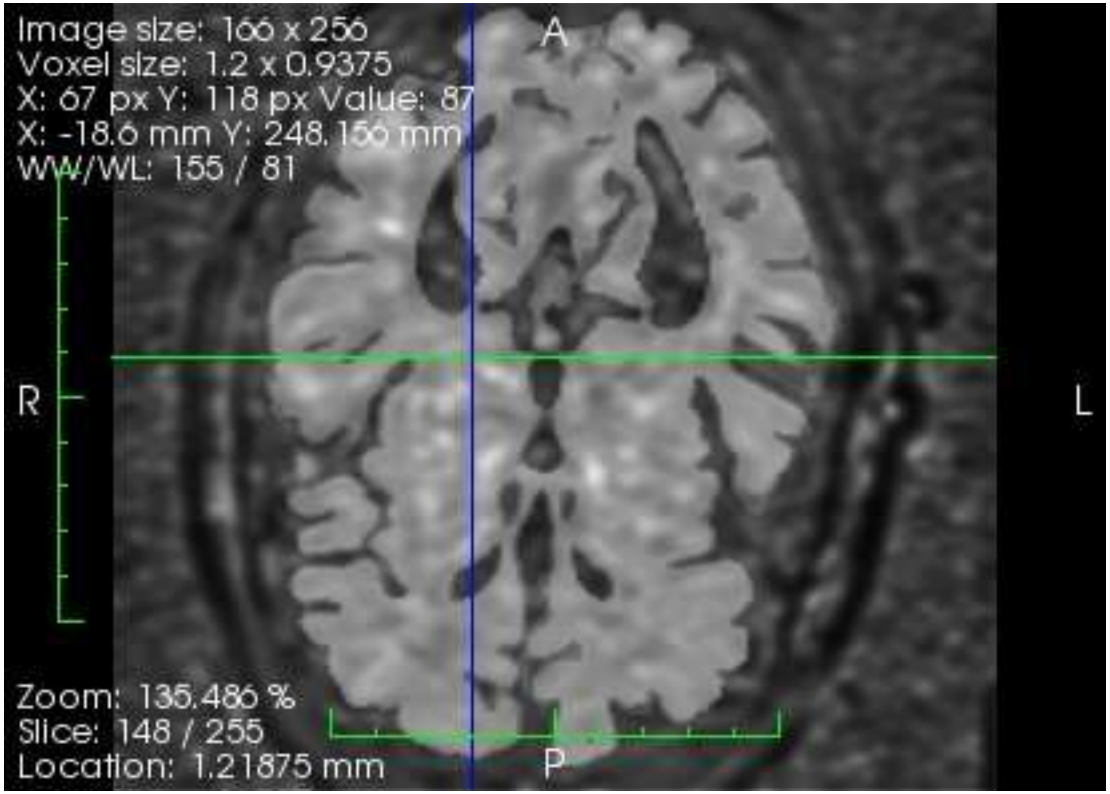

Log Jacobian Integrated on the brain mask

Consistent measures at the voxel and regional level

Pilot experiment

- 8 ADNI MCI subjects, longitudinal 6-months scans from baseline to T36.
- GM+WM segmentation at baseline (BET+FAST from FSL)
- N3 algorithm for intensity correction.

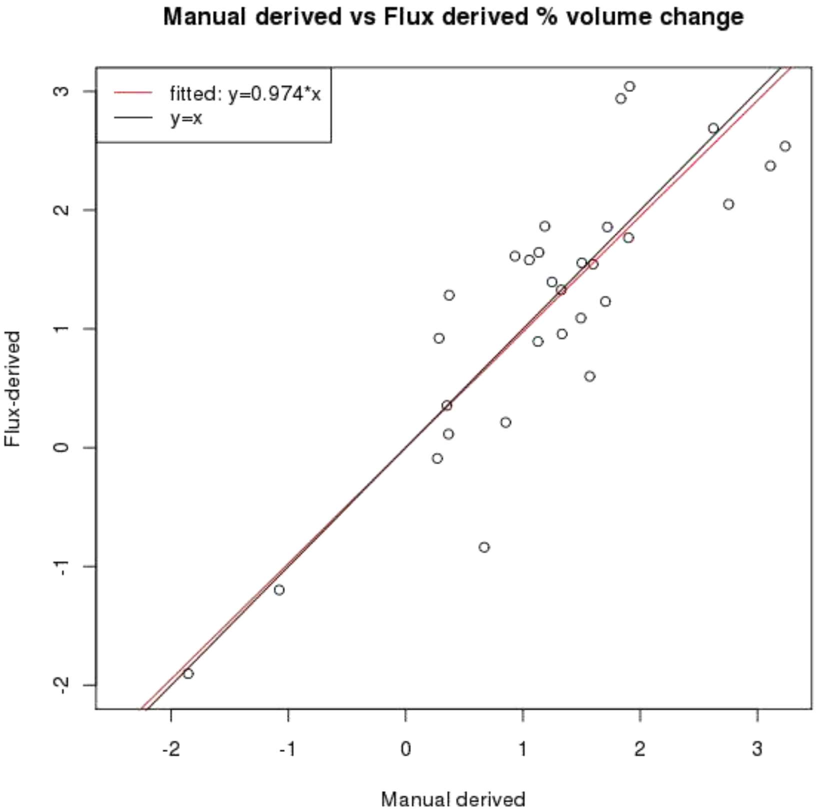

Correlation with ground truth

- Log-demons Flux vs manual volume: 0.90
- KNBSI vs manual volume: 0.85

Current challenges for longitudinal studies

Consistency of the temporal trajectory

- Robust estimation of longitudinal changes at multiple time points

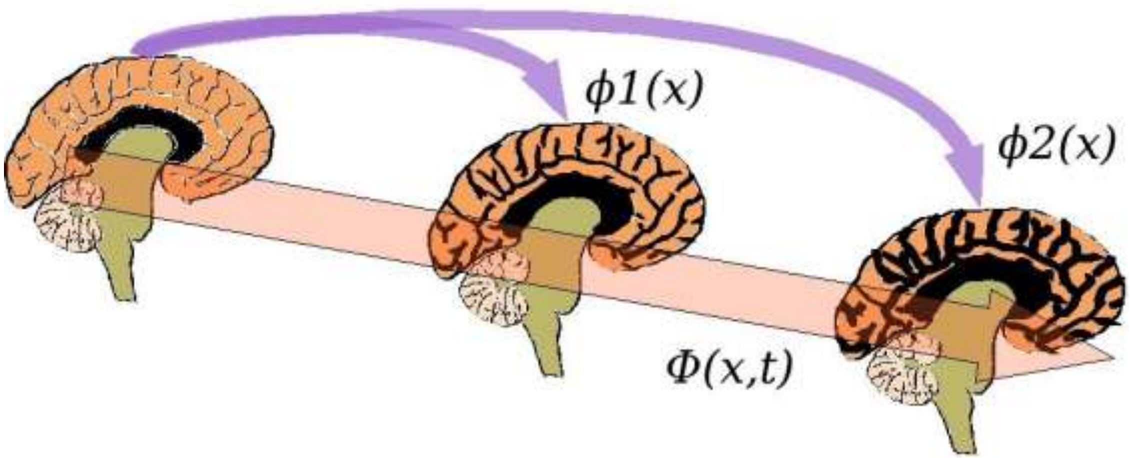

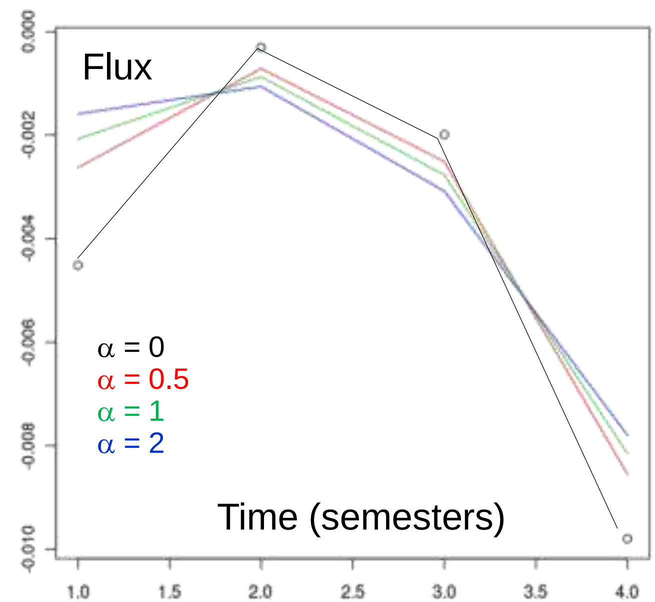

- Regularize the temporal trend
- Without loosing accuracy

Current challenges for longitudinal studies

Patient specific evolution → model of the population trend

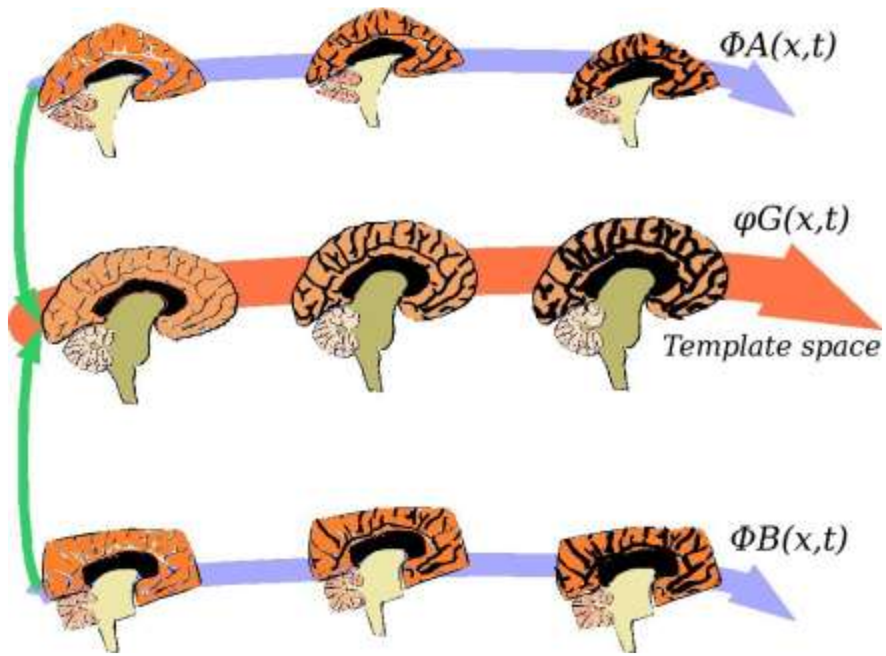

What is the right parallel transport of trajectories?

Roadmap

Goals and methods of Computational anatomy

Statistical computing on manifolds

A Riemannian framework for tensor computing

Currents: an embedding space for curves and surfaces

Log-Euclidean statistics on image deformations

Conclusion and challenges

Statistics on geometrical objects

A consistent statistical framework based on a Riemannian metric

An efficient algorithmic toolbox based on the Exp map

- Gauss-Newton for Karcher mean
- Filtering, convolution = weighted means
- Gradient descent = geodesic walking
- Intrinsic explicit numerical scheme for Laplace Beltrami

What about non complete manifolds?

- E.g. Power metrics for tensors
- Accumulation at boundaries for diffusion?

2nd order geometry tools: connection, parallel transport

- Comparison of deformation sequences [Cao,Miller,Younes, Neuroimage09]
- Should it be consistent with the metric?

Statistics on geometrical objects

How to chose or estimate the metric?

- Invariance principles, learning the metric?
- Anatomical deformation metrics?

Is the Riemannian metric the minimal structure?

- No bi-invariant metric but bi-invariant means on Lie groups [V. Arsigny]
- Change the Riemannian metric for a connection?

From finite to infinite dimensions

- Efficient algorithms for diffeomorphisms?
- What are we loosing with static velocity fields?

Challenges of Computational Anatomy

Applications

- Medical Image Analysis (registration evaluation, DTI)
- Building models of living systems (spine, brain, heart…)

Build models from multiple sources

- Curves, surfaces [cortex, sulcal ribbons]
- Volume variability [Voxel/deformation &Tensor Based Morphometry]
- Probing the information highways of the brain with DMRI [fibers, tracts, atlas]

From descriptive statistics to modeling and to personalized medicine

- Knowledge discovery
- Modeling
- Personalized digital medicine

Thank You!

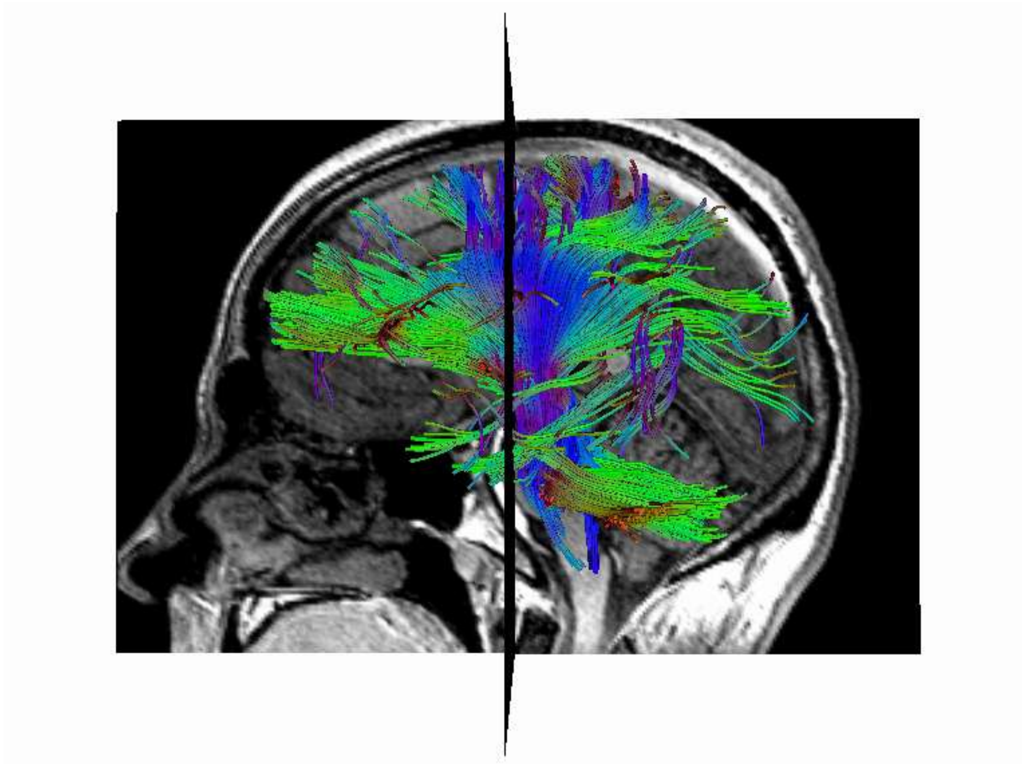

Publications: http://www.inria.fr/sophia/asclepios/biblio

Software: http://www.inria.fr/sophia/asclepios/software/MedINRIA.

Special thanks to Pierre Fillard for many illustrations!

Acknowledgements

Image guided therapy

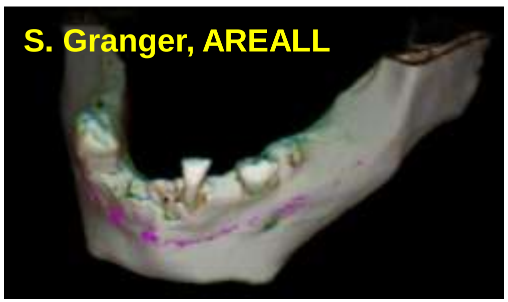

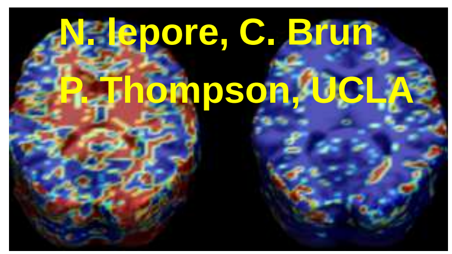

Brain imaging

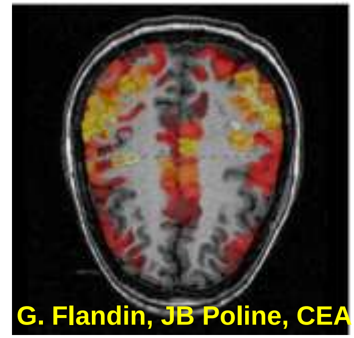

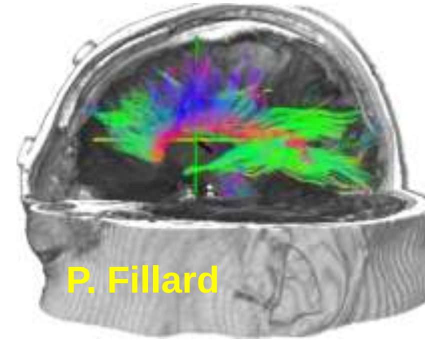

Computational anatomy

Confocal microscopy

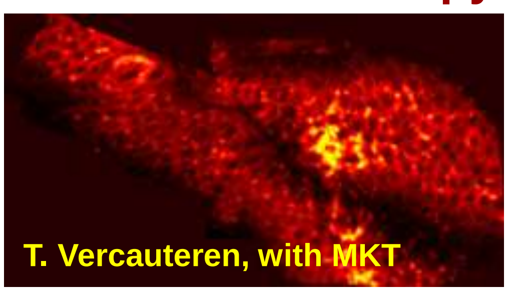

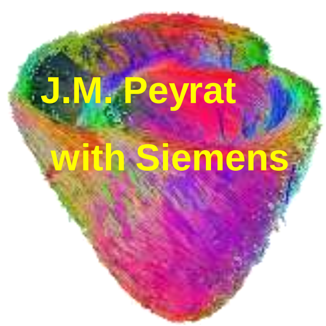

www.inria.fr/sophia/asclepios/ [publications | software]

Acknowledgements

Image guided therapy

- Brain surgery (Roboscope): A. Roche and P. Cathier
- Dental implantology: S. Granger, AREALL
- Liver puncture guidance: S. Nicolau and L. Soler, IRCAD
- Mosaicing confocal microscopic images: T. Vercauteren, MKT

Brain imaging

- Geometry and statistics for fMRI analysis: G. Flandin, J.-B. Poline, CEA
- Inter-subject non-linear registration: P. Cathier, R. Stefanescu, O. Commowick

Computational anatomy

- Associated team Brain Atlas with LONI: P. Thompson, P. Fillard, V. Arsigny
- Growth and variability: S. Durrleman
- Spine shape: J. Boisvert, F. Cheriet, Ste Justine Hospital, Montreal.
- ACI Agir / Grid computing: T. Glatard and J. Montagnat, I3S.

Epidaure / Asclepios Team

- N. Ayache, G. Malandain, H. Delingette
- … and all the current and former team members.